Defining the end of pluripotency in mouse embryonic stem cells

Studien zum Ende der Pluripotenz in embryonalen Stammzellen der Maus

Doctoral thesis for a doctoral degree
at the Graduate School of Life Sciences,
Julius-Maximilians-Universität Würzburg,
Section Biomedicine

submitted by

Nadine Obier

from
Halle (Saale)

Würzburg, 2010

Submitted on: .....

Office stamp

Members of the *Promotionskomitee:*

Chairperson:	Prof. Thomas Müller
Primary Supervisor:	Prof. Albrecht Müller
Supervisor (Second):	Prof. Ulrich Scheer
Supervisor (Third):	Prof. Constanze Bonifer

Date of Public Defence: .....

Date of Receipt of Certificates: .....

Contents

1 Summary

Stem cells with the particular potential to self renew and to differentiate into multiple cell lineages are fascinating cell types for basic and applied research. Pluripotent embryonic stem (ES) cells are derived from the inner cell mass (ICM) of preimplantation embryos. Upon differentiation ES cells can give rise to cells of ecto-, meso- and endoderm including germ cells. In contrast, multipotent adult stem cells are more restricted in their differentiation outcomes, they differentiate into cells of their tissue of origin. For example, hematopoietic stem cells (HSCs) that reside in hemogenic tissues such as the bone marrow (BM) differentiate into hemato-/lymphoid cell lineages. Upon differentiation of stem cells not the genome, but the epigenetic regulation changes. Differentiation-associated epigenetic changes generate cell types with distinct phenotypes and functions. For stem cell-based therapies it is important to deeper understand the relation between epigenome and cellular function.
In the scope of this thesis I aimed to analyze cultures of differentiating stem cells with respect to gene expression, chromatin regulation and differentiation potential.
For the analysis of global histone modification levels, which represent one mechanism for epigenetic regulation, flow cytometric protocols were established that allow single cell measurements. By applying this methodology decreased histone acetylation levels were shown in differentiated ES cell populations. In contrast, comparable histone acetylation levels were observed in differentiated and undifferentiated BM cells.
In addition, I investigated effects of the histone deacetylase (HDAC) inhibitor trichostatin A (TSA) on murine BM cells, comprising also HSCs. Upon TSA treatment the frequency of cells with *in vitro* and *in vivo* hematopoietic activity was increased, while lineage committed cells underwent apoptosis.
Next, the loss of pluripotency was assessed in differentiating ES cell cultures. Using short-term *in vitro* differentiation protocols marker-based analyses and functional assays were performed. Functionally pluripotency was diminished after 2 days of differentiation as assessed by colony formation, embryoid body (EB) formation and cardiomyogenic differentiation approaches. In contrast, pluripotency marker expression was reduced at later time points. Further, the application of distinct differentiation systems (aggregation EB, clonal EB or monolayer (ML) culture) had an impact on the progression and homogeneity of differentiation cultures. To further study the end of pluripotency, differentiated ES cells were placed under ES cell culture conditions. The data suggest that 3 days differentiated ES cells had passed a point of no return and failed to regain Oct4-eGFP expression and that HDAC inhibitor treatment selectively killed differentiated ES cells.
Finally, I aimed to study the effect of EED - a core subunit of the histone methylating Polycomb repressive complex 2 (PRC2) - on ES cell chromatin and function. ES cells lacking EED showed loss of histone H3 lysine 27 trimethylation (H3K27me3) accompanied by increased histone acetylation and reduced H3K9me3 levels. Despite typical ES cell morphology and pluripotency marker expression, EED knockout (KO) ES cells exhibited altered nuclear heterochromatin organization, delayed chromatin mobility and a failure in proper differentiation. Conclusively, my data provide insights into the epigenetic regulation of stem cells. Particu-

larly, the results suggest that HDAC inhibitor treatment was detrimental for differentiated BM as well as for differentiated ES cells and that ES cells after 3 days of differentiation had lost pluripotency. Further, the data demonstrate that EED KO ES cells self renewed, exhibited morphology and pluripotency marker expression similar to wild type ES cells, but failed to differentiate. This indicates an important role of EED not only for undifferentiated but also for differentiating ES cells.

2 Zusammenfassung

Stammzellen mit ihrer besonderen Fähigkeit sich selbst zu erneuern und zu differenzieren stellen einen faszinierenden Zelltyp für Grundlagenforschung und angewandte Wissenschaften dar. Pluripotente embryonale Stammzellen (ES Zellen), die aus Zellen der inneren Zellmasse von Präimplantationsembryonen etabliert werden, können ekto-, meso- und endodermale Zelltypen sowie Keimzellen hervorbringen. Im Gegensatz dazu sind multipotente adulte Stammzellen in ihrem Entwicklungspotential eingeschränkt, sie differenzieren sich zu allen Zelltypen ihres Gewebes. Zum Beispiel hämatopoetische Stammzellen (HSZs), die sich in Blut-bildenden Geweben wie dem Knochenmark befinden, vermögen sich in alle Blutzellen zu differenzieren. Während der Differenzierung von Stammzellen ändert sich nicht deren Genom, sondern ihre epigenetische Regulation. Durch epigenetische Mechanismen werden Zelltypen mit verschiedensten Phänotypen und Funktionen generiert. Für Stammzelltherapien ist ein tieferes Verständnis des Zusammenhangs von Epigenom und zellulärer Funktion wichtig.
Im Rahmen dieser Dissertation war es mein Ziel, differenzierende Stammzellkulturen auf ihre Genexpression, ihre Chromatinregulation und ihr Differenzierungspotiential hin zu analysieren.
Um Histonmodifikationen, die einen möglichen Mechanismus epigenetischer Regulation darstellen, global untersuchen zu können, sind zunächst, durchflusszytometrische Protokolle etabliert worden, die die Analyse einzelner Zellen ermöglichen sollten. Mit dieser Methode konnten reduzierte Levels von Histonazetylierung in differenzierten ES Zellen gezeigt werden. Im Gegensatz dazu beobachtete ich vergleichbare Levels von Histonazetylierung in unreifen und reifen Knochenmarkzellen.
Zusätzlich untersuchte ich die Wirkung des Histondeazetylase-Inhibitors (HDI) Trichostatin A (TSA) auf Knochenmarkzellkulturen, in denen auch HSZs enhalten sind. Nach Behandlung mit TSA erhöhte sich der Anteil von Zellen mit *in vitro* und *in vivo* hämatopoetischer Aktivität, während vor allem differenzierte Zellen in Apoptose gingen.
Außerdem wurde der Verlust der Pluripotenz in differenzierenden ES Zellkulturen untersucht. Marker-basierte Analysen und funktionelle Tests wurden mit ES Zellen durchgeführt, die kurzfristig *in vitro* differenziert wurden. Es stellte sich heraus, dass nach funktionellen Gesichtspunkten die Pluripotenz bereits nach 2 Tagen Differenzierung deutlich reduziert war, beurteilt anhand der Fähigkeit Kolonien zu bilden, embryoide Körperchen (EK) zu formieren und zu kontrahierenden Herzmuskelzelltypen zu differenzieren. Im Gegensatz dazu verringerte sich die Expression von Pluripotenzmarkern erst zu späteren Zeitpunkten. Ich habe weiterhin beobachten können, dass die Wahl des Differenzierungssystems (Aggregations-EK, klonale EKs oder als adhärente Einzelzellschicht) einen Einfluss auf den Fortschritt und die Homogenität der Differenzierung hatte. Um das Ende der Pluripotenz genauer zu untersuchen, wurden differenzierte ES Zellen zurück in ES Zellkulturbedingungen gebracht. Die Ergebnisse deuten an, dass 3 Tage differenzierte ES Zellen einen Punkt überschritten haben, an dem eine Rückkehr zur Pluripotenz allein durch Kulturbedingungen noch möglich ist. Durch die Behandlung mit HDIs starben selektiv differenzierte ES Zellen.
Des Weiteren war es Ziel dieser Arbeit, den Einfluss von EED - einer essentiellen Unterein-

heit des Histon-methylierenden Polycomb repressive complex 2 (PRC2) - auf das Chromatin und die Funktion von ES Zellen hin zu analysieren. ES Zellen ohne EED wiesen neben dem bereits bekannten Verlust der Trimethylierung von Histon 3 an Lysin 27 (H3K27me3), global reduzierte H3K9me3 Levels sowie erhöhte Histonazetylierung auf. Trotz typischer ES Zell-Morphologie und normaler Expression von Pluripotenzgenen, besaßen EED knockout (KO) ES Zellen eine veränderte Organisation der Heterochromatinstruktur im Zellkern, eine verlangsamte Chromatinmobilität und Probleme bei der Differenzierung.
Zusammenfassend gewähren meine Daten Einblick in die epigenetische Regulation von Stammzellen. Im Besonderen konnte ich zeigen, dass die Behandlung mit HDIs für differenzierende Knochenmarkzellen und differenzierende ES Zellen nachteilig war und zu deren selektivem Zelltod führte. Die hier durchgeführten Analysen ergaben, dass ES Zellen nach 3 Tagen Differenzierung das Ende der Pluripotenz erreicht hatten. Schließlich zeigten die Versuche mit EED KO ES Zellen, dass sie sich zwar selbst erneuerten und morphologisch identisch mit wildtypischen ES Zellen waren, jedoch Defekte bei der Differenzierung besaßen. Dies deutet darauf hin, dass EED nicht nur für undifferenzierte ES Zellen wichtig ist, sondern auch während der Differenzierung von Bedeutung ist.

3 Abbreviations

7AAD	7 amino actinomycin D
ac	acetylation
AFP	alpha fetoprotein
AP	alkaline phosphatase
approx.	approximately
ATRA	all trans retinoic acid
BM	bone marrow
Bry	brachyury
BSA	bovine serum albumine
ChIP	chromatin immunoprecipitation
d	day(s)
DAPI	4',6-diamidino-2-phenylindole
DMEM	Dulbecco's modified eagle medium
DMSO	dimethylsulfoxide
Dnmt	DNA methyltransferase
dNTP	deoxynucleotide triphosphate
dps	day(s) post sort
EB	embryoid body
ECL	enhanced chemiluminescence
EED	embryonic ectoderm development
e.g.	*exempli gratia*, for example
EGF	epidermal growth factor
eGFP	enhanced green fluorescent protein
EpiSC	epiblast stem cell
ES	embryonic stem
et al.	*et alii*, and others
EZH2	enhancer of zeste 2
FACS	fluorescence activated cell sorting
FCS	fetal calf serum
FGF	fibroblast growth factor
FisH	fluorescence *in situ* hybridisation
GSK3	glycogen synthase kinase 3
h	hour(s)
H	histone
HAT	histone acetyltransferase
HD	hanging drop
HDAC	histone deacetylase
HMT	histone methyltransferase
HPC	hematopoietic progenitor cell

HPSC	hematopoietic progenitor and stem cell
HRP	horseradish peroxidase
HSC	hematopoietic stem cell
ICM	inner cell mass (of blastocyst)
i.e.	*id est*, that is
IL	interleukine
IMDM	Iscove's modified Dulbecco's medium
K	lysine
KDM	histone lysine demethylase
KO	knockout
LIF	leukemia inhibitory factor
Lin	lineage
LKS	Lin^-, c-Kit^+, $Sca1^+$
LT	long-term
MACS	magnetic cell separation
MBD	methyl-CpG-binding domain protein
MC	methylcellulose
me	methylation
MEF	mouse embryonic fibroblast
MEK	mitogen-activated protein kinase/ERK kinase
MTG	monothioglycerol
NSC	neural stem cell
PBS	phosphate buffered saline
PRC2	Polycomb repressive complex 2
PWM	Pokeweed mitogen
RT	room temperature
s	second(s)
Sca1	stem cell antigen 1
SCF	stem cell factor
SDS	sodium dodecylsulfate
SDS-PAGE	sodium dodecylsulfate polyacrylamide gel electrophoresis
SSEA1	stage specific embryonic antigen 1
ST	short-term
SUZ12	suppressor of zeste 12
TC	tissue culture
trxG	Trithorax group
TSA	trichostatin A
TSS	transcriptional start site
VPA	valproic acid

4 Introduction

4.1 Stem cells

4.1.1 Characteristics of stem cells

The evolution of multicellular organisms brought about the establishment of hierarchic cellular systems with tightly regulated cell proliferation and differentiation processes [1]. Stem cells constitute the cellular origin of various adult tissues and organisms. Stem cells are functionally defined by their capability to self renew and their potential to differentiate into multiple cell lineages [2, 3]. The fertilized egg of vertebrates, *i.e.* a zygote, is the stem cell with the highest developmental potential. This cell can self renew by giving rise to blastomeres with the same potential. The zygote itself and blastomeres are considered totipotent stem cell types, because they can differentiate into every cell type of an entire multicellular individual [4]. In contrast, pluripotent stem cells can generate all embryonic cell types but they fail to differentiate into extraembryonic tissue like trophectoderm. Pluripotent stem cells are generated in the inner cell mass (ICM) of blastocyst stage embryos. Placed in *in vitro* cultures ICM cells give rise to pluripotent embryonic stem (ES) cell lines that can be stably propagated in culture [5, 6]. Upon injection into blastocysts ES cells take part in normal multicellular development of the embryo. ES cell lines were so far generated from mouse, human and other species [7, 5, 6, 8]. Besides in the embryo, stem cells have crucial functions also in the adult body. Here they are the origin of tissue regeneration and cellular homeostasis, as they generate offspring that can replace aged and injured cells [9, 10, 11, 12, 13]. Adult stem cells are multi- or unipotent, *i.e.* they generate differentiated cells of their stem cell system. They reside in specialized niches within the organ or tissue that they can reconstitute [14, 15]. For instance, adult neurogenesis is achieved by a small population of neural stem cells (NSCs) which are located in the subventricular zone of the lateral ventricle [16]. Similarly, hematopoietic stem cells (HSCs) reside in trabecular structures of the bone marrow (BM) [17]. While ES cells exhibit high proliferation rates, adult stem cells often persist in a quiescent state and therefore rarely divide [18].
Stem cells are of particular interest for basic and applied research. For example, stem cell model systems can serve to address fundamental epigenetic questions, as upon differentiation of stem cells not the genetic information but rather the chromatin is modified [19]. ES cells are utilized in studies that aim to model *in vitro* embryogenesis and test for embryotoxic substances [20, 21]. Finally, stem cells are in the focus of therapeutic approaches to cure or replace aged and injured tissues or organs. In the future, pluripotent ES cells with their broad differentiation potential could be used for guided differentiation towards specific directions as in the context of tissue replacement.

4.1.2 Embryonic stem cells: pluripotency, differentiation and reprogramming

ES cells are *in vitro* derivatives of ICM cells of blastocyst-stage embryos [6]. Like ICM cells ES cells are pluripotent and can differentiate into all ecto-, endo- and mesoderm cell lineages

including germ cells. Murine ES cells can be maintained *in vitro* in an undifferentiated, self renewing state [6]. Typically ES cells grow as packed colonies on a layer of mouse embryonic fibroblasts (MEFs) in media supplemented with leukemia inhibitory factor (LIF). LIF binds to gp130 / LIF receptor and activates STAT3 via the JAK/STAT signaling pathway [22]. Subsequently, expression of factors like Nanog, Klf4 and c-myc is induced by STAT3, thereby promoting the undifferentiated state [23, 24, 25]. ES cells exhibit a highly regulated molecular network of transcription factors that enables the maintenance of the groundstate of pluripotency [26]. Oct4, Sox2 and Nanog represent core pluripotency transcription factors which act in concert on downstream targets and on an autoregulatory base [27]. The homeodomain transcription factor Oct4 belongs to the POU family of transcription factors. Oct4 is expressed in totipotent cells and subsequently in the ICM of blastocysts but not in the trophectoderm, where it is repressed by Cdx2 [28, 29]. Apart from ES cells, epiblast stem cells and germ cells also express Oct4. In ES cells Oct4 protein levels are kept within a defined range, as too low levels cause the loss of pluripotency and stimulate differentiation into trophectoderm [30]. On the other hand, high levels induce ES cell differentiation into endo- and mesodermal directions [30]. Oct4 and Sox2 proteins form heterodimers which can bind their own promoters in order to sustain Oct4 and Sox2 gene expression.
In vivo the epiblast of a preimplantation blastocyst develops into primed epiblast cells upon nidation. While ES cells are established from preimplantation blastocysts, epiblast stem cells (EpiSCs) can be derived from primed epiblast cells and propagated *in vitro* [31] (Scheme 4.1). Recently, it became obvious that murine ES cell cultures are not homogenous but rather heterogenous. For example gene expression analyses of single ES cells revealed that expression levels of pluripotency factors like Rex1, Nanog, SSEA1 or Stella vary to a great extent and are fluctuating [32, 33, 34, 35, 36]. It is hypothesized that cells with lower levels of these factors are similar to EpiSCs (*i.e.* they are epiblast-like cells), but that this cell population can occasionally revert to groundstate of pluripotency under standard ES cell conditions. It was further reported that a serum-free culture medium supplemented with inhibitors of glycogen synthase kinase 3 (GSK3) and mitogen-activated protein kinase/ERK kinase (MEK) allows the maintenance of ES cells as a homogenous population without fluctuation towards epiblast-like cells [37]. GSK3 and MEK inhibitors block signal pathways that are active in lineage committing ES cells. Under these groundstate conditions ES cells are not dependent on external stimuli like LIF and do not differentiate. Recent studies also demonstrate the conversion of EpiSCs to ES cells by appropriate culture conditions in the presence of LIF or small molecules [38, 39].
The question of whether cells are pluripotent can be assessed on different levels of stringency. While the expression of pluripotency markers gives first hints about a cell's developmental potential, functional parameters are more reliable. A more stringent test is the assessment of ES cell growth and multilineage differentiation potential *in vitro*. Pluripotent ES cells form typical colonies when self renewing and generate embryoid bodies (EBs) upon withdrawal of LIF or GSK3/MEK inhibitors. Upon differentiation induction ES cells spontaneously and undirectedly start to express molecular programs of differentiated cells. *In vivo* upon subcutaneous injection, ES cells form teratomas that are constituted of differentiated cells of the three germ layers [40]. The formation of germline-competent chimeras after injection of ES cells into blastocysts represents the most stringent test for pluripotency [41]. By using tetraploid blastocysts, which can only form extraembryonic tissue but fail to develop into the embryoblast, injected truly pluripotent ES cells give rise to the entire embryo [42].
The remarkable *in vitro* differentiation potential of ES cells makes them an interesting cell

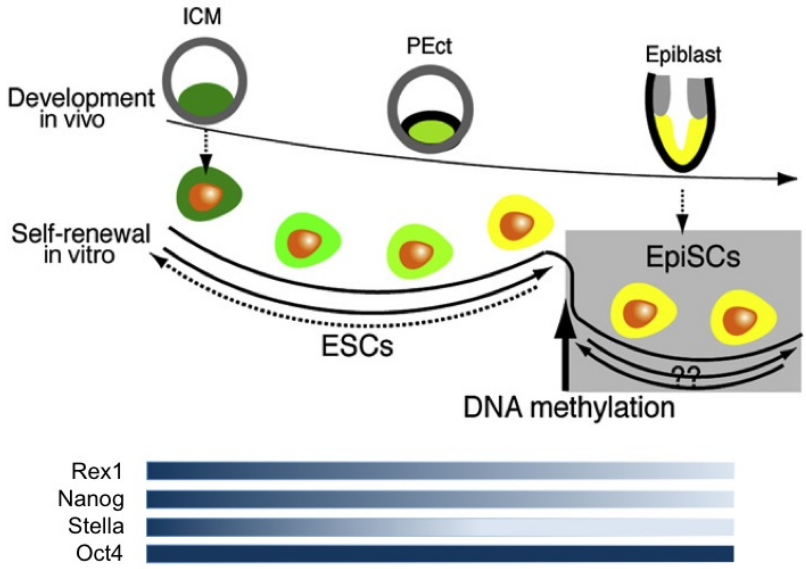

Scheme 4.1: **Embryonic and epiblast stem cells.**
Embryonic stem (ES) cells are derived from the inner cell mass (ICM) of early blastocyst stage embryos. Epiblast stem cells (EpiSCs) are established for *in vitro* culture from postimplantation blastocysts. ES cells like EpiSCs express similar levels of the pluripotency marker Oct4 and can differentiate to cells of all 3 germ layers. They differ in expression levels of several genes like Rex1, Nanog or Stella. Female EpiSCs exhibit an inactivated X chromosome with methylated DNA. Cultures of ES cells where found to be heterogeneous because cells undergo interconvertible fluctuations between cellular identities similar to ES cells and others similar to EpiSCs (epiblast-like cells). (modified from Hayashi *et al.* [36])

type for tissue replacement approaches. With the establishment of human ES cells approx. 10 years ago ES cell-based cell replacement strategies came within closer reach [8]. In October 2010 Geron Corporation initiated a first clinical trial of human ES cell-based therapy [43]. ES cells were so far successfully differentiated towards many clinically relevant cell types including cardiomyocytes, dopaminergic neurons and pancreatic beta-cells [44, 45, 46, 45]. However, potential remnants of undifferentiated ES cells within differentiated cell populations display a considerable risk of teratoma-tumor formation upon transplantation [47, 45]. Therefore, it is essential to define safety criteria and standardized differentiation protocols before clinical application.
Usually, upon *in vitro* differentiation murine ES cells form EBs that represent aggregates of differentiating ES cells [48, 49]. For that a defined number of differentiating ES cells is clustered to one EB by gravity in hanging drops (HDs) of differentiation medium. For differentiation of ES cells towards hematopoietic cell types it was reported that the formation of EBs in semisolid medium yielded higher hematopoietic differentiation outcomes than the formation of EBs by ES cell aggregation [50]. For this purpose, individual EBs emerge from single differentiating ES cells in a methylcellulose (MC)-based medium that prevents random clustering. Alternatively, ES cells can also be differentiated as adherently growing monolayer (ML) cells in the absence of LIF [51]. To a certain extent the ongoing differentiation within EBs mimics embryonic development, but different cell lineages stochastically appear during *in vitro* ES cell differentiation. To further direct differentiation towards defined cell types, cell type-specific selection methods and/or cell type-specific growth conditions must be applied

[44].
The studies on pluripotency not only involve differentiation strategies, but also include the analyses of mechanisms that lead to reprogramming of differentiated cells towards cell types with higher developmental potential. So far different methods of reprogramming of somatic towards pluripotent cells were successfully developed [52]: somatic cell nuclei are reprogrammed upon transfer into enucleated oocytes (somatic cell nuclear transfer [SCNT]), somatic cells are reprogrammed upon fusion to ES cells or by ectopic expression of Oct4, Sox2 and Klf4 (induced pluripotent stem [iPS] cells). In all 3 approaches it is most probably the activity of pluripotency factors (either in the oocyte-plasm, in the ES cell-plasm or directly by the expression of pluripotency factors) which induces reprogramming. Especially the identification of the 'magic cocktail' using Oct4, Sox2, Klf4 (and c-myc) transgenes by Takahashi and Yamanaka set a milestone in rational pluripotency and reprogramming research [53]. The directed reprogramming approach with defined factors allows deeper molecular analyses helping to better understand regulation of pluripotency. Until now iPS cells could successfully be generated from many species including human [54]. They are hardly distinguishable from normal ES cells, even though recent reports raise the issue of an epigenetic memory and incomplete reprogramming dependent on the somatic tissue of origin [55, 56].

4.1.3 Hematopoietic stem cells

Hematopoietic stem cells (HSCs) are multipotent adult stem cell types that can differentiate into all hemato-/lymphoid blood cell lineages [57, 58]. In small numbers they reside in the bone marrow (BM) where they undergo either symmetric or asymmetric cell division to give rise to either two daughter HSCs, two hematopoietic progenitor cells (HPCs) or to one HSC and one HPC [59]. In the BM niches HSCs underly extrinsic and intrinsic signals that regulate their self renewal, differentiation and migration [60]. The hematopoietic system is characterized by a hierarchic structure [61] (Scheme 4.2). HSCs at the top of the hierarchy combine a high self renewal potential with a low cell division rate. They are referred to as long-term repopulating (LT) HSCs. Short-term (ST) HSCs exhibit equal unrestricted differentiation capacity, but their pool is depleted earlier as they show limited self renewal potential. ST-HSCs can differentiate into multipotent progenitors (MPPs) which likewise have the capability to form all types of blood cells but their self renewal potential is further restricted. MPPs display a rapidly dividing cell population and their derivatives are either common lymphoid or common myeloid progenitors (CLPs, CMPs) [61]. Hematopoietic progenitor and stem cells (HPSCs) can be isolated from the BM or after mobilization from the peripheral blood. Their purification is based on the presence or absence of specific surface marker proteins that are characteristic for LT-/ST-HSCs. For instance, murine LT-HSCs are defined by the following marker status: $CD34^-$, $Sca1^+$, $Thy1.1^+$, $c\text{-}Kit^+$, Lin^-, $Flk2^-$ [62]. Sca1 represents stem cell antigen 1, c-Kit is the receptor for the stem cell factor (SCF) and lineage (Lin) markers are proteins expressed on the surface of committed cells (including lymphocytes [CD4, CD8, B220], macrophages [Mac1], granulocytes [Gr1] and erythrocytes [Ter119]). BM cells with the marker signature Lin^-, $c\text{-}Kit^+$ and $Sca1^+$ (short: LKS cells) comprise LT-HSCs, ST-HSCs but also MPPs [62]. On the basis of their individual marker expression profiles HSCs and HPSCs can be purified by fluorescence activated cell sorting (FACS). For experimental transplantation in the mouse model but also in human settings HPSCs can be given intravenously, whereupon the cells re-invade into BM niches of the recipient by a process named

homing [63, 64]. Today, HSCs are used in multiple clinical settings as therapeutics [65]. The hematopoietic system constitutes the best and longest studied stem cell system.
In contrast to various embryonic and adult stem cell types, efficient *ex vivo* expansion of HSCs remains challenging, despite the enormous efforts that were undertaken over the past decades [66]. Previously it was reported that ectopic expression of the homeotic transcription factor HoxB4 leads to expansion of HSCs *ex vivo* [67]. Later it could be shown that purified HSCs of human umbilical cord blood origin can be expanded by treatment with the nucleoside analog 5-aza-2'-deoxycytidine (5azaD) and trichostatin A (TSA), an inhibitor of histone deacetylases (HDAC), respectively [68, 69]. During the last years the design of artificial HSC niches using biopolymer matrices also led to a limited expansion of HSCs [70, 71]. Very recently, a small molecule screen by Boitano *et al.* identified an aryl hydrocarbon receptor antagonist, StemRegenin1, that supports robust *ex vivo* HSC expansion [72].

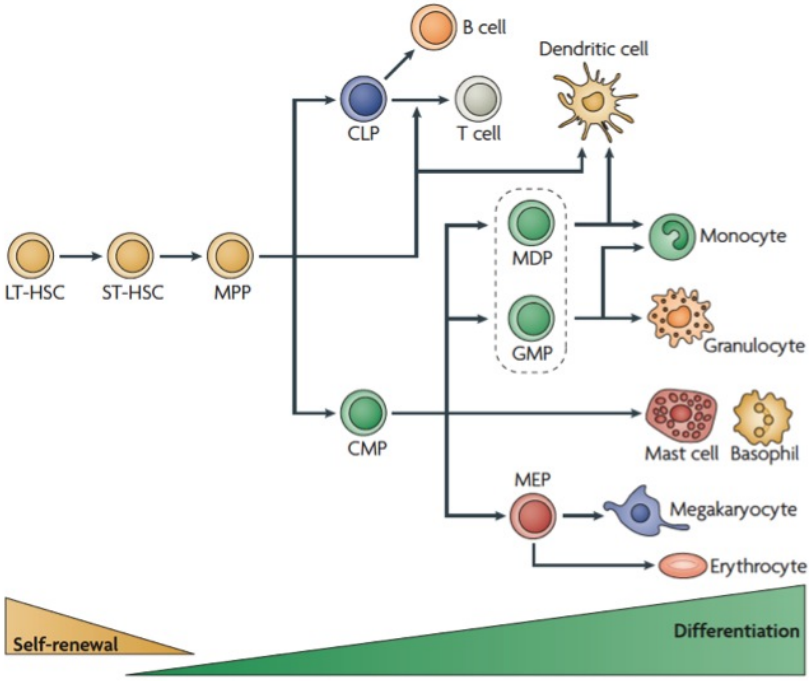

Scheme 4.2: **Hematopoietic stem cell systemt.**
Multipotent hematopoietic stem cells (HSCs) have the potential to self renew and to differentiate into all hemato-/ lymphoid cell lineages. Self renewal capacity is highest in long-term (LT) HSCs which can long-term and multilineage reconstitute irradiated recipients. Short-term (ST) HSCs have a limited self renewal potential, while multipotent progenitors (MPP) can not self renew but have full differentiation capability. Common lymphoid and myeloid progenitors (CLP, CMP) represent first committed cell types and give rise to all blood lineages including erythrocytes, lymphocytes, granulocytes, megakaryo-/thrombocytes and macrophages. (modified from Rosenbauer *et al.* [61])

4.2 Epigenetics

4.2.1 Epigenetic mechanisms

Cells store genetic information in the base sequence of their genomic DNA. Upon mitosis this information is propagated through the equal distribution of duplicated DNA to the 2 daughter cells. With the emergence of multicellular organisms and the specialization of distinct tissues, cells with identical genomes but different cellular functions developed. Though the information of approx. 20,000 genes is present in all cells of the body, individual gene activity strongly depends on the respective cell type. Thus, cells develop cell type-specific chromatin that enables the activation of some genes and the inhibition of others. Epigenetics is the study of inherited changes in phenotype or gene expression caused by mechanisms other than changes in the underlying DNA sequence. These changes remain through cell divisions [73].
Stem cells represent a powerful tool for the investigation of epigenetic mechanisms. During self renewal epigenetic information must be preserved and propagated whereas upon differentiation epigenetic properties change [74]. Deeper insights into epigenetics are needed to better understand the molecular regulation of stem cells.
Mechanisms that result in different gene activity comprise chemical modification of DNA and histones, functionally versatile non-coding RNAs, transcription factors and chromatin compaction. Also transcription factors that activate cell type-specific gene expression programs function on an epigenetic level [75]. Enzymes with the activity to methylate DNA at CpG sites are called DNA methyltransferases (Dnmt) [76]. The methylation of DNA is generally accompanied by the inactivation of genes. The silencing of genes via DNA methylation is believed to be stable and persistent, however, in recent years different DNA demethylating mechanisms were uncovered. These include the direct removal of methyl residues via demethylating enzymes or alternative pathways that utilize DNA repair enzymes [77]. Methylated DNA serves as a binding site for methyl-CpG-binding domain proteins (MBD) that can recruit other chromatin modifying proteins and complexes. Generally these complexes further mediate gene silencing.
Histones are proteins that function in the ordered package of DNA into structural units [78]. Two molecules of histone H3 and H4 form together with H2A and H2B the octamer spool around which 146 bp of DNA are wound. This structure is named nucleosome. N-terminal histone tails of core histones are reversibly and covalently modified by acetylation, methylation, ubiquitination, phosphorylation, SUMOylation, citrullination or ADP-ribosylation. These modifications are either directly involved in the activation of gene expression (*e.g.* histone acetylation) or they function as recognition sites for protein complexes. By recruitment of defined multifactorial protein complexes the expression or silencing of corresponding genes is modulated. The genome-wide pattern of histone modifications in a particular cell type is referred to as histone code, which is hypothesized to contain epigenetic information like the base pair code of DNA contains genetic information [79]. However, the histone code is not universal as different histone modifications can be recognized by more than one protein complex and hence, the subsequent effects can be of different nature [80]. In recent decades mechanisms of histone acetylation and methylation were extensively studied. While the existence of enzymes that add acetyl-groups (histone acetyl transferases, HAT) or remove them (histone deacetylases, HDAC) is well established, the discovery of histone lysine demethylases (KDM) besides well-known histone methyltransferases (HMT) was a recent event [81, 82, 83]. Lysine residues of histones H3 and H4 can be mono-, di- or trimethylated. The quantity

and position of lysine methylation plays an important role in whether the modifications are associated with transcriptional activation or repression. For example, the trimethylation of histone H3 at lysine (K) residue 4 (H3K4me3) is generally present at transcriptionally active loci whereas H3K27me3 is associated with repressed genes.
Further epigenetic mechanisms comprise non-coding RNAs [84]. They can function as microRNAs to either degrade transcripts or inhibit translation of target mRNA. Also it was reported that non-coding RNA molecules can bind to genomic DNA and thereby recruit protein complexes that recognize non-coding RNA like an adaptor.
Generally chromatin within mammalian nuclei is composed of transcriptionally active euchromatin and transcriptionally inactive heterochromatin [85]. In heterochromatin nucleosomes are densely assembled with a high degree of compaction, thus leading to inaccessible DNA and silenced genes. In contrast, euchromatin is characterized by rather loosely packed nucleosomes that are accessible to the transcriptional machinery. DNA methylation and hypoacetylated histones are enriched in heterochromatin, whereas unmethylated DNA and hyperacetylated histones are present in euchromatin. The movement of nucleosomes along DNA which results in compaction or decondensation is achieved by ATP-dependent nucleosome remodeling complexes. These complexes push nucleosomes like beads on a string and thereby regulate eu-/heterochromatin and gene activity epigenetically [86].

4.2.2 Histone acetylation and HDAC inhibition

Histone acetylation represents one mechanism of epigenetic regulation by which gene activity can be modulated. Two principle mechanisms are operating [87]: firstly, the acetylation of histone lysine residues weakens the electrostatic affinity of the negatively charged DNA and the positively charged histones. Therefore, chromatin structure becomes loosened and DNA is more accessible for transcription factors and RNA polymerases. Secondly, acetylated lysine residues serve as recognition sites for bromodomain protein complexes. In this case it is decisive which position the acetylated lysine residue has and which type of histone is involved. The sites of acetylation include at least four highly conserved lysine residues of histone H4 (K5, K8, K12 and K16), five of histone H3 (K9, K14, K18, K23 and K27), as well as less conserved sites in histones H2A and H2B [88]. The catalytic reaction of acetylation is performed by HAT enzymes that transfer an acetyl group from acetyl CoA resulting in ε-N-acetyl lysine. The deacetylation of histones is accomplished by HDAC enzymes. So far, 11 members of the HDAC family have been identified. They are subdivided into 4 classes: class I comprises HDAC 1, 2, 3, 8, class II contains HDAC 4, 5, 6, 7, 9, 10, class III includes the sirtuins and class IV is represented by HDAC 11 [89]. Acetylation of histones is balanced in an equilibrium by the 2 opposing enzymatic activities. Recent data suggest that HDACs and HATs are simultaneously present at regulatory sites of active genes allowing fast and flexible modulation of gene expression [90].
The activity of HDACs can be reduced by treatment with HDAC inhibitors, thereby indirectly inducing histone hyperacetylation [91]. Classical HDAC inhibitors affect class I and II HDACs by interacting with their catalytic domains. One of these inhibitors is the Streptomyces metabolite TSA, a hydroxamic acid [92]. Also aliphatic acid compounds such as valproic acid (VPA) inhibit HDACs. Beneficial effects in clinical application of HDAC inhibitors were determined rather empirically. VPA is in use as anti-epileptic drug since long time and it is currently under investigation for several cancer treatment approaches including leukemia [93, 94]. TSA is under clinical test as anti-inflammatory agent [95]. Whether the

therapeutic efficacy of these compounds is based on the resulting histone hyperacetylation remains however questionable. As different HDAC inhibitors exert distinct disease-specific effects, it is possible that drug-specific (side) effects other than HDAC inhibition are responsible for the entire spectrum of HDAC effects. Further, HDACs were also shown to affect deacetylation of non-histone proteins such as tubulin [96, 97]. Thus, HDAC inhibition potentially affects multiple biological processes besides chromatin regulation. To date reports on TSA describe various effects on different cell types: exposure of leukemic U937 cells to TSA results in growth inhibition and induction of apoptosis [98]; TSA treatment of fetal brain-derived NSCs increases neuronal and decreases astrocyte differentiation [99]; addition of TSA to MEFs transduced with reprogramming genes enhances iPS cell-generation [100]; together with the Dnmt inhibitor 5azaD TSA leads to net expansion of $CD34^+$ human cord blood cells [69, 68].

4.2.3 Epigenetics of pluripotent cells

The remarkable differentiation potential of pluripotent cells is mirrored in their chromatin organization. Especially hyperdynamic chromatin plasticity and bivalently regulated genes in ES cells represent exceptional and pluripotency-associated features.

Hyperdynamic chromatin

Several discoveries within the last decade shed light on a highly flexible and permissive state of chromatin in ES cells [101]. Flexibility of gene expression is a hallmark feature of ES cells which can only be achieved if respective genes are not permanently silenced. An open and unrestricted chromatin architecture is therefore a fundamental prerequisite for this state.
Electron microscopy of ES cell nuclei revealed that their chromatin is homogeneous, decondensed and rich in euchromatin. In contrast, differentiated nuclei exhibit frequent, distinct heterochromatin domains [102, 103]. While heterochromatin domains in ES cells are rather diffuse, upon differentiation to NSCs they become more defined with distinct boundaries [104]. Euchromatin is generally associated with a transcriptional activity of genes, and indeed global transcription levels are elevated in ES cells as compared to differentiated cells [102]. The dynamics, *i.e.* the molecular exchange rates, of chromatin proteins are higher in ES cells than in differentiated progeny [104, 105]. By fluorescence recovery after photobleaching (FRAP) analyses of GFP-tagged proteins like heterochromatin protein 1 (HP1), histone H1 or core histones, fast and highly mobile chromatin fractions were discovered in pluripotent cells [104]. Global levels of histone modifications which are accompanied by gene activity are higher in ES cells than in differentiated cells. Histone modifications such as H3K9ac but also H3K14ac, H3K4me3 and H3K36me3 are prevalent in undifferentiated ES cells [104, 106, 102, 107, 108, 109]. In contrast, levels of repressive histone modifications, like H3K9 methylation or HP1, become globally elevated upon differentiation [104, 102, 106, 109, 110, 111].
High chromatin dynamics and large euchromatin proportions are most probably the result of ATP-dependent chromatin remodeling complexes [112]. These enzymes are responsible for the generation of an accessible DNA configuration and for opening chromatin structures. These enzymes are highly abundant in undifferentiated ES cells and comprise BAF250B, Bptf, BAF155 and Chd1 [102, 113, 114, 115, 116, 117, 118].
Thus, the chromatin of pluripotent ES cells is characterized by an overall and high accessibil-

ity and transcriptional hyperactivity, thereby preventing permanent silencing of genes which are associated with cell lineage commitment. However, to avoid uncontrolled expression of genes that are not required at the groundstate of pluripotency, cells must interpose flexible repressive regulatory mechanisms. One example for this are bivalently controlled chromatin domains.

Bivalent chromatin domains

Bivalent chromatin domains are characterized by the simultaneous presence of repressive H3K27me3 and activating H3K4me3 marks at regulatory sites of genes which are involved in lineage commitment, differentiation and tissue development [119, 120] (Scheme 4.3). As the repressive H3K27me3 modification appears dominant over H3K4me3, bivalent genes are expressed at only low levels in pluripotent ES cells. However, upon differentiation respective genes can either be immediately activated by removing the H3K27me3 modification via specific KDMs or expression can stably be repressed by demethylation of H3K4. This mechanism, which leads to a flexible epigenetic control of gene expression programs upon external or internal stimuli, is not only a feature of pluripotent but also of multipotent HPSCs [121, 122, 123]. The activating methylation of H3K4 is catalyzed by Trithorax group (trxG) proteins that comprise 8 different enzymes, *e.g.* MLL1, MLL2, SET1A and ASH1 [83]. At least 6 different proteins were identified as H3K4-specific KDMs (like LSD1 or JARID1A). Methylation of H3K27 is accomplished by EZH2 or its homolog EZH1 which are the core subunits of the Polycomb repressive complex 2 (PRC2) [125]. Two demethylating enzymes, KDM6A (UTX) and KDM6B (JMJD3), were described for lysine 27 [83].
For the efficient repression of bivalent genes upon lineage commitment different mechanisms are discussed. While in ICM and in ES cells genes are silenced by H3K27me3 and subsequent recruitment of PRC1 and RING1B-mediated H2A ubiquitination, in extraembryonic lineages genes are repressed via recruitment of Suv39H1 to H3K27me3, leading to subsequent H3K9 and DNA methylation [126, 127].

Polycomb repressive complex 2

The PRC2 consists of 3 core subunits: EZH1/2 (enhancer of zeste), EED (embyonic ectoderm development) and SUZ12 (suppressor of zeste) [128] (Scheme 4.4). The homologs EZH1 and EZH2 represent the executing H3K27 HMT enzymes, the two can substitute for each other [125]. EED exists in 4 different isoforms that are the result of different translational start sites in the EED mRNA [129]. Stability of the PRC2 is dependent on the presence of all 3 subunits. Knockout (KO) ES cell lines of EZH2, SUZ12 and EED were successfully generated [125, 130, 131]. Interestingly, only EED KO or EZH2 KO combined with EZH1 RNAi-mediated knockdown (KD) leads to loss of H3K27 mono-, di- and trimethylation. EZH2 KO and SUZ12 KO reduce di- and trimethylation while H3K27me1 remains unaffected.
Neither EZH2 nor EED or SUZ12 can directly bind to target DNA motifs. Currently different models for the interaction of PRC2 with its target regions are discussed. It was described that EED binds with its WD40 domains to unmodified histone H3 but also specifically to H3K27me3 and H3K9me3 modified histones [132, 133, 134]. The interaction with H3K27me3 was shown to enhance the enzymatic activity of EZH2 allosterically, thus promoting H3K27 methylation. Thereby the repressive modification is transmitted to new histones during DNA replication and epigenetic heritability is achieved. Recently the interplay between non-coding

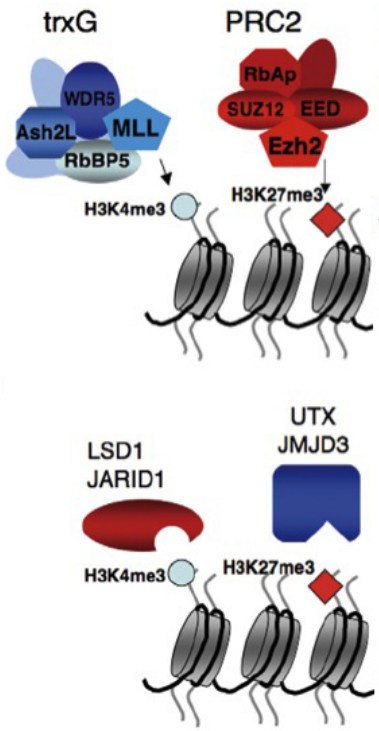

Scheme 4.3: **Regulation of bivalent chromatin domains in ES cells.**
Bivalently regulated chromatin domains simultaneously carry histone marks associated with gene activation (H3K4me3) and repression (H3K27me3). Bivalently regulated genes are repressed or expressed at only low levels in ES cells. They are related to development and differentiation. Bivalent genes are poised for future expression by the presence of activiating H3K4me3 marks. While Trithorax group proteins (trxG)) catalyze H3K4 methylation and Polycomb repressive complex 2 (PRC2) perform H3K27 methylation, specific lysine demethlyases (KDMs) remove respective methylation marks. Therefore, bivalent genes become stably repressed by H3K4 demethylation via LSD1 or JARID1 and expression of bivalent genes is mediated by the removal of H3K27 trimethylation by UTX or JMJD3. (modified from Pietersen *et al.* [124])

RNAs and PRC2 was discovered as a mechanism for gene targeting [135, 136]. It was shown that non-coding RNAs polymerized from PRC2-repressed genes serve as connector between genomic sites and SUZ12.
Besides the core subunits of PRC2 further proteins were identified to be assembled into the multifactorial PRC2 complex, *e.g.* Dnmt, Suv39h1, HDACs and Jarid2 [137, 138, 139, 140, 141, 142]. Notably, the presence of Jarid2 in the PRC2 was suggested to guide the complex to its target sites, as Jarid2 contains a DNA binding domain. Further, Jarid2 most probably interacts via SUZ12 and Jarid2 was found to be co-localized with PRC2 and its respective histone modification in ES cells [143, 144, 145, 146].
The PRC2 complex plays an important role in the establishment and maintenance of the distinct ES cell chromatin, as the H3K27me3 histone mark has essential gene regulatory functions, particularly the repression of development-associated genes. Thus, it is not surprising that in ES cells the expression of EED is directly regulated by Oct4. As a direct consequence EED expression is decreased during differentiation [147]. Furthermore, EED is necessary for successful reprogramming of somatic B lymphocytes upon fusion with ES cells [148]. ES cells lacking EED are unable to perform fusion-based reprogramming of B lymphocytes even if simultaneously merged to another wild type ES cell, indicating an inhibitory

effect of EED^{negative} nucleo- or cytoplasm on reprogramming.
In vivo EED KO embryos die during mid gestation (E10.5) [149]. Similarly chimeric embryos derived from the injection of EED KO ES cells into blastocysts die at comparable developmental stages [150]. Despite elevated transcription levels of PRC2 target genes in EED KO ES cells, the expression of pluripotency-associated genes remains unperturbed, and differentiation - at least to a certain extent, including cell types of the 3 germ layers - is possible. However, an additional deletion of the PRC1 member RING1B in EED KO ES cells results in completely abrogated differentiation [151]. PRC1 and PRC2 act redundantly to repress development-associated genes in ES cells. Thus, the derepression of all of these genes blocks ES cell differentiation.
The PRC2 complex and its members were also shown to exhibit non-chromatin, cytosolic functions. EZH2 is involved in actin polymerization and EED is linked to TNF receptor signaling [152, 153]. In addition, PRC2, particularly EZH2, is linked to several cancers and supposed to be responsible for epimutations [154].
Thus, a better understanding of chromatin regulation by PRC2 will shed light on elementary developmental processes but also on disease-related mechanisms.

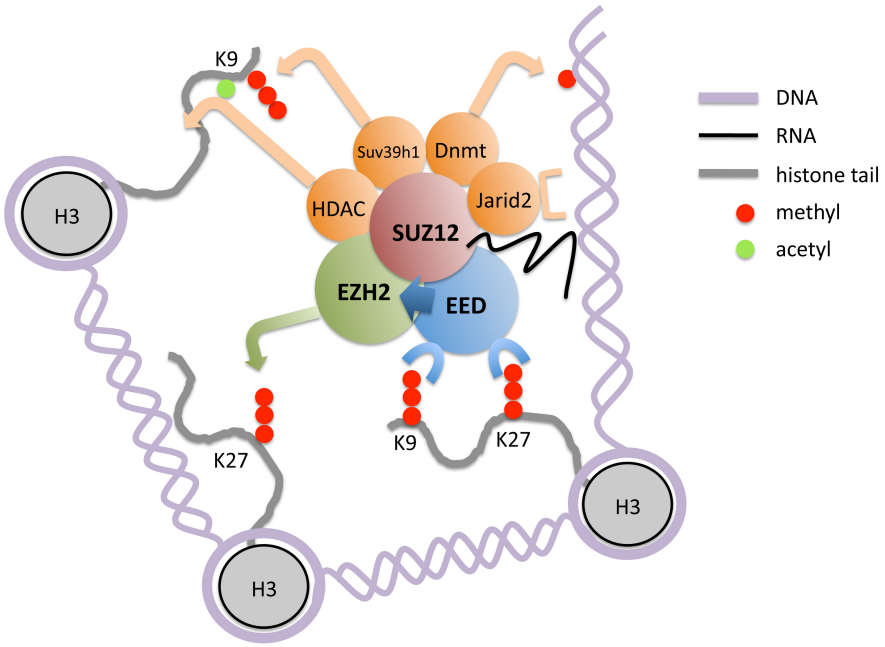

Scheme 4.4: **Polycomb repressive complex 2.**
The Polycomb repressive complex 2 (PRC2) is composed of the core subunits SUZ12, EED and EZH2. Additional proteins found to be assembled with PRC2 are histone deacetylases (HDACs), the H3K9 histone methyltransferase (HMT) Suv39h1, DNA methyltransferases (Dnmts) and Jarid2. EED can directly bind to H3K9me3 and H3K27me3. Binding to H3K27me3 leads to allosterical activation of the H3K27 HMT activity of EZH2. Genomic targeting of PRC2 is assumed to be mediated via either direct DNA interaction of Jarid2 which binds to SUZ12 or via non-coding RNAs that recruit SUZ12 to target loci. Histone octamers are displayed as grey spheres, only one copy of histone H3 and its N-terminus is exemplarily denoted per octamer.

4.3 Scientific aims of this thesis

Our current knowledge about the molecular regulation of adult and embryonic stem cells points to important roles of epigenetic mechanisms. In the scope of this thesis I aimed to analyze cultures of differentiating hematopoietic and embryonic stem cells with respect to gene expression, chromatin structure and stem cell function. The first part of the work focuses on the analysis of HDAC inhibitor effects on cell death, differentiation and HPSC activity in *ex vivo* murine BM cell cultures. The second part comprises studies on the early *in vitro* differentiation progression of mouse ES cells. It includes analyses on the influence of differentiation protocols on the loss of pluripotency. Further, I address the question of whether short-term differentiated ES cells can revert to pluripotency by re-addition of LIF in the presence or absence of HDAC inhibitor treatment. The final part of this thesis deals with the functional and chromatin-associated exploration of ES cells that lack the PRC2 core member EED. A detailed understanding of stem cell regulation on the molecular level is essential for deeper insights into normal and diseased stem cells functions.

5 Results

5.1 Establishing chromatin flow cytometric protocols

Analyses of defined cells, such as rare stem cells, within heterogeneous cell populations concerning chromatin modifications is technically challenging. As flow cytometry allows the analysis of subpopulations, because it measures on the single cell level, I aimed to establish protocols by which global levels of histone modifications can be determined for individual cells and for marked subpopulations.

5.1.1 Detection of nuclear antigens

In order to have access to the desired antigens within the chromatin inside the nucleus, different fixation and permeabilization approaches with variations in their harshness were tested. In total, 3 different methods were applied: fixation in 4% formaldehyde and permeabilization by saponin-supplemented buffers, fixation and permeabilization in ice-cold alcohol or fixation and permeabilization by formamide and heat. It turned out that different antibodies require different fixation strategies for successful staining. Two protocols were sufficient to cover all antibodies used. In summary, all antibodies and the corresponding protocols are listed in Table 5.1. For intranuclear staining cells were fixed and permeabilized prior to incubation with primary and secondary antibodies. In order to test for unspecific signals produced by background staining, cells were subjected to flow cytometric analysis with or without fixation as well as with or without primary antibody incubation. Figure 5.1 A shows that only fixed and permeable cells which were incubated with primary and secondary antibodies exhibited increased fluorescence signals over negative control levels. This indicates that the primary antibody recognizes intracellular antigens only and that the secondary antibody had neither inside nor outside the cell unspecific affinities.

Table 5.1: Antibodies used for chromatin flow cytometry.

Specificity	Species, isotype	Company	Order number	Antibody per 100 μl staining solution [ng]	Protocol
H3	rabbit, polyclonal	Abcam	ab1791	600	A, B
H3K4me3	rabbit, polyclonal	Abcam	ab8580	500	A, B
H3K27me3	mouse, IgG3k	Abcam	ab6002	1,000	B
H3K27me3	rabbit, polyclonal	Diagenode	CS-069-100	250	A, B
H3K9me2	mouse, IgG2ak	Abcam	ab1220	250	A, B
H3K9ac	rabbit, polyclonal	Abcam	ab10812	100	A, B
H3K9/14ac (pan-acH3)	rabbit, polyclonal	Upstate	06-599	500	A
H4	rabbit, polyclonal	Upstate	07-108	1,000	A, B
H4K8ac	rabbit, polyclonal	Upstate	06-760	250	A, B
H412ac	rabbit, polyclonal	Upstate	06-761	250	A, B
H416ac	rabbit, polyclonal	Upstate	06-762	250	A, B
H4K5/8/12/16ac (pan-acH4)	rabbit, polyclonal	Upstate	06-598	250	A, B
Isotype control	rabbit, polyclonal	Dianova	rabpolypureisotc	250	A, B

To further prove that the fluorescence signals were indeed located inside the nucleus, cytospin samples of chromatin flow cytometrically stained cells were prepared, DNA was counterstained with Hoechst 33258 and the subcellular distribution of staining signals was examined. As displayed in Figure 5.1 B signals of immunofluorescently stained histone modifications were exclusively located inside the nuclei.

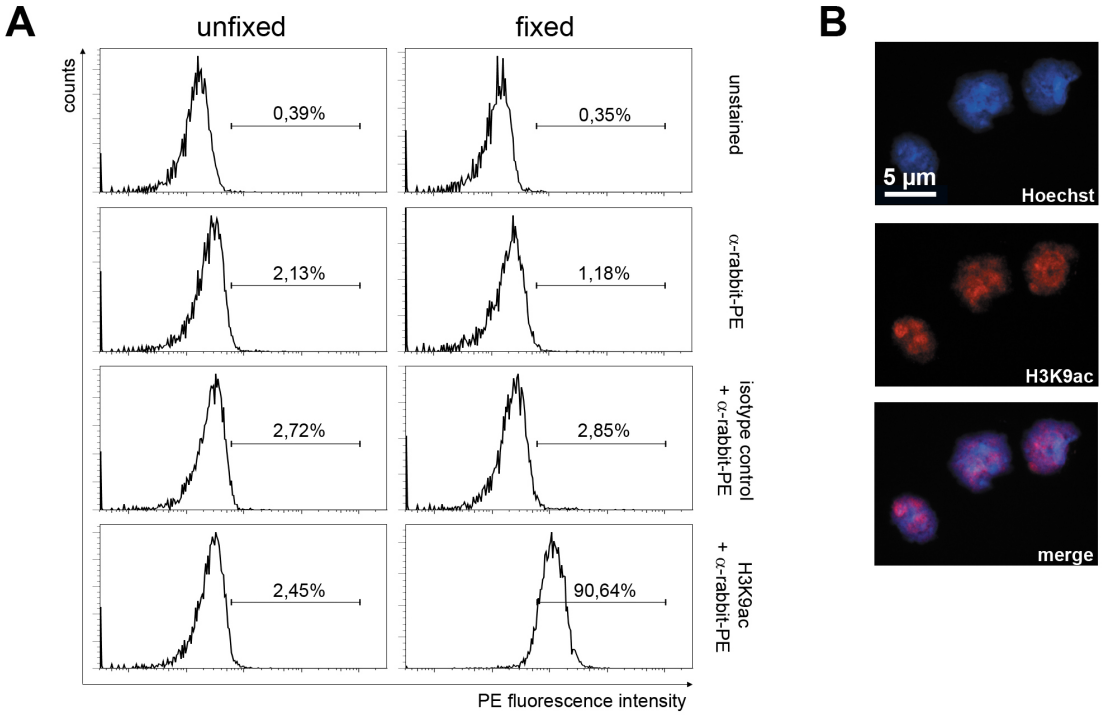

Figure 5.1: **Chromatin flow cytometry detects nuclear antigens in ES cells.** A) Analysis of ES cells with secondary, isotype control or anti-H3K9ac antibodies. Primary antibodies were detected by anti-rabbit secondary antibodies (phycoerythrin, PE). ES cells were incubated without fixation in FACS buffer or cells were fixed and permeablized (protocol A). Histogram showing PE fluorescence intensities and percentages of positive cells. B) Fixed ES cells were immunofluorescently stained with H3K9ac-specific antibody using flow staining procedures. Cells were cytospun and DNA was counterstained (Hoechst 33258). One representative analysis of 3 individual experiments is shown.

5.1.2 Specificity of measurement

To prove that the chromatin flow cytometry approach specifically displays epitopes, firstly I analyzed ES cells prior and post treatment with the HDAC inhibitor TSA (Figure 5.2 A). As HDAC inhibition results in histone hyperacetylation, cells were immunofluorescently stained with an antibody specific for H4K16ac. Flow cytometric analysis revealed an increase in global H4K16ac levels in TSA-treated cells, while histone H4 signals, used as a control, remained unchanged. A similar increase in H4 acetylation signal was verified by Western blot analysis. TSA-induced histone hyperacetylation was detected with all antibodies recognizing acetylated lysine residues listed in Table 5.1 (data not shown).

Secondly, trimethylation levels of H3K27 were analyzed in EED KO and in wild type ES cells (Figure 5.2 B). EED KO ES cells lack a critical component of the PRC2 that is involved in the methylation of H3K27 [131]. Flow analysis of EED KO and of wild type ES cells clearly showed a reduction of global H3K27me3 levels in EED KO as compared to wild type cells, whereas the H3 signal persisted at unchanged levels. The reduction in H3K27me3 signal was also seen in Western blot analyses.
Together, the data show that chromatin flow cytometry specifically detects nuclear antigens in ES cells.

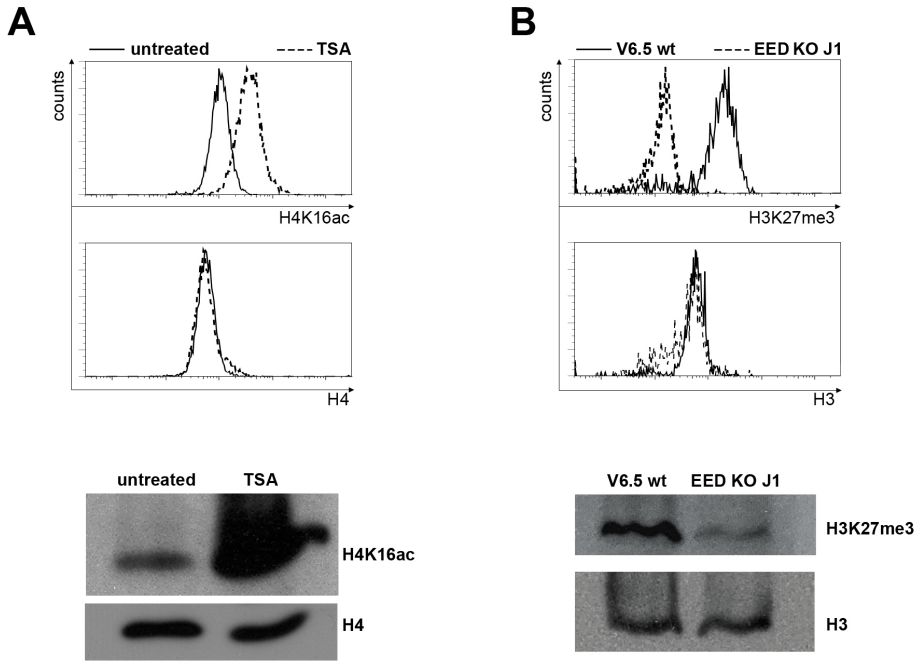

Figure 5.2: **Chromatin flow cytometry specifically detects histone modifications.** A) Flow cytometric (top) and Western blot (bottom) analysis of ES cells +/- TSA (9 h, 150 nM) stained with H4K16ac- and H4-specific antibodies. Representative analyses are shown (flow cytometry, n = 4; Western blot, n = 3). B) Flow cytometric (top) and Western blot (bottom) based comparison of wild type and EED KO ES cells with H3K27me3- or H3-specific antibodies. Representative analyses are shown (flow cytometry, n = 4; Western blot, n = 2).

5.1.3 Studies on histone modification levels in differentiating ES cells

Flow cytometry in general allows the simultaneous analysis of multiple parameters. To make use of this advantage I combined the detection of a cell surface marker with the assessment of an intranuclear histone modification level. Upon differentiation mouse ES cells lose the surface marker SSEA1 [32]. V6.5 ES cells were differentiated for 7 days as EBs in the presence of 0.1 μM all trans retinoic acid (ATRA) and subsequently singularized, fixed and double stained for extracellular SSEA1 levels and the H3K9ac histone modification. As depicted in Figure 5.3, about 75% of the differentiated ES cells showed low levels of SSEA1 whereas only 20%

were SSEA1^{positive}. Electronic gating of SSEA1^{positive} and SSEA1^{negative} cells, respectively, revealed that the H3K9ac level was higher in the SSEA1^{positive} subpopulation than in the SSEA1^{negative} cells. Histone H3 levels, however, were similar in the two subpopulations.
In summary, these data show that chromatin flow cytometry allows the simultaneous detection of surface and intranuclear antigens and that different global chromatin modification levels can be distinguished in individual cells of heterogeneous, differentiating ES cell populations.

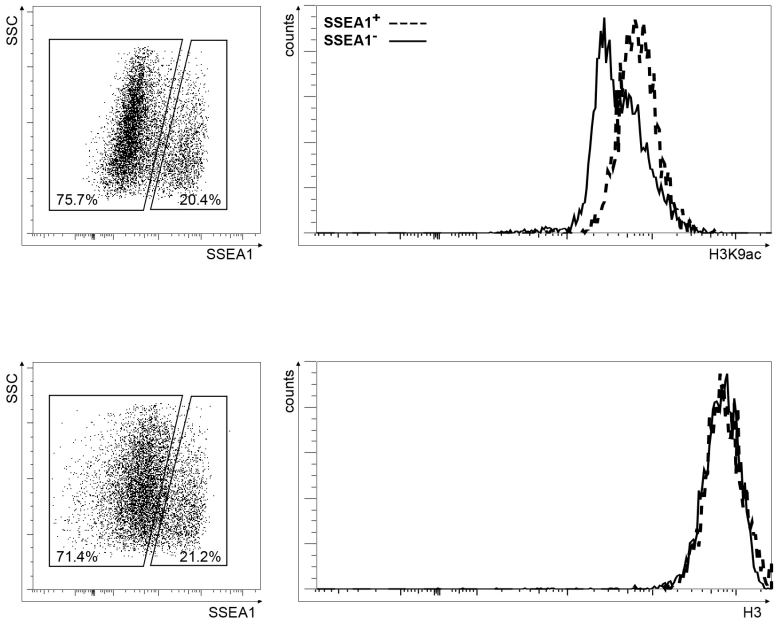

Figure 5.3: **Chromatin flow cytometry detects altered histone modification levels upon ES cell differentiation.** Flow cytometric analysis of surface marker SSEA1 and intranuclear H3K9ac (top) or H3 (bottom) levels in 7 days differentiated ES cell cultures. SSEA1^{positive} and SSEA1^{negative} cells were gated (left) and plotted in histogram overlays according to H3K9ac levels (right). One representative analysis of 3 individual experiments is shown.

5.2 Analyzing the effect of HDAC inhibition on the hematopoietic potential of BM cells

The chromatin and epigenome of pluripotent ES cells and of multipotent adult stem cells, like HSCs, mirrors their capability to self renew and to differentiate. In the scope of this thesis, I analyzed histone acetylation in BM cells and the effect of TSA treatment on the hematopoietic activity of BM cells.

5.2.1 Global histone acetylation in BM cells

By applying chromatin flow cytometry in combination with lineage marker antibodies, which recognize macrophages, granulocytes, erythrocytes, T- and B-lymphocytes, I compared global levels of pan-acetylated histone H4 (pan-acH4) in the immature Lin^- population, including HSCs, to mature Lin^+ cells. As shown in Figure 5.4 A, pan-acH4 levels in Lin^- and Lin^+ cells were similar. However, if treated with the HDAC inhibitor TSA, global pan-acH4 levels were elevated whereas H3 levels remained unchanged (Figure 5.4 B).
In order to measure not only histone acetylation levels but also the activity of HDAC enzymes, an HDAC activity assay was performed on nuclear extracts of either Lin^+ or $Lin^{-/int}$ BM cells which were separated by MACS technology. The results obtained from this colorimetric assay are depicted in Figure 5.4 C. As expected, nuclear extracts of BM cells pretreated with TSA showed significantly reduced HDAC activity levels. As the majority of unfractionated BM cells consists of lineage committed Lin^+ cells, the HDAC activity of whole BM extracts and Lin^+ cells were on a comparable level. However, the $Lin^{-/int}$ BM cells exhibited a significantly elevated HDAC activity with a more than 1.5-fold increase.
Together, these data show that the executing enzymes that remove acetyl-groups from histones are more active in the uncommitted $Lin^{-/int}$ compartment. However, this has no consequences on global histone acetylation states.

5.2.2 Effect of TSA treatment on in vitro and in vivo hematopoietic activity

Treatment with the HDAC inhibitor TSA was previously shown to expand $CD34^+$ human umbilical cord blood cells with hematopoietic repopulating activity [68]. Therefore, I aimed to analyze whether TSA treatment would also affect hematopoietic activity of mouse BM cells. For the analysis of TSA treatment effects on *in vitro* and *in vivo* hematopoietic activity, BM cells were cultured *ex vivo* in medium supplemented with IL3, IL6 and SCF for two days in the absence or presence of increasing concentrations of TSA. Subsequently cells were placed into *in vitro* and *in vivo* assays to estimate their hematopoietic activity.
First, freshly isolated and cultured BM cells were subjected to a flow cytometric analysis in order to obtain information about the frequency of LKS cells, which comprise HPSCs. The analysis revealed that the percentage of LKS cells increased slightly during a 2-day culture period from 1.25% to 2.72% (Figure 5.5 A). However, increasing concentrations of TSA could raise the LKS cell frequency to more than 18%, which is a 10-fold increase as compared to freshly isolated BM cells. Also VPA, another HDAC inhibitor, showed similar effects on the percentage of LKS cells.
The influence of TSA treatment on cell numbers was examined by counting living cells before and after treatment and culture. Figure 5.5 B (left panel) displays the decline of living cells with increasing concentrations of TSA. Less than 10% of the initially plated cells were alive af-

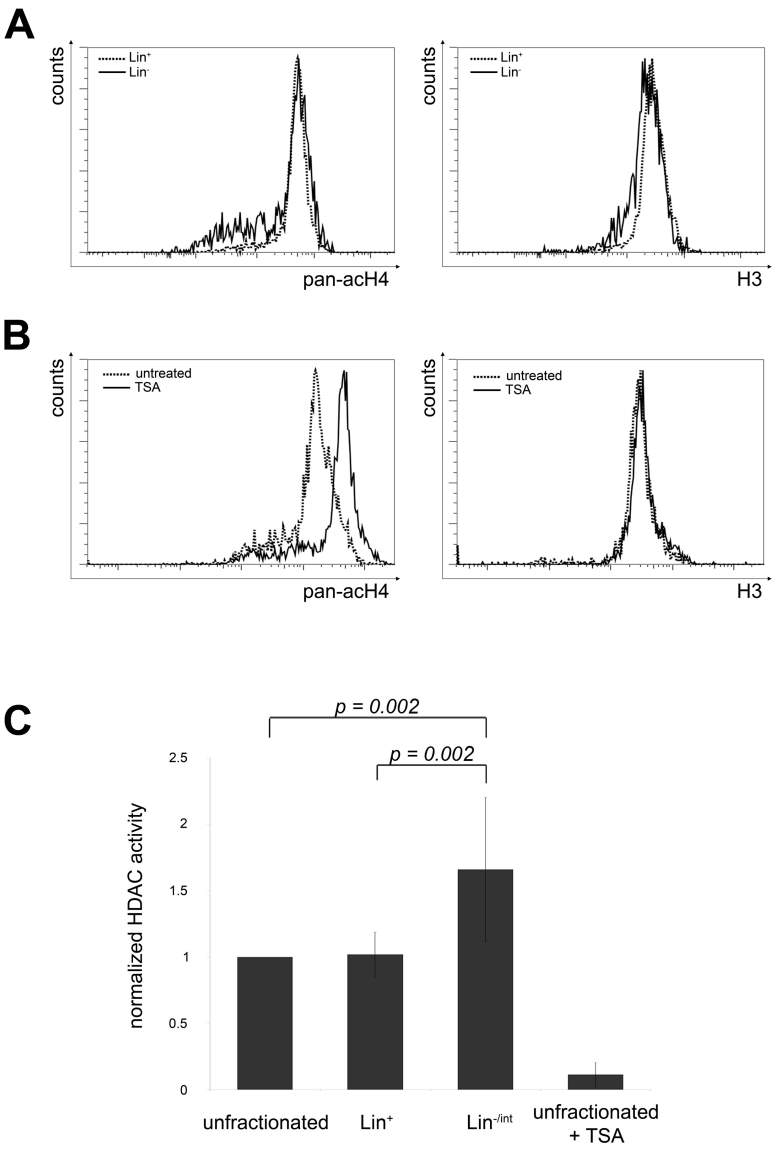

Figure 5.4: **Lin$^-$ and Lin$^+$ BM cells have similar histone H4 acetylation levels, but different HDAC activities.** A) Histone H4 acetylation status of electronically gated Lin$^+$ and Lin$^-$ BM subpopulations analyzed by pan-acH4- (left) and H3- (right) specific intranuclear flow cytometry. A representative analysis of three independent experiments is shown. (B) Histone H4 acetylation status of BM cells cultured with or without TSA. Fresh BM cells were cultured for 4 h with/without 150 nM TSA and stained with pan-acH4- (left) and H3- (right) specific antibodies for flow cytometry. C) HDAC activity in nuclear extracts of separated Lin$^{-/int}$ and Lin$^+$ BM cells by a fluorimetric HDAC activity assay. A TSA-treated extract is shown as control. Normalized means and standard deviations of HDAC activities are plotted. From three individual cell separation procedures and sample preparations, a total of nine measurements was obtained for each cellular fraction. Including correction for multiple testing, statistical significance had a level of $P < 0.005$.

ter a 2-day treatment period with 50 nM of TSA. By subjecting BM cells to a methylcellulose (MC)-based colony formation assay the relative colony forming capacity, which reflects HPC activity, was determined. The number of colonies which formed from 5,000 cells increased in BM cells which were cultured and treated with 50 nM TSA (Figure 5.5 B, middle). However, as only few cells survived 50 nM TSA treatment, the corresponding absolute number of CFCs was less in 50 nM TSA-treated than in 5 or 10 nM TSA-treated cultures (Figure 5.5 B, right panel). In order to measure more primitive HPCs, a secondary CFC assay was performed by plating primary into secondary MC cultures. Compared to untreated or 10 nM TSA-treated cells, BM cells which were treated with 50 nM TSA formed 6-fold more secondary colonies (Figure 5.5 B, lower panel).
As the proof of *in vivo* repopulation of irradiated recipients is the most stringent test of HPSCs, 20,000 freshly isolated and in parallel cells cultured for 2 days +/- TSA were transplanted into lethally irradiated mice. Peripheral blood was analyzed for donor cell contribution 16 weeks after transplantation. Cultured and TSA-treated BM cells were derived from the Ly5.1 mouse strain, whereas recipients and co-transplanted competing BM cells carried Ly5.2 leukocyte antigens. Flow cytometric analysis for $Ly5.1^+$ cell frequencies in the peripheral blood showed that the donor contribution decreased 4-fold from 20% to 5% when BM cells were *ex vivo* cultured for 2 days (Figure 5.5 C). Importantly, mice that received 50 nM TSA-treated BM cells possessed an average of 50% of donor cells in their peripheral blood.
These data indicate that upon 50 nM TSA treatment the relative frequency of phenotypical, *in vitro* colony forming and *in vivo* repopulating HPSCs is increased, though high TSA concentration caused more than 90% of cell death. A net expansion of HPCs with *in vitro* colony forming potential could only be determined for BM cells treated with low concentrations of TSA.

5.2.3 Selective cell survival upon TSA treatment

To address the question of whether TSA affects differentiation and selectively induces cell death, freshly isolated BM cells were separated with respect to their grade of lineage commitment into Lin^+ and $Lin^{-/int}$ subpopulations by MACS. Separated cell populations were cultured for 2 days with growth factors in the absence or presence of TSA. As shown in Figure 5.6 A, in the two separated subpopulations cell numbers declined upon TSA treatment, however, more cells of the $Lin^{-/int}$ subpopulation survived.
Additionally, I examined the cultured and treated $Lin^{-/int}$ subpopulation regarding apoptosis and Lin marker expression. Figure 5.6 B illustrates a representative flow cytometric analysis. $Lin^{-/int}$ cells gained Lin marker surface expression during a 2-day culture period without TSA, suggesting commitment and differentiation. However, the frequency of Lin^+ cells was reduced in a dose-dependent manner when cells were treated with TSA (Figure 5.6 B, C). The analysis further revealed that treatment with 50 nM TSA resulted in a higher proportion of Lin^- cells within the living ($AnnexinV^{negative}$) cell population (Figure 5.6 B, D).
Together, this indicates that TSA treatment induces apoptosis preferentially in Lin^{int} and in Lin^+ cells.

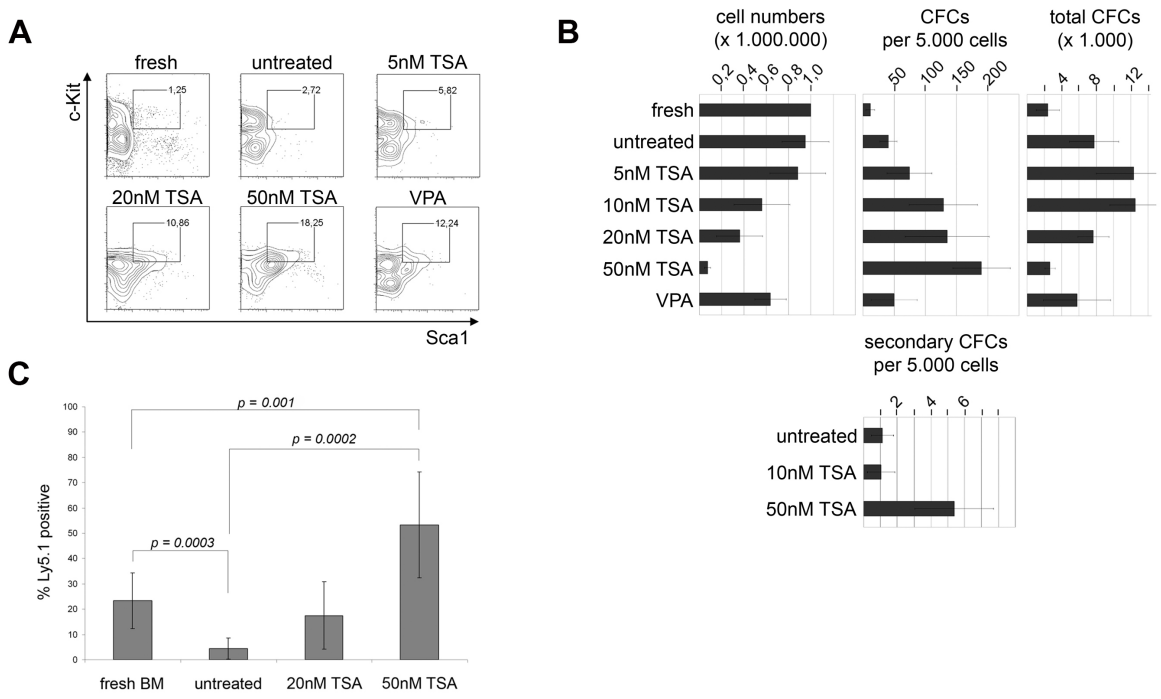

Figure 5.5: **HDAC inhibition by TSA results in higher frequencies of *in vitro* and *in vivo* HPSCs.** Analyses were done with either freshly isolated BM cells or with BM cells cultured for 2 days in medium supplemented with IL3, IL6 and SCF with or without HDAC inhibitors. A) The results of c-Kit- and Sca1-specific FACS analyses of gated Lin^- cells of fresh BM and BM cells cultured for 2 days either with or without increasing concentrations of TSA or VPA are shown. A representative analysis is shown. Lin^-, c-Kit^+ and $Sca1^+$ (LKS) cell frequencies are indicated (gates); n=4. B) Total cell numbers of BM cultures are displayed directly after plating (fresh) or after 2 days of treatment with increasing amounts of TSA or VPA. Also shown are CFC frequencies per 5,000 cells and absolute CFC numbers [absolute CFC number = (CFC numbers/5,000 cells) / cell number of day-2 cultures). Cells were cultured for 2 days in the absence or presence of TSA or VPA. Living cells were counted by trypan blue staining and equal cell numbers were seeded into methylcellulose (MC) medium. Colony numbers were counted after 10 days of culture. Mean values and standard deviations are shown (n=5). Secondary CFC frequencies in untreated and treated BM cultures (bottom). BM cells were cultured for 2 days in either the absence or presence of TSA; then equal numbers of living cells were seeded in MC medium. On day 10, colony frequencies were determined, followed by isolation of cells from primary cultures. Equal cell numbers were re-plated into secondary MC cultures. Colony numbers of secondary cultures were counted at day 10 post plating. Mean values and standard deviations are displayed (n=3). C) Engraftment potential of TSA-treated BM cells. Donor reconstitution of irradiated mice with fresh BM cells or BM cells cultured with or without TSA. Ly5.1 BM cells were cultured for 2 days in the absence or presence of TSA. Cells were injected into irradiated Ly5.2 recipients together with Ly5.2 competitor BM cells. Peripheral blood cells of transplant recipients were analyzed by flow cytometry for the presence of donor (Ly5.1) and recipient cells 16 weeks post transplantation. Percentages of Ly5.1 donor cells are indicated. Analyses are shown from two independent experiments comprising eight recipients per cell sample. Mean values and standard deviations are indicated. Including correction for multiple testing, statistical significance had a level of $P < 0.005$.

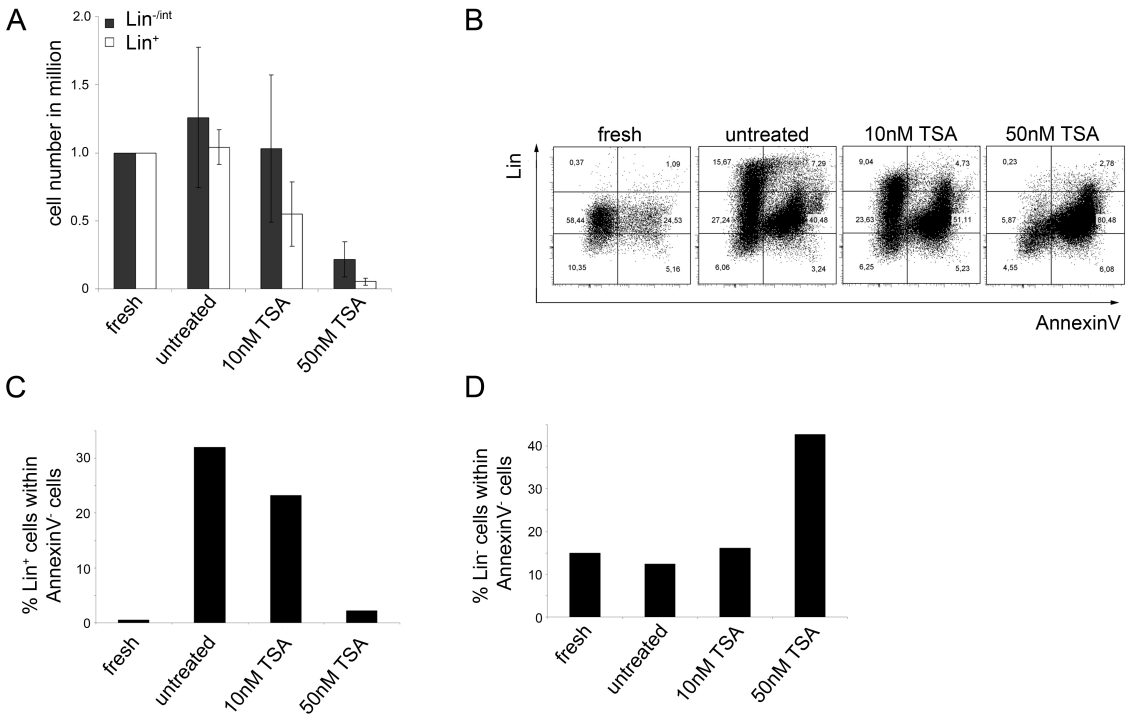

Figure 5.6: **TSA treatment preferentially kills mature BM cells.** A) Cell numbers of MACS-separated Lin^+ and $Lin^{-/int}$ BM cells are shown after 2 days of culture with/without TSA (n=3). B) Flow cytometric analysis of $Lin^{-/int}$ BM cells directly after MACS separation (fresh) and after 2 days of culture (untreated, 10 nM, 50 nM TSA). Cells were analyzed for Lin expression and for apoptosis (by AnnexinV staining). Gates (Lin^-, Lin^{int}, Lin^+) were defined according to unstained and Lin^+ MACS-separated BM cells. A representative analysis is shown (n=3). C) Percentages of Lin^+ cells and D) percentages of Lin^- cells within the alive, $AnnexinV^{negative}$ cell population. Data in C and D were taken from the plot shown in B. The total number of $AnnexinV^{negative}$ cells was always set to 100% (C, D).

5.3 Studying differentiation of pluripotent mouse ES cells

Pluripotent mouse ES cells are *in vitro* derivatives of ICM cells from murine E3.5 preimplantation blastocysts. ES cells can be maintained infinitely as stable cell lines that self renew without losing differentiation potential [6]. The presence of LIF and feeder cells in standard ES cell culture conditions activates the transcription factor network including Oct4, Sox2 and Nanog which maintains ES cells in a groundstate of pluripotency [155, 156]. By differentiation induction, either *in vitro* or *in vivo*, pluripotent ES cells can give rise to cell types of all three germ layers and germ cells. The following section contains analyses on early steps of *in vitro* ES cell differentiation induced by the withdrawal of LIF and feeder cells.

5.3.1 Differentiation potential of different ES cell lines

Here I aimed to analyze the loss of pluripotency in mouse ES cells which were differentiated as EBs. Distinct ES cell lines underlie clonal variation which is reflected by different cellular reactions upon differentiation induction. Thus, in order to minimize observations that are based on cell line-specific properties, the differentiation experiments were performed with 3 different ES cell lines. D3 ES cells (129/Sv X 129/Sv) were grown on gelatin-coated tissue culture (TC) dishes [157], whereas V6.5 (129/Sv X C57BL6) and OG2 (CBA X C57BL6) ES cells were regularly grown on MEF feeder layers [42, 158]. For EB formation 1,000 ES cells were clustered to one EB per hanging drop (HD) in differentiation medium (Scheme 5.1). EBs were cultured for up to 7 days. Figure 5.7 A shows light microscopic pictures of the ES cells and the corresponding EBs. At individual days defined numbers of EBs were harvested, dissociated, cells were counted and cell numbers per EB were determined (Figure 5.7 B). Also the diameters of EBs were measured microscopically, results are given in Figure 5.7 C.
During differentiation the 3 ES cell lines showed different proliferation behaviors, which was reflected by differences in the cell numbers per EB and EB size differences. D3 cells divided most rapidly but during the last 2 days of differentiation they failed to continue to proliferate, as the EB size decreased and the cell numbers remained unchanged. In contrast, V6.5 and OG2 cells proliferated continuously. The maximum diameter of D3 EBs was accomplished at day 5. This diameter was comparable to the maximum diameter of OG2 EBs at day 7. Thus, due to faster proliferation, D3 EBs reached a maximal size earlier. A maximal EB size might be limited to a diameter that still allows sufficient diffusion of nutrients.
A marker of pluripotent ES cells is SSEA1 on the cell surface [32, 159, 160]. In Figure 5.8 flow cytometric data are depicted reflecting the relative frequencies of SSEA1^{high}, SSEA1^{medium}, SSEA1^{low} and SSEA1^{negative} cells within ES and EB cells of the 3 lines. As the expression of SSEA1 is fluctuating within a certain range in ES cell cultures [32], ES cells (day 0 of differentiation) of all 3 lines showed medium and high SSEA1 expression, as expected. Interestingly, clustering of 1,000 ES cells to one EB for 1 day increased the proportion of SSEA1^{high} cells 2-fold. Steadily, SSEA1 levels declined during proceeding differentiation and at day 4 cells reached SSEA1 levels similar to undifferentiated ES cells. However, after 7 days of differentiation SSEA1 levels differed among the 3 lines. While most OG2 and V6.5 ES cell-derived cells showed medium SSEA1 levels, most D3 cells were SSEA1^{low}.
These data suggest, that (i) SSEA1 is not a stringent marker for pluripotency, because its levels decline late during differentiation, that (ii) the fluctuation towards SSEA1^{high} levels are favored during early differentiation and that (iii) different ES cell lines vary in their dynamics of SSEA1 down-regulation.

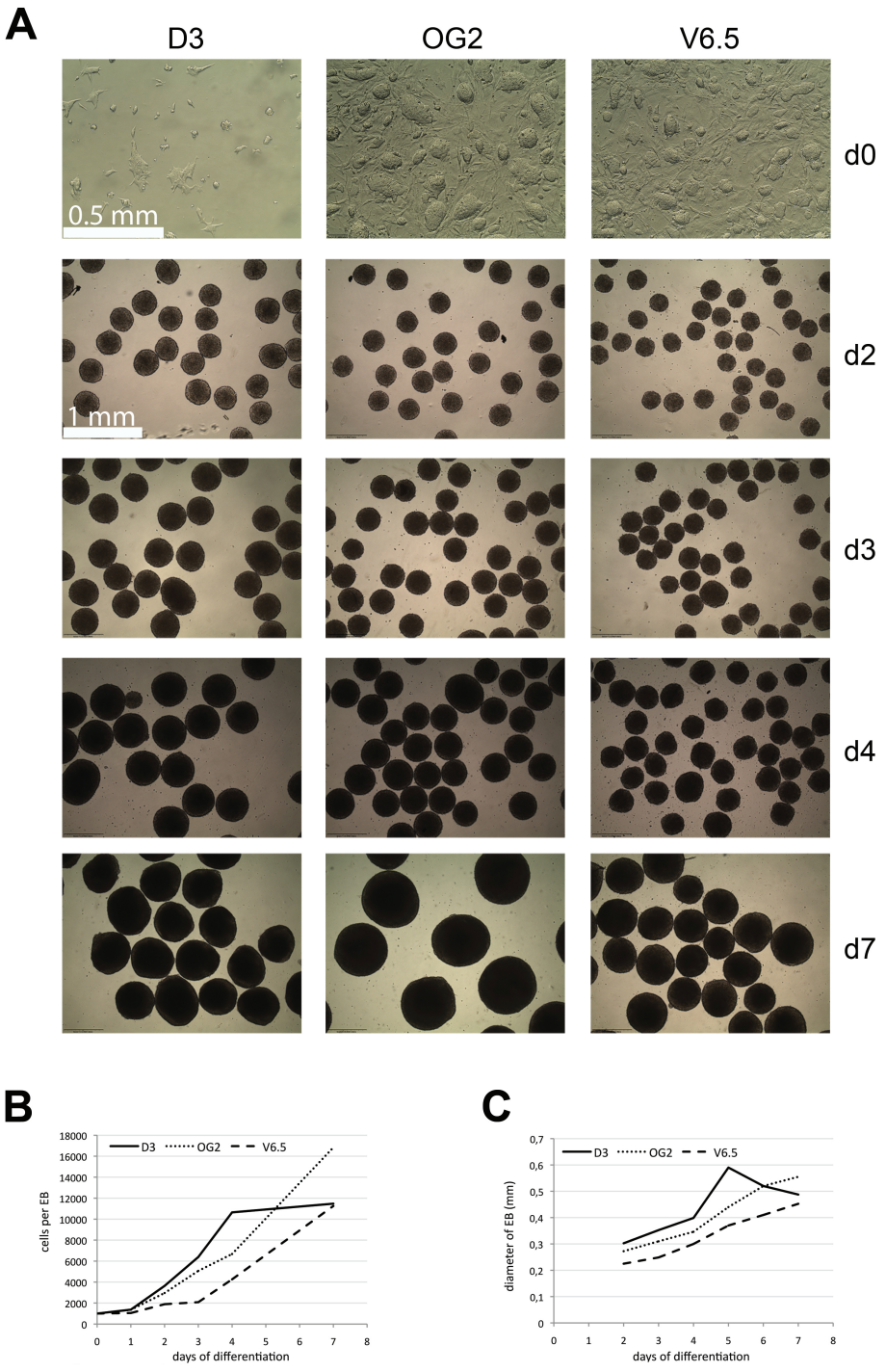

Figure 5.7: **D3, OG2 and V6.5 wild type ES cells have different proliferation kinetics upon EB differentiation.** A) Light microscopic photographs of undifferentiated D3, OG2 and V6.5 ES cells (day 0; d0) and differentiated EBs (day 2 to day 7; d2-7). In each case 1,000 ES cells were clustered to one EB by HD differentiation procedure for 2 days, cells were subsequently maintained in suspension culture. B) Cell numbers per EB are shown for the 3 cell lines at the indicated days of differentiation. Defined numbers of EB were harvested, dissociated and cell numbers were determined (n=3). C) Diameters of EBs at day 2-7 of differentiation were obtained by software analyses of microscopic pictures (n=3).

Besides the cell surface marker SSEA1, expression of a set of pluripotency- and differentiation-associated genes was analyzed (Figure 5.9). Unexpectedly, for all cell lines the expression of pluripotency-associated genes was up-regulated in 1-day differentiated cells *versus* ES cells, before levels declined at day 7 of differentiation. I did not observe a clear and steady down-regulation but rather slight reduction with considerable fluctuation. V6.5 cells showed still highest expression levels of Oct4, Sox2, Rex1 and Nanog after 7 days of differentiation as compared to the other 2 ES cell lines, while almost no endodermal AFP transcription could be detected. OG2 cells immediately and exclusively expressed AFP at day 1, whereas D3 cells expressed the endodermal marker after more than 4 days. In contrast, the mesodermal differentiation analyzed by Bry gene expression started early and strongly in D3 cells, while in OG2 and V6.5 cells, Bry was detected at day 7. The ectodermal lineage, measured by Nestin expression, appeared in all cell lines at day 4 with a maximum expression. OG2 cells expressed highest levels of Nestin.
Together, while pluripotency marker genes were still found to be expressed after 4 and 7 days at levels comparable to undifferentiated ES cells, ecto-, meso- and endoderm-associated markers were up-regulated reflecting ongoing differentiation. Simultaneous detection of markers for undifferentiated cells and differentiated cells could be the result of mixed heterogeneous cell populations.
ES cells have the capability to self renew while maintaining their pluripotent character and to differentiate to all embryonic cell lineages upon differentiation induction. Here, it was analyzed how fast these features were lost during *in vitro* differentiation in 3 different ES cells lines.
ES cells self renew by forming clonal colonies under standard ES cell culture conditions. In a colony forming assay the potential of ES and EB cells to form colonies with alkaline phosphatase (AP) activity was compared. Figure 5.10 A displays the percentage of self renewing CFCs in ES cell cultures and among differentiated EB cells. All 3 lines showed declining frequencies of CFCs with proceeding differentiation times, indicating a loss of self renewal capacity. Especially during the first 2 days of differentiation the frequency of CFCs dropped to approx. 30%. Notably, the potential to form colonies differed in the 3 undifferentiated ES cell cultures. The percentage of CFCs varied from approx. 100% CFCs in D3 and OG2 ES cells to only 40% in V6.5 ES cells.
By performing EB formation assays I next compared the potential of the 3 ES cell lines and their differentiated EB cells to proliferate under differentiation conditions in MC. Therefore, feeder-free ES cells or dissociated EB cells after 1 to 7 days of differentiation were plated into semisolid medium without LIF to allow clonal proliferation yielding EBs. The 3 ES cell lines varied in their EB formation frequency: 140 out of 1,000 D3 ES cells developed EBs, 100 of 1,000 OG2 ES cells formed EBs. Only 60 EBs developed per 1,000 V6.5 ES cells (Figure 5.10 B). Despite these dissimilarities the frequency of EB forming cells declined during differentiation in all 3 lines. OG2 and V6.5 cells reached a minimum of EB forming cells after 2 days of differentiation, whereas in D3 cell cultures EB formation potential was still present after 3 days.
In order to analyze the differentiation potential towards spontaneously contracting cardiomyocytes, I next applied the 'beating body' assay to either ES cells or their differentiated progeny [161]. Therefore, EBs were generated by the HD method and subsequently single EBs were placed into wells of gelatin-coated 48-well plates. Contractile properties of individual EBs were analyzed after 10 days by microscopy. Figure 5.10 C summarizes the frequency of contracting EBs which were formed by undifferentiated ES or by differentiated EB cells. Again

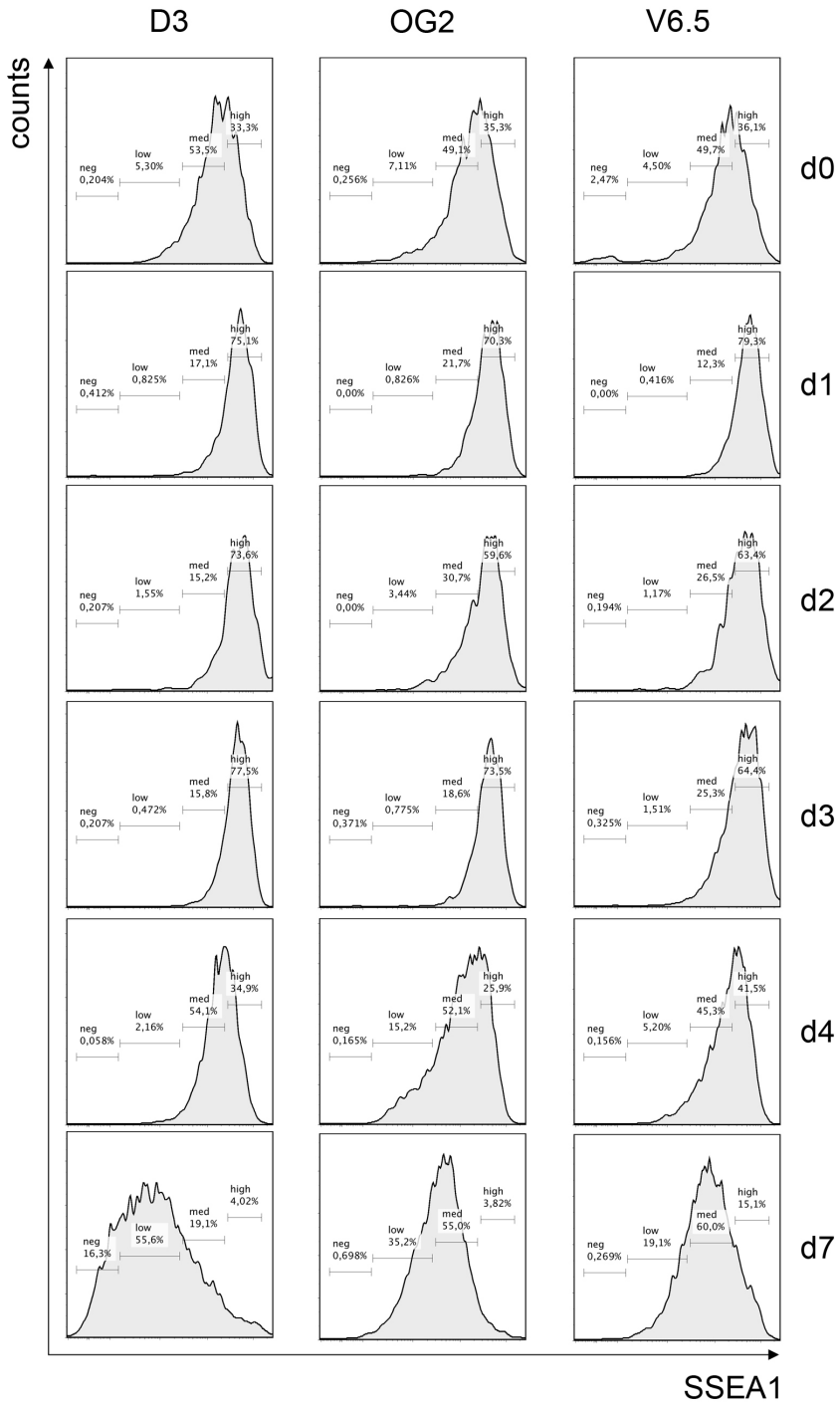

Figure 5.8: **SSEA1 surface expression is slowly diminished upon EB differentiation.** Undifferentiated ES cells (d0) and differentiated EB cells harvested at days 1, 2, 3, 4 or 7 of differentiation were stained with primary SSEA1-specific and subsequently with secondary anti-mouse-Cy3 antibodies. Shown are representative flow cytometric histogram plots with corresponding gate frequencies for SSEA1^{negative}, SSEA1^{low}, SSEA1^{medium} and SSEA1^{high} subpopulations (n=3).

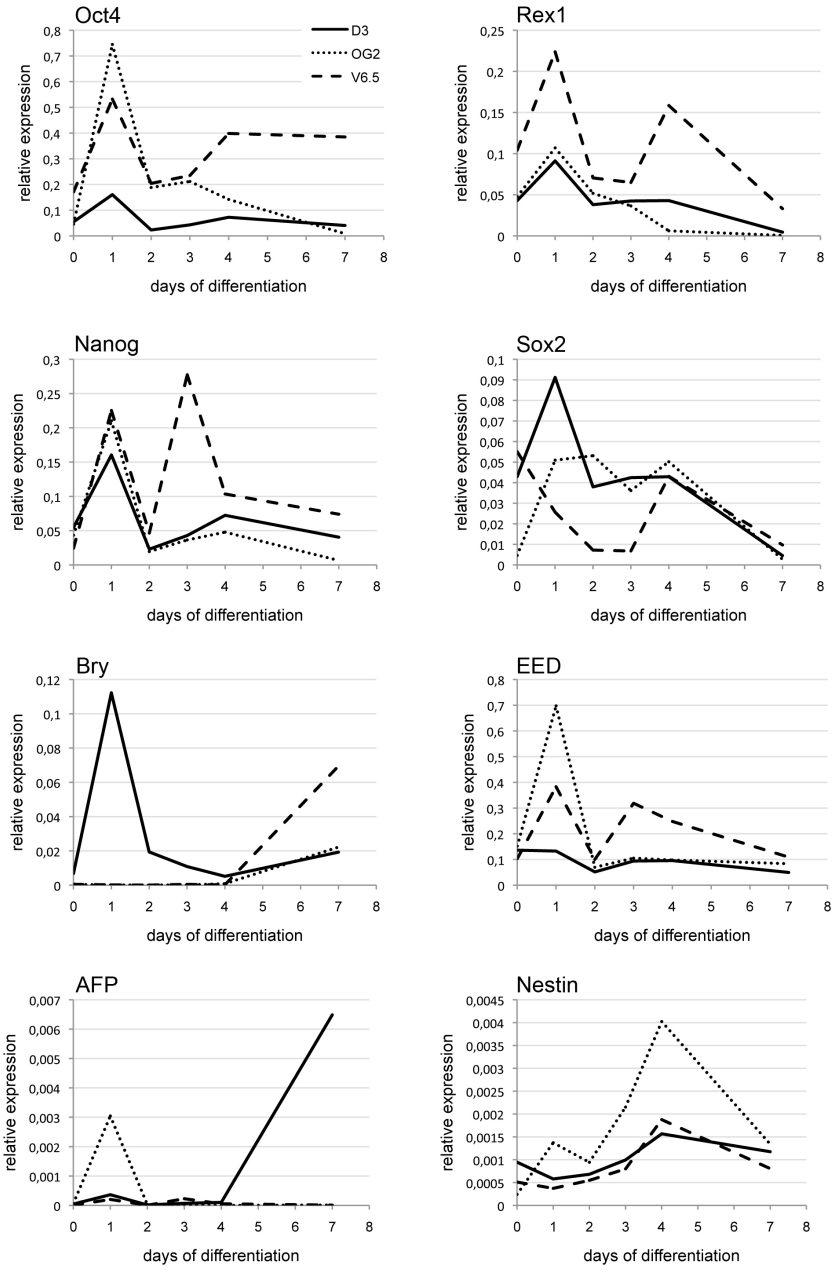

Figure 5.9: **Gene expression in D3, OG2 and V6.5 ES cells during EB differentiation.** RNA was prepared from undifferentiated ES cells (d0) or differentiated EB cells harvested at days 1, 2, 3, 4 or 7 of differentiation. cDNA was synthesized and realtime PCR was performed with primers specific for pluripotency genes (Oct4, Rex1, Nanog, Sox2) or for ecto-, meso- and endodermal markers (Nestin, Bry, AFP) as well as for EED.

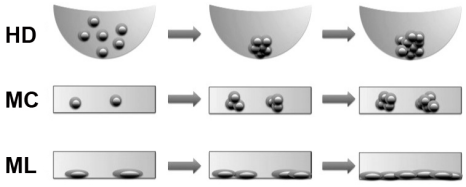

Scheme 5.1: ***In vitro* differentiation methods for murine ES cells.** ES cells form EBs by clustering in hanging drops (HD) or by clonal proliferation in a semisolid methylcellulose (MC) medium. When attached to tissue culture (TC) surface ES cells also differentiate as monolayer (ML) cells.

the 3 undifferentiated ES cell lines differed in their efficiency to generate 'beating bodies'. All EBs formed by D3 and V6.5 ES cells contained contracting cells, whereas only 20% of the OG2 ES cell-derived EBs were contracting. Interestingly, in V6.5 and OG2 cells the potential to differentiate to cardiomyocytes was lost after 1 and 2 days of differentiation induction, respectively. For D3 cells, which were differentiated for 3 days and subsequently subjected to the 'beating body' assay, no contracting cardiomyocytes were observed anymore. However, in 4-day and 7-day differentiated D3 EB cells there were 40% and 10% of wells containing contracting EBs. Maybe after 4 or 7 days of differentiation first progenitors of cardiomyocytes appeared in D3 EB cultures. Hence, if subjected to the 'beating body' assay, previously differentiated cardiomyogenic cells could induce contraction. Cardiomyocytes are a mesoderm-derived cell type and gene expression analysis of the mesoderm inducer brachyury (Bry) revealed unexpectedly early expression in the course of D3 ES cell differentiation (Figure 5.9). This indicates a favored mesodermal lineage commitment and fits to the overall high efficiency of 'beating body' formation (Figure 5.10).
Altogether, these assays showed that the self renewal and differentiation capacity of ES cells decreased when cultured under differentiation conditions for 3 days. However, individual ES cell lines behaved differently with regards to their colony and EB formation capacity, especially in the undifferentiated state.

5.3.2 Progression of differentiation as a consequence of differentiation method

Differentiation of mouse ES cells is generally induced by withdrawal of LIF and feeder cells from culture conditions. Different methods of differentiation were described in the literature and in the scope of this thesis I focused on 3 distinct protocols, which are summarized in Scheme 5.1 [49]. ES cells can be clustered by gravity in HDs of differentiation medium, yielding EBs of similar size. EBs can also be formed from single ES cells in semisolid MC differentiation medium, avoiding stochastic aggregation and resulting in clonal-derived EBs [162]. Alternatively, ES cell differentiation can be induced by culturing ES cells as an adherent ML on TC plastic surfaces in differentiation medium [51].
In order to compare the impact of the differentiation method on the loss of pluripotency I measured eGFP levels in OG2 cells which express eGFP under the control of a transgenic distal Oct4 enhancer that is active in ICM and ES cells [158]. Figure 5.11 shows a flow cytometric analysis of Oct4-eGFP expression in undifferentiated OG2 ES cells and in differentiated EB cells. EBs were either formed clonally in MC or by clustering in HDs. Oct4-eGFP levels started to decrease at the 3rd day of differentiation. However, at day 4 and 7 it became obvious that EB cells in MC steadily and homogeneously lost Oct4-eGFP expression, whereas

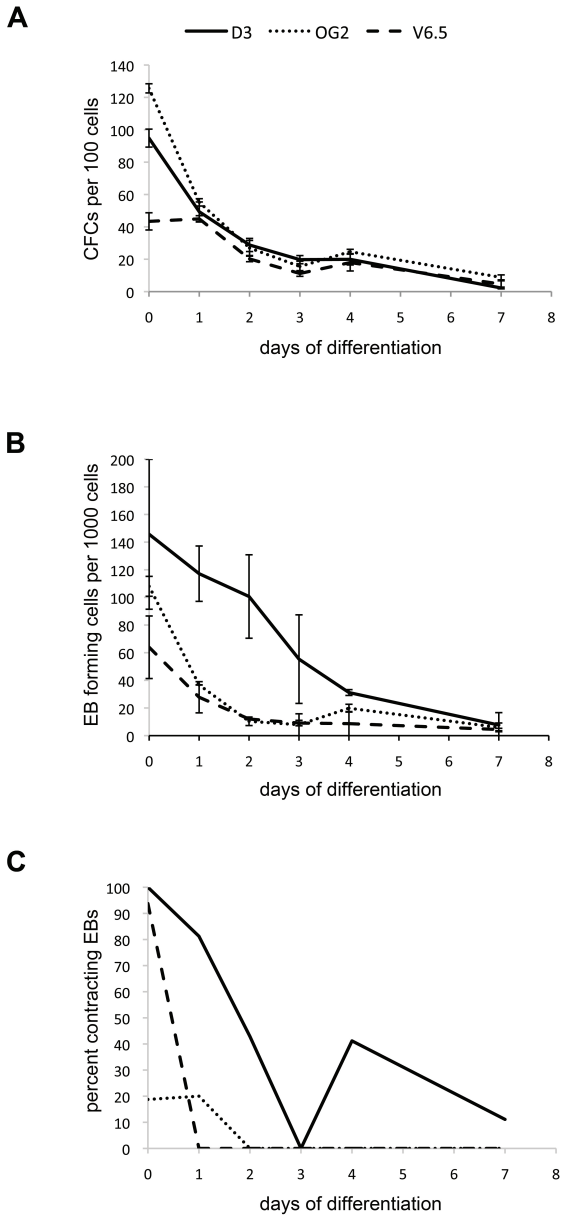

Figure 5.10: **D3, OG2 and V6.5 ES cells lose functional properties of pluripotency upon HD EB differentiation.** A) Undifferentiated ES (d0) and EB cells after 1, 2, 3, 4 or 7 days of *in vitro* differentiation were reseeded into ES cell culture conditions. Developing colonies were stained for AP activity and colonies were counted. Displayed are the percentages of CFCs for the respective days of differentiation and for the 3 cell lines (n=3). B) Undifferentiated ES (d0) and EB cells after 1, 2, 3, 4 or 7 days of differentiation were plated into MC medium to determine clonal EB formation capacity. Shown are the numbers of EBs formed of 1,000 cells seeded at the given days of differentiation and for the 3 cell lines (n=3). C) Undifferentiated ES (d0) and EB cells after 1, 2, 3, 4 or 7 days of differentiation were used as initial cellular material for a 'beating body' assay. Frequencies of contracting EBs were enumerated after a total of 15 days (2 days HD, 3 days suspension, 10 days attached EBs), percentages are depicted (n=1).

HD EB cells split up to heterogeneous subpopulations of cells with no Oct4-eGFP expression, medium and high levels of Oct4-eGFP.
Further the localization of Oct4-eGFP^{high} cells within 7-day old HD EBs was investigated by cryosectioning and fluorescence microscopy. The analysis revealed that a couple of Oct4-eGFP^{positive} cells were located particularly in the center of the EB and formed islet-like clusters (Figure 5.12).
Similarly to EB differentiation, OG2 ES cells which were differentiated as ML started to exhibit reduced Oct4-eGFP levels at day 3 (Figure 5.13). However, the uniformity and progression of differentiation seemed to depend on the density of cells within the ML, *i.e.* the degree of confluence. Starting with less ES cells resulted in more uniformly differentiated cells at day 6, while high initial cell numbers gave rise to subpopulations of cells with no and with high Oct4-eGFP levels. Light microscopic imaging of high density seeded ML differentiation cultures revealed colony-like structures of cells growing on a confluent layer of differentiated ES cells, as shown in Figure 5.14. Indeed, the colony-like nests of cells turned out to be eGFP^{positive} whereas the layer underneath appeared less intense in fluorescence (data not shown).
In summary, these results show that - as evidenced by Oct4-eGFP expression - differentiation proceeded more efficiently and uniformly when ES cells started the differentiation process isolated and not in close proximity to other ES cells. This suggests an influence of the microenvironment provided by (differentiating) ES cells on the loss of pluripotency.

5.3.3 Reversibility of Oct4-eGFP expression after differentiation-induced loss

Previously it was reported that the levels of some pluripotency-associated proteins are fluctuating in ES cells without affecting pluripotency [34]. Besides Rex1, Stella and SSEA1 also Nanog levels are subjected to fluctuations, most probably as a result of a reversible shift between embryonic stem cell and epiblast stem cell identity [32, 33, 34, 35, 36]. Alternating levels of Oct4 RNA or protein were so far not shown. Therefore I aimed to examine whether differentiated ES cells with reduced Oct4-eGFP expression levels can regain ES cell expression levels of Oct4-eGFP under standard ES cell culture conditions. For this purpose I differentiated OG2 ES cells for 3 days as HD EBs until about half of the cells showed Oct4-eGFP signals clearly below ES cell levels. Cells of dissociated EBs were sorted by FACS with respect to their eGFP fluorescence intensity into an Oct4-eGFP^{high} and Oct4-eGFP^{medium} subpopulation. Separately, sorted cells were cultured under ES cell conditions and Oct4-eGFP levels were analyzed (Figure 5.15, 5.16 and Scheme 5.2).
Figure 5.15 gives the percentages of Oct4-eGFP^{high}, Oct4-eGFP^{medium}, Oct4-eGFP^{low} and Oct4-eGFP^{negative} populations in undifferentiated ES cells, in 3 days differentiated EB cells as well as in sorted EB cells, respectively. After FACS-sorting Oct4-eGFP^{medium} and Oct4-eGFP^{high} cells were cultured for 4 and 6 days under standard ES cell conditions. As HDAC inhibitors were reported to have a beneficial effect on reprogramming efficiency of Oct4^{negative} MEFs to Oct4^{positive} iPS cells, I additionally treated differentiated cells with 20 nM TSA during the first 24 h of ES cell culture [100]. The experiment revealed that differentiated EB cells with medium Oct4-eGFP expression levels after 4 days in ES cell culture continued to lose Oct4-eGFP expression as more than 80% of cells were Oct4-eGFP^{negative}. However, the subpopulation of Oct4-eGFP^{high} cells increased from 0.5% immediately after sorting to 2.9% in the untreated culture and to 8.6% upon TSA treatment. After 6 days of ES cell culture conditions the frequency of Oct4-eGFP^{high} cells increased to 30.3% in the absence and to

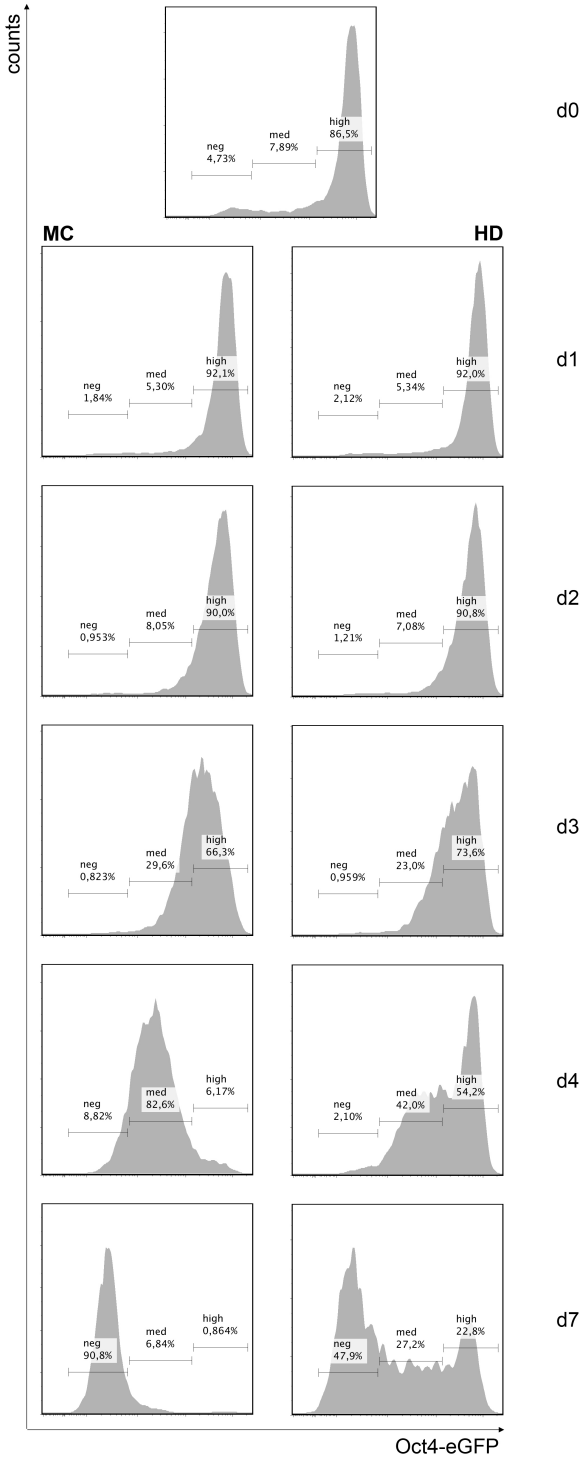

Figure 5.11: **EBs derived from clustered ES cells exhibit a higher grade of cellular heterogeneity than single cell-derived EBs.** Oct4-eGFP levels of undifferentiated OG2 ES cells (d0) and differentiated cells were flow cytometrically determined. Levels are shown as histogram plots with gate frequencies for $eGFP^{negative}$, $eGFP^{medium}$ and $eGFP^{high}$ subpopulations. ES cells were either differentiated in semisolid MC (left panel) or as clustered EBs in hanging drops (HD, right panel). A representative analysis of two individual experiments is given.

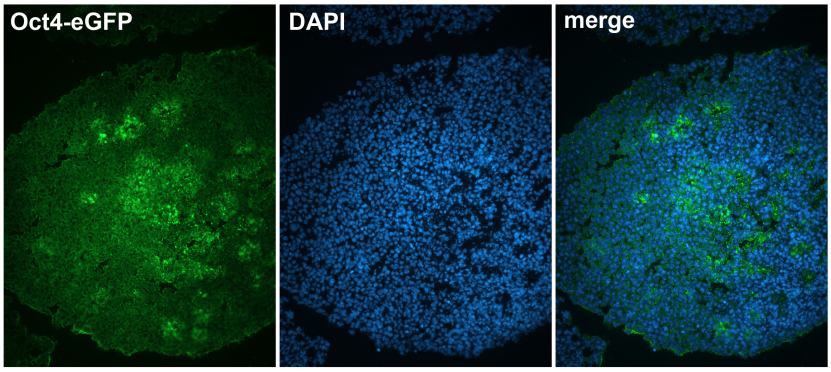

Figure 5.12: **Subpopulations of Oct4-eGFP^{positive} cells are located in central regions of EBs and form clusters.** OG2 ES cells were differentiated for 7 days as HD EBs. EBs were embedded, frozen and sectioned. Nuclei were visualized by DAPI staining. Magnification: 10x.

67.1% in the presence of TSA, respectively. Differentiated cells which had been sorted for high eGFP levels also showed some Oct4-eGFP^{medium}, Oct4-eGFP^{low} and Oct4-eGFP^{negative} cells after 4 days, indicating ongoing differentiation. Again the transient TSA treatment led to larger proportions of Oct4-eGFP^{high} cells. This became even more evident after 6 days of culture when 87% of the cells became Oct4-eGFP^{high}. Also the fluorescence intensity was increased (shown by the right-shifted peak).
Together, two observations were notable from this analysis: firstly, though most of the Oct4-eGFP^{medium} cells lost Oct4-eGFP expression during 4 days in ES cell culture, some cells maintained high Oct4-eGFP expression levels. The proportion of Oct4-eGFP^{high} cells increased after a total of 6 days post sort. This could be the result of re-gaining of Oct4-eGFP expression by cells that were Oct4-eGFP^{negative} or it was the result of a selective expansion of Oct4-eGFP^{high} cells deriving from a contamination with undifferentiated ES cells during the FACS-sort procedure. Secondly, a transient TSA treatment of differentiated ES cells led to higher frequencies of cells with high Oct4-eGFP expression, which might be due to either a reprogramming effect or to selective survival of a contaminating Oct4-eGFP^{high} subpopulation.
Though the purity of the sorted cell populations after FACS appeared to be high, I decided to ascertain whether contamination with eGFP^{high} cells in the sorted eGFP^{medium} samples was the reason for cells with high levels of Oct4-eGFP expression. For this purpose, different numbers of 3 days differentiated and sorted eGFP^{medium} OG2 cells were plated into ES cell culture conditions. As displayed in Figure 5.16 A, after sorting there was a contamination with Oct4-eGFP^{high} cells of only 0.56%, suggesting that about 1 out of 200 cells was Oct4-eGFP^{high}. Sorted cells were plated at the following concentrations: 100, 200, 400, 800, 1,600 and 3,200 cells per plate. After 2, 4 and 6 days flow cytometric analyses were done to control for Oct4-eGFP expression levels. Figure 5.16 B (untreated cells) summarizes the frequencies of Oct4-eGFP^{high}, Oct4-eGFP^{medium}, Oct4-eGFP^{low} and Oct4-eGFP^{negative} cells according to the gates shown in Figure 5.16 A. After 2 days analyses showed that the more cells had been plated out, the larger was the proportion of Oct4-eGFP$^{low/medium/high}$ cells. Also the fraction of Oct4-eGFP^{high} cells increased from day 2 to day 6 at all cell densities. Figures 5.16 C and D give respective gate frequencies for cells that were treated for 24 h with the HDAC inhibitors TSA or VPA. Compared to untreated cultures the overall frequency of Oct4-eGFP^{low} cells,

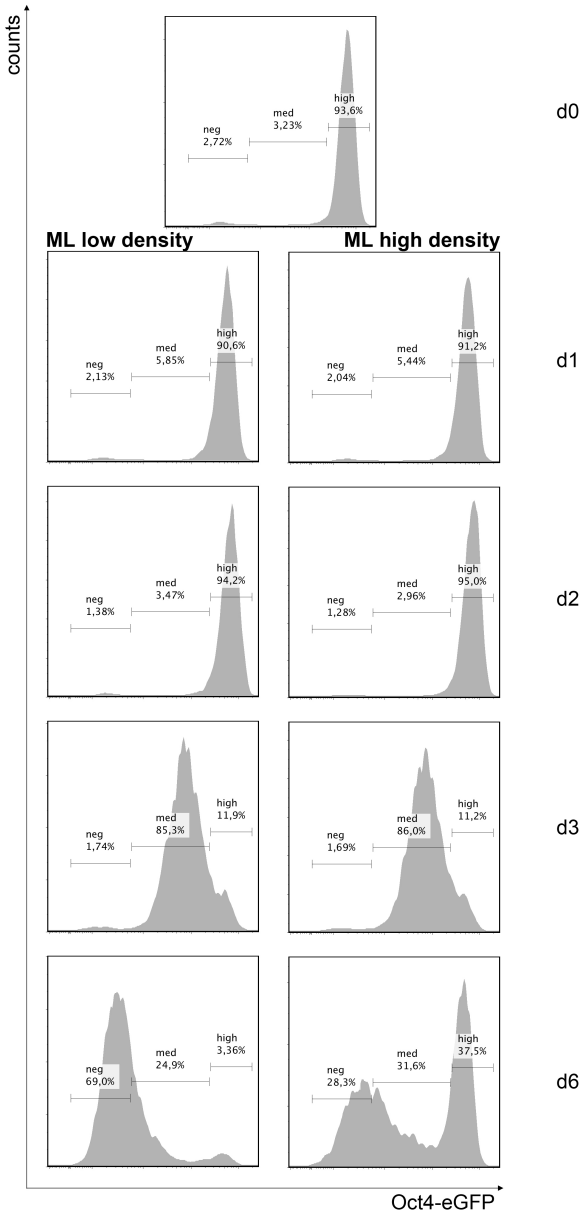

Figure 5.13: **ML differentiation cultures with confluence exhibit higher cellular heterogeneity than low-density ML cultures.** Oct4-eGFP transgene levels of undifferentiated OG2 ES cells (d0) and of differentiated cells were flow cytometrically determined. Expression levels are shown as histogram plots with gate frequencies for Oct4-eGFP^{negative}, Oct4-eGFP^{medium} and Oct4-eGFP^{high} subpopulations. ES cells were differentiated on TC-grade dish surfaces. Low density (left panel) cultures started with $1 \cdot 10^5$ cells for day 6 cultures, with $3 \cdot 10^5$ cells for day 3 cultures, with $5 \cdot 10^5$ cells for day 2 cultures or with $5 \cdot 10^5$ cells for day 1 cultures. High density (right panel) cultures started with $5 \cdot 10^5$ cells for day 6 cultures, with $6 \cdot 10^5$ cells for day 3 cultures, with $1 \cdot 10^6$ cells for day 2 cultures or with $>1 \cdot 10^6$ cells for day 1 cultures. (n=2).

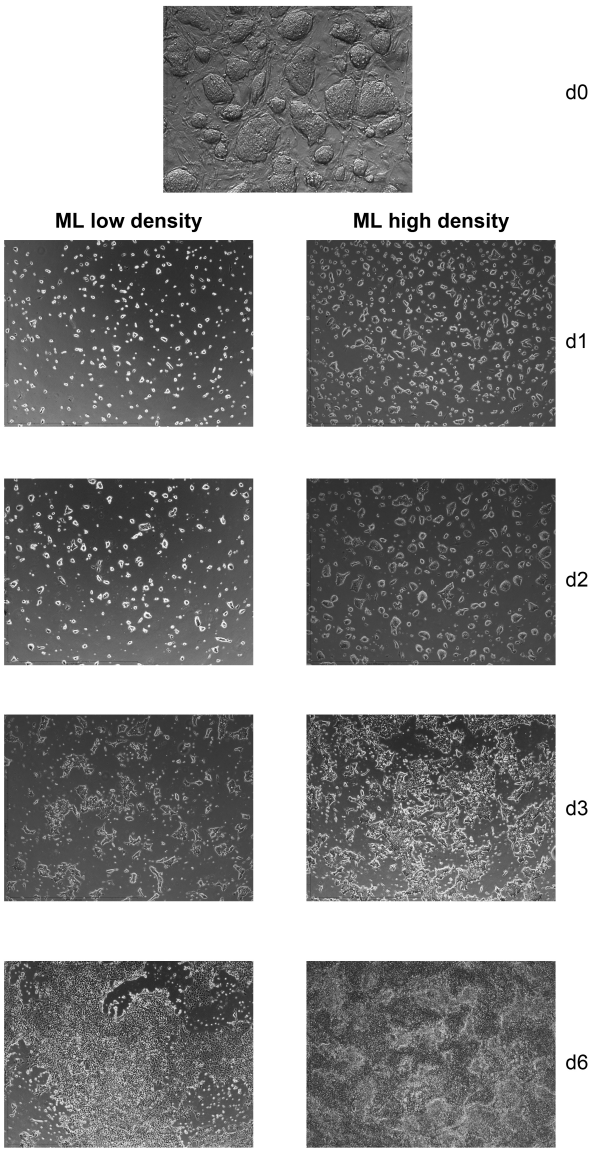

Figure 5.14: **ML differentiation cultures with confluence establish multilayer, colony-like growth properties.** Light microscopic photographs of undifferentiated OG2 ES cells and of ES cells differentiated under ML differentiation conditions at days 1 to 6. Low density (left panel) cultures started with $1 \cdot 10^5$ cells for day 6 cultures, with $3 \cdot 10^5$ cells for day 3 cultures, with $5 \cdot 10^5$ cells for day 2 cultures or with $5 \cdot 10^5$ cells for day 1 cultures. High density (right panel) cultures started with $5 \cdot 10^5$ cells for day 6 cultures, with $6 \cdot 10^5$ cells for day 3 cultures, with $1 \cdot 10^6$ cells for day 2 cultures or with $>1 \cdot 10^6$ cells for day 1 cultures. (n=2).

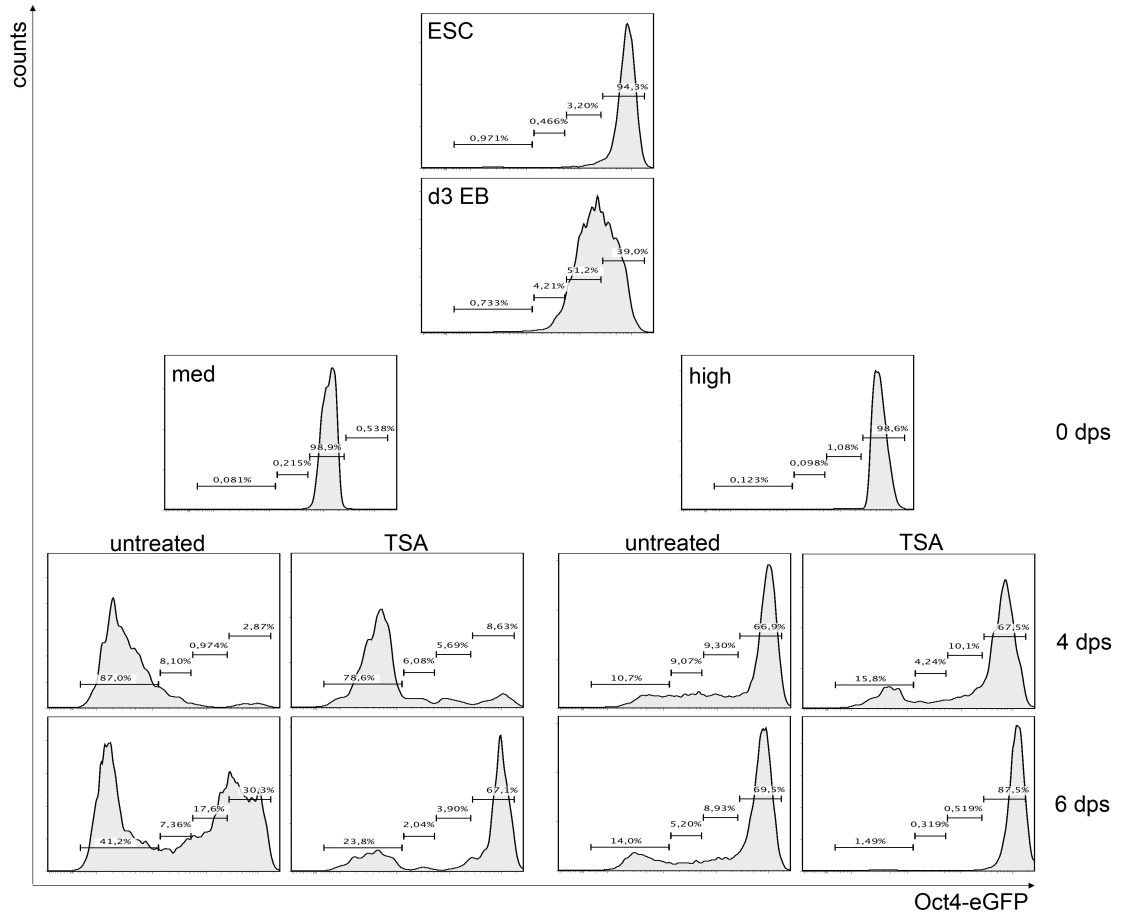

Figure 5.15: **Transient TSA treatment affects the frequency of Oct4-eGFP^{positive} cells in differentiated and rescued ES cell cultures.** Flow cytometrically Oct4-eGFP levels of the following cells were determined and plotted as histograms with gate frequencies of Oct4-eGFP^{negative}, Oct4-eGFP^{low}, Oct4-eGFP^{medium} and Oct4-eGFP^{high} cells: OG2 ES cells (ESC), HD EB cells after 3 days of differentiation prior to sort (d3 EB) and immediately post sort (*i.e.* 0 days post sort, [dps]) for medium (left panel) and high (right panel) eGFP levels. Also shown are Oct4-eGFP^{medium} and Oct4-eGFP^{high} sorted cells after 4 and 6 days of subsequent ES cell culture conditions (4 dps and 6 dps) without (untreated) or with (TSA) 24 h treatment with 20 nM TSA.

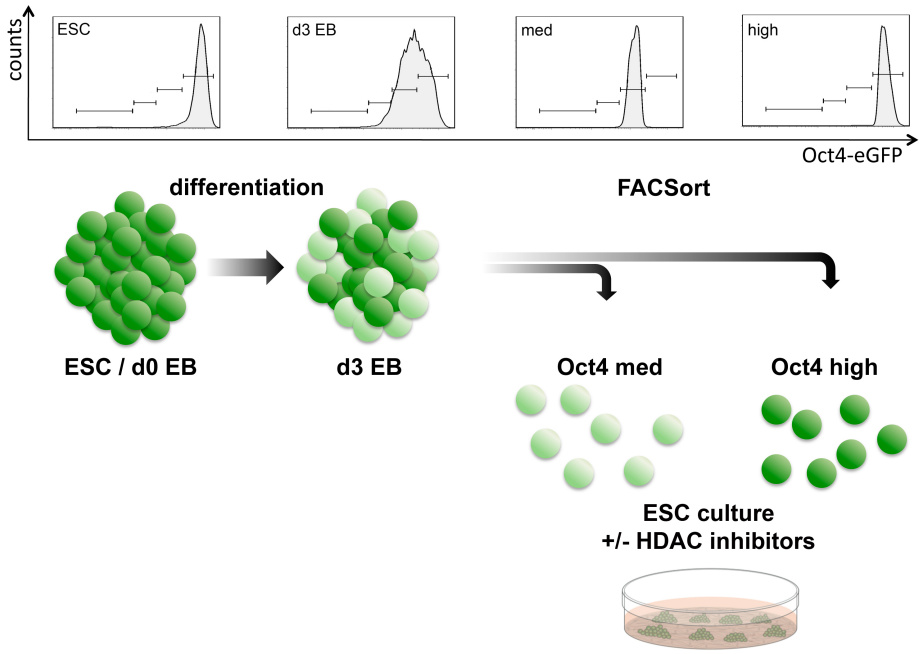

Scheme 5.2: **Experimental strategy for reversibility of Oct4-eGFP expression.** OG2 ES cells were differentiated for 3 days as HD EBs. Next, EBs were dissociated and cells were FACS-sorted into Oct4-eGFP^{medium} and Oct4-eGFP^{high} cells. Different numbers of sorted cells were cultured in the absence or presence of HDAC inhibitors under standard ES cell conditions for 2, 4 or 6 days before reanalysis for Oct4-eGFP expression by flow cytometry.

but not of Oct4-eGFP^{medium} and Oct4-eGFP^{high} cells was clearly reduced after 2 days of ES cell culture. The more cells were cultured the less Oct4-eGFP^{negative} cells were detected after 2, 4 and 6 days. Interestingly, after 6 days of culture at the lowest cell number (100 cells) the frequencies of Oct4-eGFP^{high} cells were at comparable low levels in untreated, in TSA- and in VPA-treated cell cultures. Further, the highest percentages of Oct4-eGFP$^{medium/high}$ cells were detected in HDAC inhibitor-treated samples with high cell number plateing.
These results indicate that Oct4-eGFP^{high} cells were probably a result of contaminating, selectively proliferating cells, because even after 6 days only few Oct4-eGFP^{positive} cells were detected when started with 100 cells. Additionally, the low percentage of Oct4-eGFP^{positive} cells in the 100 cells sample after 6 days suggests that HDAC inhibition did not lead to reprogramming of Oct4-eGFP^{negative} cells to Oct4-eGFP^{positive} cells. It rather seems that HDAC inhibition resulted in a selective killing of Oct4-eGFP^{low} cells which were virtually absent upon treatment. In summary, it could not be explicitly shown whether Oct4-eGFP expression can be re-established in differentiated ES cells, however, the analyses performed indicate that ES cell culture conditions can not re-establish Oct4-eGFP expression in ES cells which once had reduced their Oct4-eGFP levels.

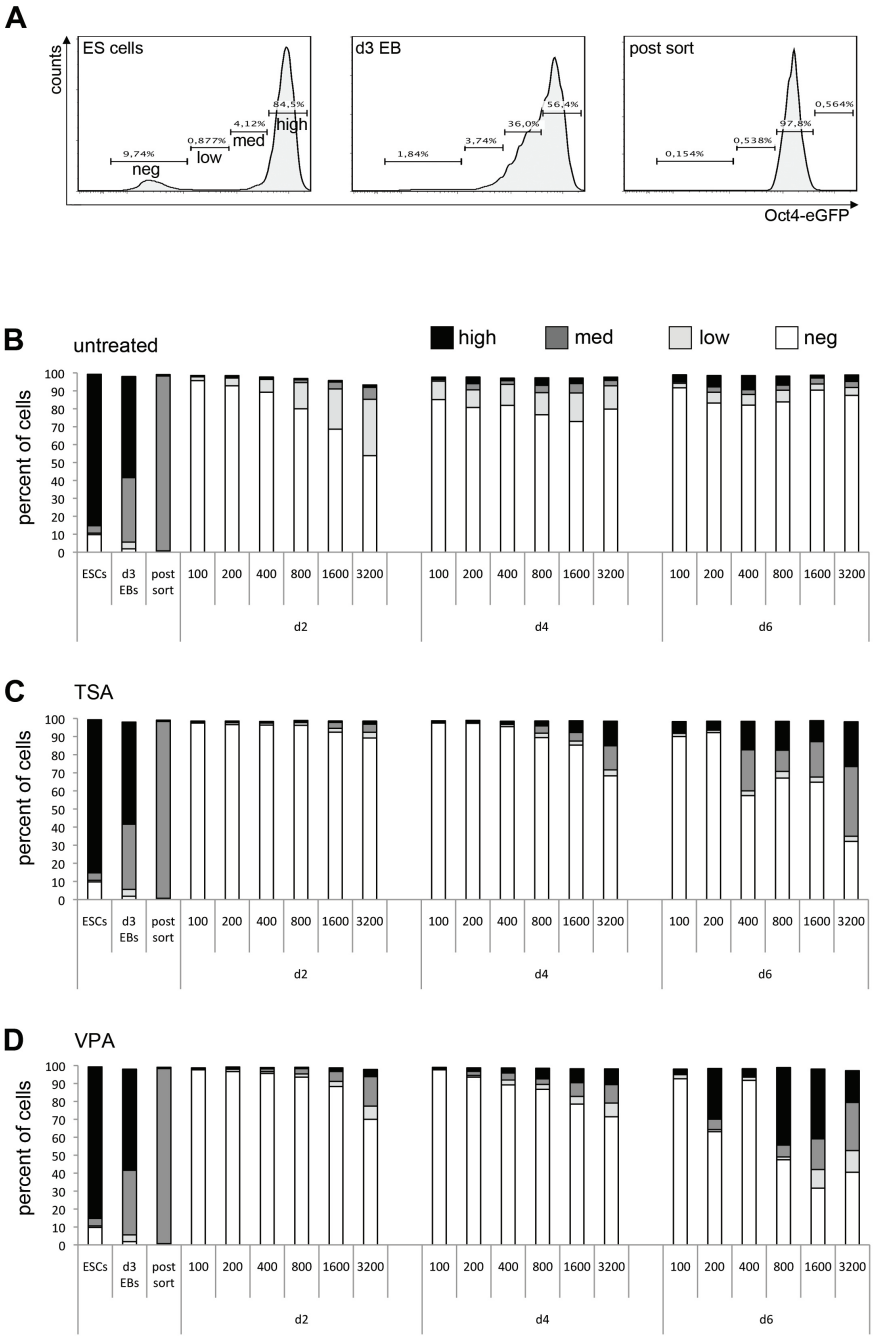

Figure 5.16: **Cell numbers and HDAC inhibitor treatment have an effect on the frequencies of Oct4-eGFP^{positive} cells in differentiated and rescued ES cell cultures.** A) OG2 ES cells were differentiated for 3 days as HD EBs and sorted for medium expression of Oct4-eGFP. Flow cyotmetric validation of Oct4-eGFP levels and gate frequencies of negative, low, medium and high subpopulations are displayed. B, C and D) Gate frequencies of Oct4-eGFP^{high}, Oct4-eGFP^{medium}, Oct4-eGFP^{low} and Oct4-eGFP^{negative} cells as defined in A) are summarized as bar diagrams. Different numbers of sorted cells were plated (100, 200, 400, 800, 1,600 and 3,200) and cultured under ES cell culture conditions. Cells remained either untreated (B) or cells were treated in the first 24 h post plating with 20 nM TSA (B) or 2 mM VPA (C). Oct4-eGFP levels were analyzed after 2, 4 and 6 days (d2, d4, d6).

5.4 Investigating the role of the Polycomb group protein EED in ES cells

Pluripotency is the central property of ES cells. It is lost when cells differentiate and become lineage-committed. While the genetic information of a cell remains unchanged, epigenetic mechanisms lead to altered chromatin states that affect gene expression and cellular function [163, 164, 165, 166, 167]. In ES cells the opposing histone modifications H3K4me3 and H3K27me3, which are simultaneously present at promoters of development-associated genes, form bivalent chromatin domains [119, 168, 120]. The PRC2 with its HMT EZH2 catalyzes the methylation of H3K27. The complex member EED is essential for a functional PRC2 complex [131] (Scheme 4.4). Here I analyzed the consequences of EED deletion on local and global chromatin structure and on the differentiation capacity of ES cells.

5.4.1 Local and global histone modifications

As the deletion of EED was reported to result in derepression of PRC2-target genes, I aimed to prove whether this was also true for the EED KO ES cells used in this study. To exclude for clonal variation of gene expression levels two wild type and two EED KO ES cell lines were analyzed in parallel. A customized real time PCR array with a panel of primers which are listed in Table 5.2 was performed. The array provides primers for genes that are associated with pluripotency, with differentiation, with chromatin modifications and with general cellular properties. Figure 5.17 shows the gene expression of two wild type and two EED KO ES cell lines relative to the housekeeping gene HPRT. Data sets were normalized to V6.5 wild type cells. However, the expression of several bivalently regulated genes could not be detected, because improper melting curves or Cp values did not allow analysis of the data (see Table 5.2). Probably, primers or PCR conditions were not optimal, though reactions were performed according to the manufacturer's protocol. Further, while expression levels of the two EED KO cell lines appeared to be similar, the two wild type ES cell lines exhibited variations for some genes, such as mixl1 or cdx2. Despite these limitations, it could be shown that expression levels of the pluripotency-associated genes oct4, myc, tert, dppa4, stat3, flp1l1 and ctr9 were not affected by EED KO, as reported previously (Figure 5.17 A). However, other pluripotency genes were up-regulated in EED KO ES cells: klf4, kit, tbx3 and tcl1 (Figure 5.17 A).
As expected, EED KO ES cells did not express eed, but normal levels of ezh2 and suz12 were observed (Figure 5.17 D). Interestingly, transcripts of the PRC1 member bmi1 were up-regulated in EED KO ES cells. Also expression levels of p16 from the Ink4a locus (Cdkn2a), for which Bmi1 is a transcriptional repressor, were elevated (Figure 5.17 C, D). Unexpectedly and in contrast to what was reported previously, an increase of expression (derepression) for the development-associated genes sox21, b-catenin, nestin, chordin, foxj3 or nodal was not observed (Figure 5.17 B). Further, transcript levels of pmaip1, which is a pro-apoptotic member of the Bcl-2 familiy, were increased in EED KO ES cells, while no elevated apoptosis rates were detected (Figure 5.17 D and data not shown).
Next, the effect of EED deletion was investigated on H3K27 trimethylation levels, as this modification is catalyzed by the PRC2. Local H3K27me3 levels at the transcriptional start sites (TSS) of differentiation-associated genes were analyzed by chromatin immunoprecipitation (ChIP) in wild type and EED KO ES cells. Figure 5.18 depicts the relative enrichment of the H3K27me3 modification at the TSS of sox21, bry, hoxa3 and pax5. In accordance to

Table 5.2: SABiosciences customized gene expression PCR array.

Category	Gene symbol	GenRefSeq	Synonym	Analyzable*
Pluripotency	Pou5f1	NM013633	Oct34	yes
	Sox2	NM011443		no
	Zfp42	NM009556	Rex1	yes
	Nanog	NM028016		yes
	Klf4	NM010637		yes
	myc	NM010849	c-myc	yes
	Sall4	NM175303		no
	Tert	NM009354	Telomerase	yes
	Dppa4	NM028610		yes
	Kit	NM021099	c-Kit	yes
	Tbx3	NM011535		yes
	Tcl1	NM009337		yes
	Stat3	NM011486		yes
	Fip1l1	NM024183		yes
	Ctr9	NM009431		yes
	Esrrb	NM011934		yes
bivalently regulated genes	Irx2	NM010574		no
	Dlx1	NM010053		no
	Nkx2.2	NM010919		no
	Sox21	NM177753		yes
	Zfpm2	NM011766		no
	Pax5	NM008782		no
	Lbx1	NM010691		no
	Evx1	NM007966		no
Primitive endoderm	AFP	NM007423	alpha fetoprotein	no
	Ctnnb1	NM007614	beta-catenin	yes
	GATA4	NM008092		no
	Sox7	NM011446		no
	Sox17	NM011441		no
	Mixl1	NM013729		yes
	GATA6	NM010258		no
Definitive endoderm	Foxa2	NM010446		no
	FABP1	NM017399	fatty acid binding protein 1	no
	FABP2	NM007980	fatty acid binding protein 2	no
	Hnf1b	NM009330		no
Ectoderm	Nes	NM016701	Nestin	yes
	Nog	NM008711	Noggin	no
	Tubb3	NM023279	beta-3-Tubulin	no
	Chrd	NM009893	Chordin	yes
	FoxJ3	NM172699		yes
	Otx2	NM144841		yes
Mesoderm	T	NM009309	Brachyury	yes
	Gsc	NM010351	Goosecoid	yes
	Acvr1	NM007394	Activin A receptor	yes
	nodal	NM013611		yes
	wnt3a	NM009522		no
	tgfb1	NM011577	TGF beta	yes
	bmp2	NM007553		no
	tal1	NM011527		no
Chromatin modifiers	eed	NM021876		yes
	ezh2	NM007971		yes
	suz12	NM199196		yes
	bmi1	NM007552		yes
	Ehmt2	NM145830	G9a	yes
	Kdm6b	NM001017426	Jmjd3	yes
	Kdm6a	NM009483	UTX	yes
	Kdm5a	XM359326	Jarid1a	yes
	HDAC1	NM008228		yes
	Dnmt1	NM010066		yes
	Dnmt3a	NM007872		yes
	Dnmt3b	NM010068		yes
	Smarca4	NM011417	BRG1	yes
	Smarca2	NM011416	BRM	no
	Mll1	NM001081049		yes
	Kdm1	NM133872	LSD1	yes
	Suv39H1	NM011514		yes
	Suv39H2	NM022724		yes
	Kdm4c	NM144787	Jmjd2c	yes
Others	Tcf4	NM013685		yes
	HoxA3	NM010452		no
	Sub1	NM011294	PC4	yes
	Cdx2	NM007673		yes
	Trp53	NM011640	p53	yes
	CDKN1A	NM007669	p21	yes
	Cdkn2a	NM009877	p16INK4a	yes
	cdk2	NM016756		yes
	Pcgf6	NM027654		yes
	Pcgf1	NM197992		yes
	Nsd1	NM008739	KMT3b	yes
	Tcf15	NM009328		yes
	Pmaip1	NM021451	Noxa	yes
	pten	NM008960		yes
Controls	B2M	NM009735	beta-2-microglobulin	yes
	HPRT1	NM013556	Hypoxanthine-guanine phosphoribosyltransferase	yes
	RPL13A	NM009438	60S ribosomal protein L13a	yes
	GAPDH	NM008084	Glyceraldehyde-3-phosphate dehydrogenase	yes
	ACTB	NM007393	beta-actin	yes

* data were considered not analyzable by following criteria: more than 1 melting curve peak or/and Cp > 30.

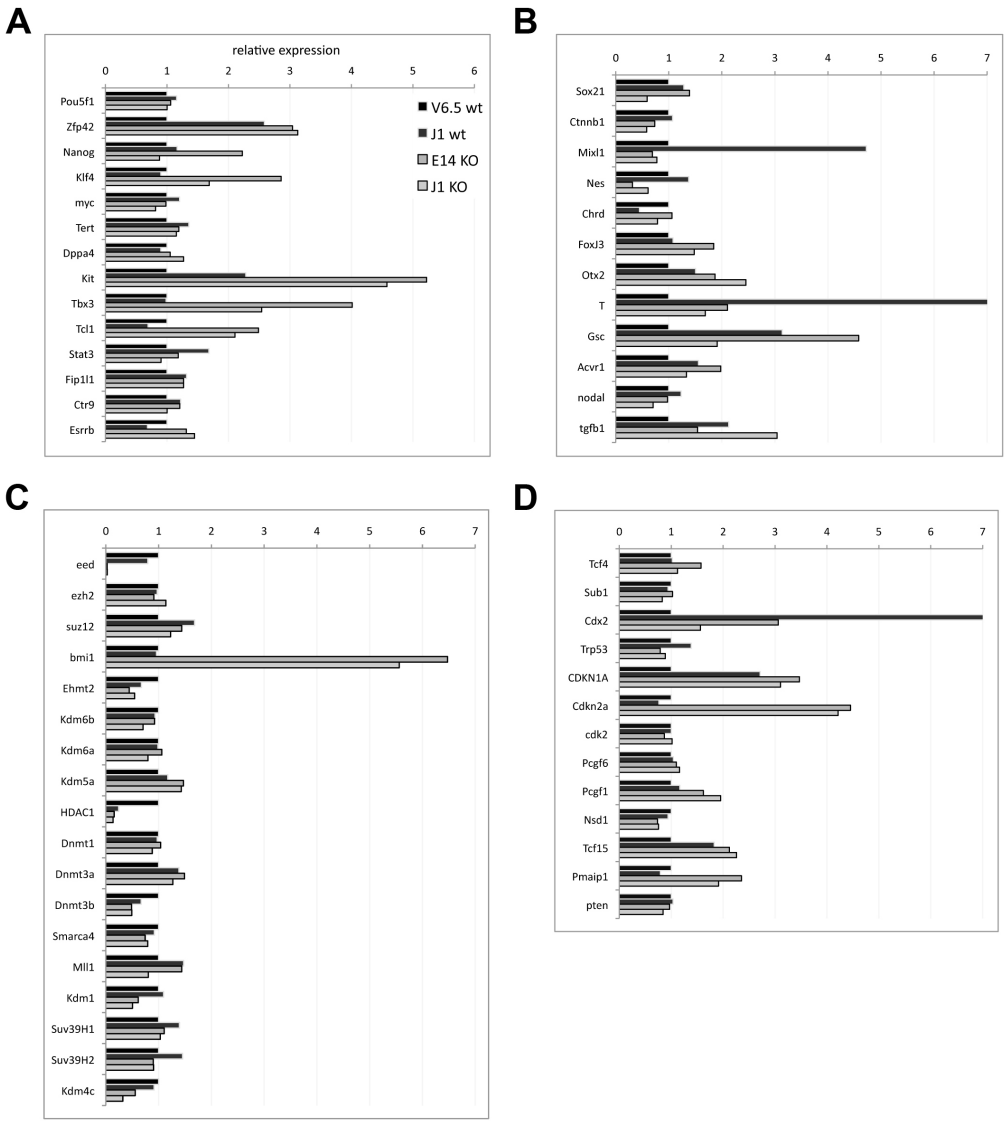

Figure 5.17: **Wild type and EED KO ES cells exhibit differential gene expression.** RNA of wild type (V6.5 and J1) and of EED KO ES cells (E14 and J1) was purified and reverse transcribed to cDNA. Real time PCR was performed in a 96 well customized PCR array format (SABiosciences, Table 5.2). Shown is expression relative to HPRT and normalized for V6.5 wild type ES cells by delta delta Cp calculation. Gene expression of the following categories are shown: A) Pluripotency-, B) Differentiation- and C) Chromatin modifier-associated genes, D) Other genes.

previous reports, upon ChIP of EED KO ES cells only low amounts of PCR fragments could be amplified, indicating the absence of the repressive modification at these genomic regions. In contrast, enrichment of the H3K27me3 modification at the TSS of these genes was detected in wild type V6.5 and J1 ES cells, as expected.
Western blot and chromatin flow cytometric analyses were performed on the two wild type and two EED KO ES cell lines to address the question of whether other histone modifications

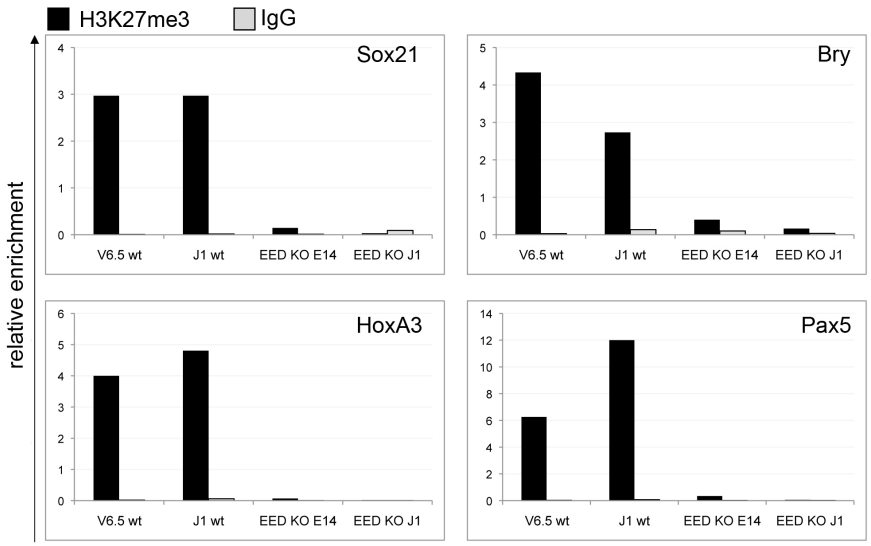

Figure 5.18: **EED KO ES cells exhibit reduced levels of H3K27me3.** Cross-linked and sheared chromatin of wild type ES cells V6.5 and J1 as well as of EED KO ES cells E14 and J1 was immunoprecipitated with anti-H3K27me3 or isotype control antibodies. Realtime PCR of the precipitated DNA was done with primers binding to transcriptional start sites of sox21, bry, hoxa3 and pax5 genes.

besides H3K27me3 were globally affected by EED depletion. As illustrated in Figure 5.19, ES cells lacking EED showed reduced H3K27me3 and slightly reduced H3K9me3 levels in comparison to wild type ES cells. Flow cytometry moreover revealed that the acetylation level of histone H4 at residues K8, 12 and 16 was elevated in EED KO cells while H3K4me3 levels remained unchanged (Figure 5.20).
By these analyses I could show that in EED KO ES cells the levels of the PRC2-catalyzed H3K27me3 modification were locally and globally depleted. However, the gene expression of *e.g.* sox21, whose TSS lacked H3K27me3, was not elevated. Additionally to H3K27me3, which is directly linked to PRC2, an increase of H4 acetylation levels and a decline of the repressive H3K9me3 modification were also observed. This indicates the existence of a crosstalk and close interdependence of histone modifying protein complexes as previously observed [169, 170, 171].

5.4.2 Global nuclear chromatin organization

While the effect of EED on local chromatin organization and histone modifications was well established in the last decade [131, 172], little is known about its role in the global chromatin architecture. Thus, I aimed to deeper analyze the chromatin of EED KO ES cells by microscopy. First the DNA of undifferentiated ES cell colonies grown on coverslips was visualized by DAPI staining. Figure 5.21 A shows exemplary colonies of V6.5 wild type and EED KO E14 ES cells. Heterochromatin regions, which comprise compact chromatin, and thus can be stained by DAPI, had different characters in wild type and KO ES cells. DAPI signals in wild type cells were equally distributed throughout the nucleus, forming

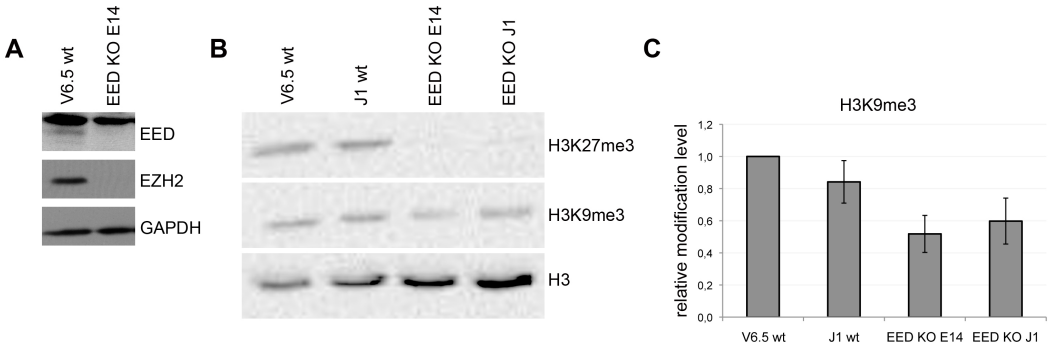

Figure 5.19: **Global levels of H3K27me3 and H3K9me3 are reduced in EED KO ES cells.** Whole cell lysates of wild type (V6.5 and J1) and EED KO ES cells (E14 and J1) were prepared. A) In V6.5 and EED KO E14 lysates EED, EZH2 and for loading control GAPDH were detected by Western blot. The EED-specific protein band runs below a larger unspecific band. B) H3K27me3, H3K9me3 as well as H3 were detected by Western blot. C) Relative intensities of H3K9me3 to H3 were obtained by densitometry of Western blot films. Values were normalized to V6.5 wild type cells. Results are displayed as bar diagram. Average and standard deviations of 4 experiments are shown.

small clusters that showed fuzzy boundaries. In contrast, in EED KO ES cells DAPI-stained areas appeared in larger and more defined clusters. An immunofluorescence analysis of the heterochromatin-associated H3K9 trimethylation affirmed that this modification was enriched in the DAPI^{positive} foci of both wild type and EED KO ES cells (Figure 5.21 B). Subsequently, the number of heterochromatin foci was counted per nucleus. Figure 5.21 C shows the distribution of heterochromatin foci as a histogram. While wild type ES cells exhibited a wide range of nuclei with varying numbers of heterochromatin foci, EED KO ES cells had a smaller variability and fewer heterochromatin foci. Figure 5.21 D gives the corresponding statistical analysis and demonstrates that the average number of heterochromatin foci in wild type ES cell nuclei is significantly higher than in EED KO ES cells. Simultaneously the mean area of single foci was quantified. The results are summarized in Figure 5.21 E. The average size of individual heterochromatin regions in EED KO ES cell nuclei was significantly larger than in wild type cells.

As cells show distinct grades of chromatin compaction during different phases of the cell cycle, the altered heterochromatin organization in EED KO ES cells could be the result of a cell cycle arrest. To analyze whether this is the case, DNA content was analyzed by flow cytometry in wild type and EED KO ES cells. Figure 5.21 F summarizes cell cycle profiles and gives percentages of cells in G1, S and G2 phase. Wild type cells comprised more cells in S phase (48.8% wt *versus* 31.1% EED KO), while EED KO ES cells contained more cells in G1 and G2. However, EED KO ES cells were not arrested in cell cycle, but showed a typical cell cycle profile for ES cells. Hence, the observed heterochromatin foci were presumably not the result of cell cycle-dependent DNA condensation.

These analyses show that the loss of EED led to an altered nuclear chromatin assembly, reflected by less and larger heterochromatin foci. However, as reduced global levels of the heterochromatin-associated H3K9me3 were observed in EED KO ES cells, this indicates that not more heterochromatin is established in EED KO cells but rather that chromatin is reorganized.

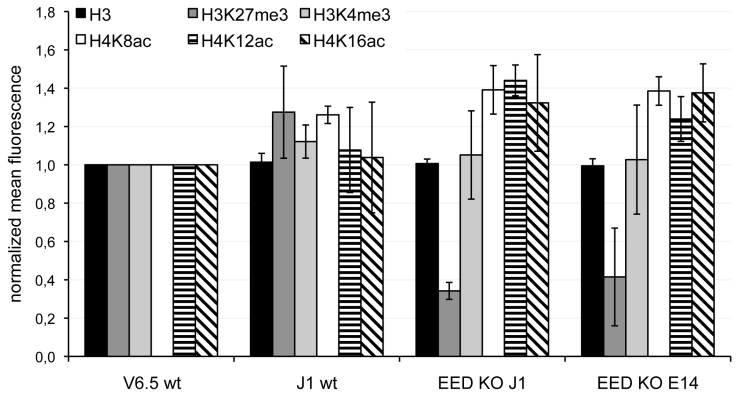

Figure 5.20: **Global levels of H4 acetylation are increased in EED KO ES cells.** Wild type (V6.5 and J1) and EED KO ES cells (E14 and J1) were subjected to chromatin flow cytometry using protocol A (see Material and Methods) and antibodies specific for H3, H3K27me3, H3K4me3, H4K8ac, H4K12ac and H4K16ac. Mean fluorescence values were normalized to V6.5 wild type levels. Average and standard deviations of 3 individual experiments are shown.

It was previously reported that ES cell chromatin shows a high degree of plasticity and is less compacted than the chromatin of committed cells to allow differentiation pathways into various directions [104]. As the observed heterochromatin structure of EED KO ES cells was more similar to differentiated cells the EED KO chromatin phenotype was further analyzed with respect to its dynamics. To this end, V6.5 wild type and EED KO E14 ES cells were transiently transfected by electroporation with a construct that contains the linker histone H1 fused to GFP. Transfected cells were subjected to FRAP analyses. The time required for fluorescence recovery after photobleaching was measured in individual ES cells. Analyses are summarized in Figure 5.21 G. The data show that fluorescence recovery of H1-GFP in V6.5 ES cells is faster than in EED KO ES cells. The time needed for 50% of total recovery was more in EED KO ES cells. However, both wild type and EED KO ES cells showed recovery rates of about 100%, indicating large proportions of mobile chromatin fractions. This result suggests that due to EED deletion not the proportion of the immobile fraction was increased. In contrast, differentiated cells were shown to have immobile chromatin fractions, resulting in incomplete FRAP recovery rates [104].
Together, heterochromatin foci in EED KO ES cells appeared more defined and distinct as compared to wild type cells, and the chromatin mobility was delayed. These characteristics are similar to but not completely matching properties of differentiated cells, indicating an intermediate state of EED ES cells between pluripotent and differentiated cells.

5.4.3 Differentiation potential of EED KO ES cells

To assess the functional consequences of EED deletion I next aimed to analyze the *in vitro* differentiation capability of EED KO ES cells. The morphology of either wild type or EED KO ES cell cultures was similar and indistinguishable (Figure 5.22 A). However, if cultures reached a critical level of confluence, wild type ES cells usually showed first signs of differentiation

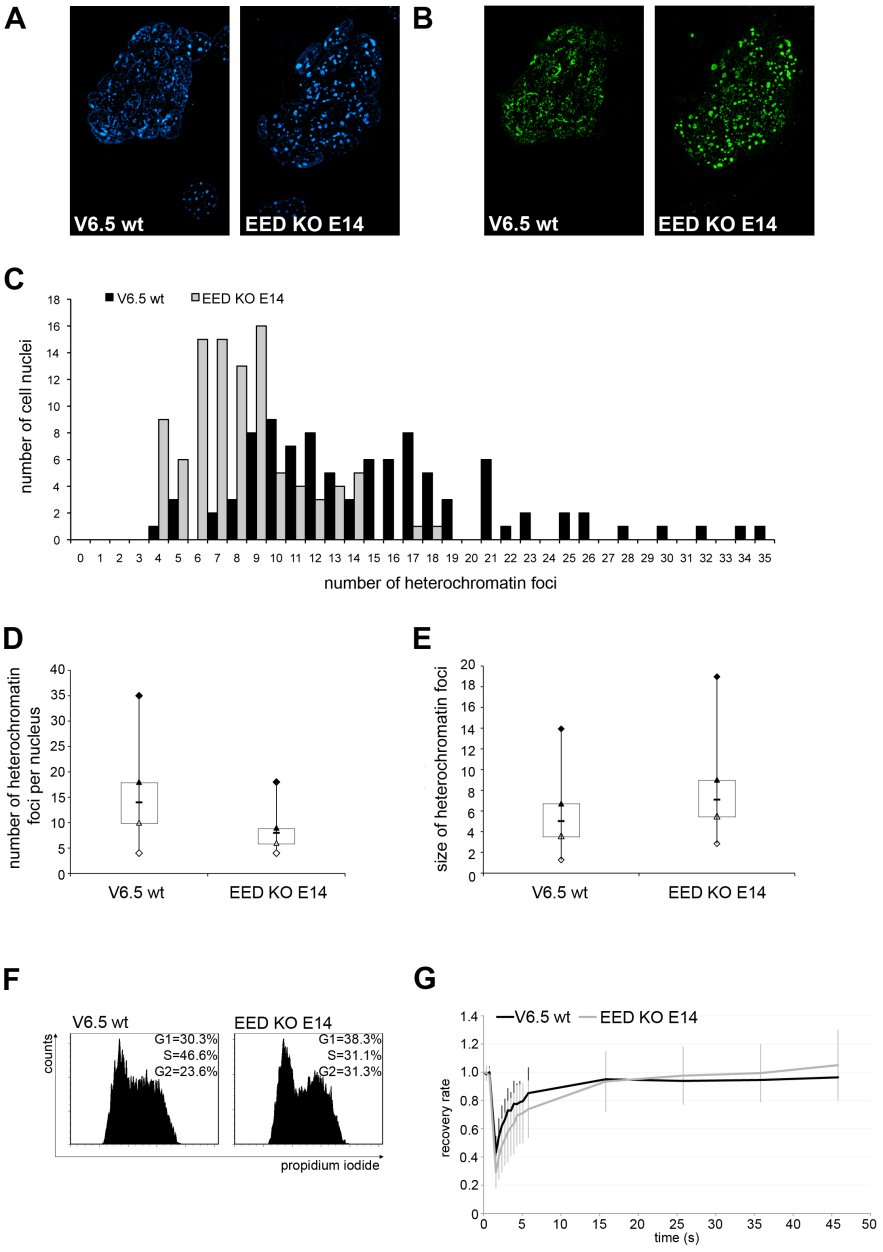

Figure 5.21: **Wild type and EED KO ES cells show different nuclear chromatin organization and dynamics.** Wild type V6.5 and EED KO E14 ES cell colonies were fluorescently stained with A) DAPI and B) with primary anti-H3K9me3 and secondary anti-rabbit-Cy2 antibodies. C) $DAPI^{positive}$ heterochromatin foci were enumerated by ImageJ software analyses. Displayed is a histogram giving the numbers of heterochromatin foci and the corresponding number of cell nuclei ($n_{wt} = 95$, $n_{KO} = 97$). D) Box plot (shown are maximum, 3rd quantile, median, 1st quantile, minimum) summarizing the number of heterochromatin foci per nucleus in V6.5 wild type and in EED KO E14 ES cells ($p < 0.001$) E) Box plot summarizing the size (*i.e.* area) per heterochromatin focus in arbitrary units. ($p < 0.001$). F) DNA of V6.5 wild type and EED KO E14 ES cells was flow cytometrically stained with propidium iodide. G1, S and G2 cell cycle phase distribution was calculated. (n=2) G) V6.5 wild type and EED KO E14 ES cells were transiently transfected with a transgenic vector containing H1-GFP. One day post transfection cells were subjected to FRAP analysis. Equally sized regions were bleached with equal laser settings and fluorescence was measured before and until 45 s after bleaching. Initial fluorescence intensity was normalized to 1 (($n_{wt} = 8$, $n_{KO} = 12$)).

with flattened and frayed colony boundaries, while these features were not observed in EED KO ES cell cultures (data not shown). By applying the 'beating body' differentiation assay, the morphology of EBs in suspension and upon transfer to adherent culture conditions were compared, as displayed in Figure 5.22 A. After clustering in HDs (day 2), EED KO E14 ES cells formed EBs of comparable size to wild type ES cells. But in the subsequent days of differentiation EED KO cells failed to proliferate and were hardly able to spread on the TC dish surface as attached EBs. Further, the contracting properties of EBs derived from wild type and EED KO ES cells were quantified (Figure 5.22 B). The two wild type cell lines exhibited different efficiencies and dynamics of 'beating body' formation. While 100% of J1 EBs were contracting at day 8 of differentiation, a maximum of 30% of V6.5 EBs were contracting at day 14 of differentiation. In contrast, no 'beating bodies' could be detected in EED KO ES cell-derived cultures even after a total differentiation period of 23 days.
ES cells and cells differentiated for 3 and 7 days were then subjected to a colony formation

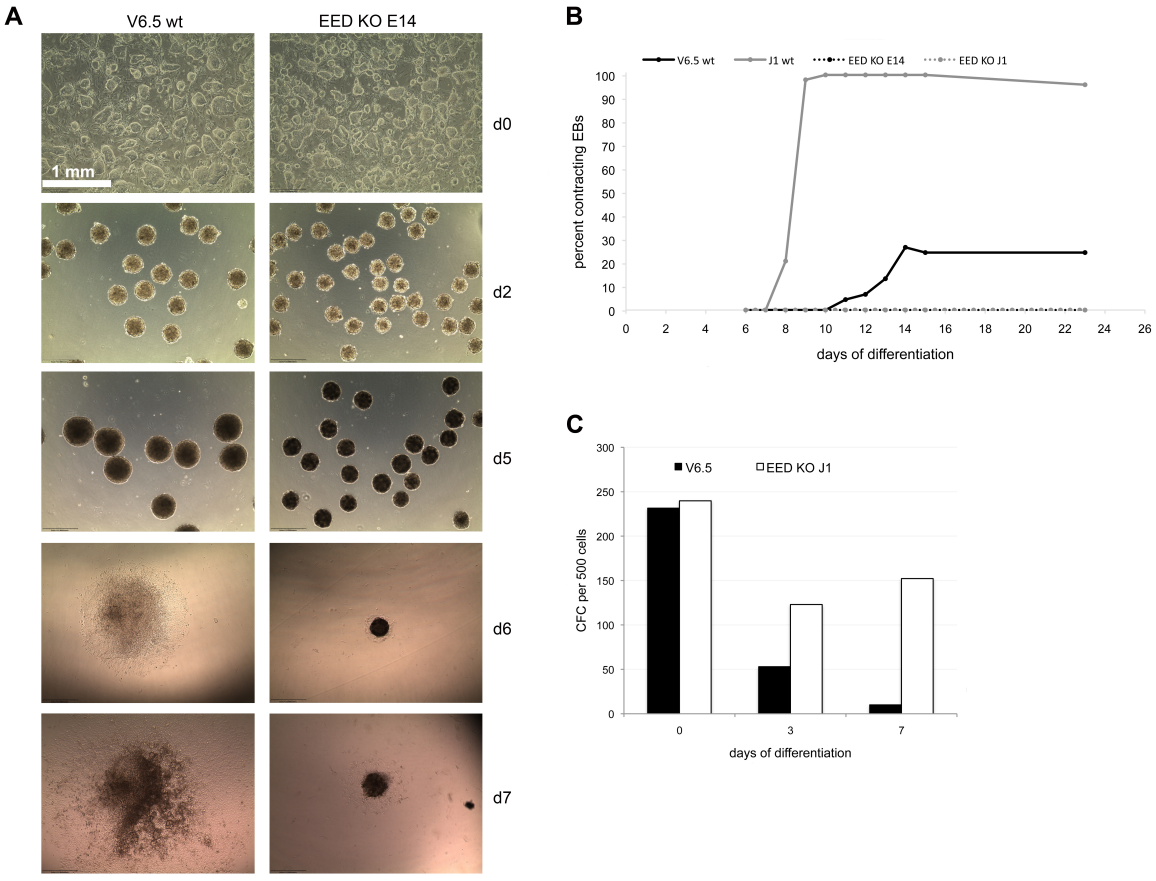

Figure 5.22: **EED KO ES cells have impaired differentiation properties.** Wild type V6.5 and EED KO E14 ES cells were differentiated as HD EBs and allowed to attach to gelatin-coated TC plastic at day 5 for the formation of contracting 'beating bodies'. A) Light microscopic photographs of wild type and EED KO ES cells (d0) and of EBs (d2, 5, 6 and 7). B) Displayed are the days of differentiation with the corresponding percentage of microscopically examined wells which contained contracting EBs. C) An AP colony formation assay was applied to wild type and EED KO ES cells (d0) as well as to 3- and 7-day old EB cells. Colonies were counted after 4 days of culture and subsequent staining for AP activity.

assay, to test whether their self renewal potential was reduced upon differentiation. As shown in Figure 5.22 C the colony formation capacity of wild type and EED KO ES cells was similar. But while wild type cells showed progressively decreasing numbers of CFCs during differentiation, EED KO cells retained a considerable proportion of CFCs even after 7 days of culture without LIF and feeder cells.
From these data I conclude that the differentiation of ES cells without EED is severely affected, with an inability to differentiate into functional cardiomyocytes *in vitro* and with a particular resistance to differentiation-induced loss of self renewal capacity.

6 Discussion

In the course of this thesis, I analyzed undifferentiated and differentiating stem cells with respect to gene expression, chromatin state and differentiation potential. Therefore protocols for the assessment of global histone modification levels in individual cells by flow cytometry were successfully established and applied to differentiating ES cell cultures, to BM cells and to EED KO ES cells. The data provide evidence that upon HDAC inhibitor treatment of BM cells the frequency of cells with *in vitro* and *in vivo* hematopoietic activity was augmented due to selective survival. Further, the results show that ES cells lost functional pluripotent character after 2 days of differentiation, while the silencing of pluripotency marker expression was delayed. The utilized differentiation protocol was shown to be determinant for the progression of differentiation. After 3 days of differentiation ES cells failed to re-activate Oct4-eGFP transgene expression when placed into ES cell culture conditions, indicating the loss of pluripotency. Finally, the analyses of ES cells lacking the PRC2 core subunit EED revealed a reorganization of heterochromatin with delayed chromatin mobility and severe differentiation deficits.
The following paragraphs discuss the results on histone acetylation, on emerging cellular heterogeneity during ES cell differentiation, on the role of EED in ES cells and on the end of pluripotency.

6.1 Histone acetylation and HDAC inhibition in stem cells and committed cell types

Parts of my work comprised the analysis of histone acetylation in hematopoietic and embryonic stem cells and their differentiated derivatives. Generally the acetylation of histones entails the expression of genes located in proximity [173].
By the optimization of flow cytometric protocols for intranuclear antigen detection I was able to analyze global histone modification levels (Figure 5.1, 5.2 and 5.3). This method can uncover distinct levels of modifications within heterogenous cell populations which is virtually not possible by Western blot. Though restricted to the detection of global modification levels without giving values for single gene loci like in ChIP approaches [174], the methodology has the potential to distinguish between subpopulations because of the advantageous multiparametric and graded analysis. Applying chromatin flow cytometry emerging subpopulations, which differed in global H3K9 acetylation levels, could be detected in differentiating ES cell cultures. SSEA1^{positive} cells (assumed to be undifferentiated cells) exhibited high global levels of H3K9ac, while SSEA1^{negative} cells (assumed to be differentiated cells) showed lower levels (Figure 5.3). However, as indicated by the asymmetric histogram curve, not all SSEA1^{negative} cells had comparably low global H3K9 acetylation levels. Cells with high H3K9ac and low SSEA1 levels might represent an additional transient subpopulation. Various reports describe changes of histone acetylation upon ES cell differentiation. McCool *et al.* observed augmented H4 acetylation in 4-day differentiated CCE murine ES cells [175], Golob *et al.* found increased

levels of H3K9ac in day 4 EBs of R1 mouse ES cells [103], whereas Lee *et al.* report strongly reduced levels of H3K9ac and pan-acH4 in differentiated CCE ES cells [106].
Even though the hyperdynamic state of ES cell chromatin is well established in the field [104], there are not only controversial results on histone acetylation but also on the overall transcriptional activity in ES cells as compared to their differentiated progeny. Elfroni *et al.* report high total mRNA levels in ES cells, while Sampath *et al.* find increased transcription and translation activity in EB cells as compared to undifferentiated ES cells [102, 176].
Interestingly, analyzing adult hematopoietic stem cells, no differences of global H4 acetylation levels in immature Lin^- *versus* committed Lin^+ BM cells were observed here, even though HDAC activity was higher in Lin^- than in Lin^+ cells (Figure 5.4 and 5.5). Based on the balanced equilibrium between histone acetylation and deacetylation, one could speculate that the opposing enzymatic activity of HATs, which could not successfully be analyzed here, is likewise increased yielding similar net global acetylation levels. High activity and metabolic rates of chromatin modifying enzymes might reflect the specific plasticity of chromatin states that enables stem cells to immediately react to intrinsic and extrinsic signals, *e.g.* by modifying crucial molecular players in order to switch the cell's chromatin and transcription. High levels of HDAC activity in Lin^- cells could further explain why immature cells selectively survived the HDAC inhibitor treatment, while mature Lin^+ cells became apoptotic (Figure 5.6). If more HDAC activity than necessary is present in Lin^- cells, HDAC inhibition will not immediately be detrimental for the cells' survival. Indeed, it could not be shown whether the elevation of histone acetylation or the selective survival of undifferentiated cells or both of it explain the relative enrichment of progenitor cells upon TSA treatment.
Similarly, in HDAC inhibitor-treated differentiated ES cell cultures I observed that Oct4-eGFP$^{medium/high}$ cells selectively survived while Oct4-eGFP^{low} cells died (Figure 5.15 and 5.16). The assessment of HDAC as well as of HAT activities in Oct4-eGFP^{high} and Oct4-eGFP^{low} cells or in SSEA1^{positive} and SSEA1^{negative} cells could further elucidate whether global histone acetylation in adult and embryonic stem cells is regulated in a similar fashion.
However, treatment of murine ES cells with TSA was reported to induce a differentiated morphology of ES cell colonies and to elevate expression of differentiation-associated genes while expression of pluripotency markers was reduced [175, 177]. In contrast, Ware *et al.* showed that the inhibition of HDACs by TSA and sodium butyrate in human and mouse ES cells increases their self renewal potential [178].
The global inhibition of HDACs is a harsh intervention in the global chromatin architecture. Despite their similarity in inhibiting HDACs, different small molecules have distinct dose-dependent side effects, including the induction of apoptosis. Different cell types can respond differently to HDAC inhibition: MEFs transduced with Oct4, Sox2, Klf4 and c-Myc are more effectively reprogrammed to iPS cells, while U937 leukemic cells undergo apoptosis and human cord blood-derived $CD34^+$ cells increase in numbers *ex vivo* [68, 98, 100].
In summary, high global levels of histone acetylation are not a general prerequisite of undifferentiated stem cells. Presumably, the sum of local histone acetylation marks at regulatory sites of particular genes are more important indicators for cellular identities.

6.2 Cellular heterogeneity in differentiating ES cell cultures

Even though mouse ES cell lines are of clonal origin and individual cells of one line are genetically identical, there is pronounced variation within cultures of a given cell line. Even

within one ES cell colony cells differ. This is not only the result of the cell's position within an individual colony, *i.e.* central or rather marginal [179], or the cell cycle stage. Recently it became obvious that mouse ES cell cultures are heterogeneous for the expression of genes like SSEA1, Stella, Rex1 and Nanog. Levels of these proteins fluctuate between low and high levels [32, 33, 34, 35, 36]. This fluctuation is likely to be the result of ES cells differentiating to epiblast-like cells and *vice versa* [36].
Assessing SSEA1 levels in undifferentiated ES cells it could be shown here that the cultures comprised cells with high and medium SSEA1 surface expression (Figure 5.8). Unexpectedly, the degree of SSEA1-heterogeneity was reduced after 1 day of EB differentiation. Under these conditions the percentage of SSEA1^{high} cells was elevated about 2-fold from 35% to 75%. I also observed increased frequencies of Oct4-eGFP^{high} cells after 1 day of HD EB differentiation (86% to 92%, Figure 5.11). Hence, this phenomenon could be explained in part by either residual feeder cells in undifferentiated samples or by an activating effect of the fresh medium on pluripotency marker expression. However, in case of SSEA1 the apparent shift towards more cells with high levels of SSEA1 must be the result of enhanced expression of SSEA1 on the surface of cells that had formerly medium levels of SSEA1. Otherwise more than 50% of cells (*i.e.* SSEA1^{medium} ES cells) must have died within 1 day, which could not be affirmed by the analysis of cell numbers (Figure 5.7). Therefore I hypothesize that the aggregation of ES cells to an EB in the first days of differentiation provides a microenvironment similar to ES cell culture conditions, that promotes and maintains pluripotency markers. Additionally, Oct4, Sox2, Nanog and Rex1 gene expression was elevated at day 1 of differentiation (Figure 5.9). Interestingly, functional parameters characterizing pluripotency were remarkably reduced after 1 and 2 days of differentiation (Figure 5.10), indicating that the presence of putative pluripotency markers (SSEA1, Oct4-eGFP or Nanog, Rex1, Sox2) is not stringently linked to a cell's function. Notably, the same cells were subjected both to functional and expression-based analyses, thus excluding potential variations in differentiation progression between individual experiments.
Next, by analyzing Oct4-eGFP levels of OG2 cells the impact of distinct differentiation methods on the loss of pluripotency was demonstrated, monitored by the loss of Oct4-eGFP. It became apparent that the HD EB differentiation method, which was also used for the experiments discussed above, resulted in a considerable heterogeneity with respect to Oct4-eGFP levels (Figure 5.11). Thus, both gene expression and functional analyses were performed with a heterogeneous mixture of cells at distinct states of differentiation. Further, cells which after 7 days of differentiation were still positive for Oct4-eGFP resided particularly in the central parts of EBs (Figure 5.12). In contrast, EBs formed by clonal proliferation in semisolid medium, that avoids the random movement and mutual clustering of single cells, homogeneously lost Oct4-eGFP. These cultures contained no Oct4-eGFP^{positive} cells after 7 days of differentiation. This strong and steady differentiation progression can be the consequence of a lack of nutritions because EBs in MC are not supplied with fresh medium, while HD EBs received fresh medium 2 days after differentiation initiation. Alternatively, as ES cells are kept separated in MC cultures this might favor fast differentiation in the absence of LIF. To test for the latter possibility I applied an alternative differentiation method with OG2 ES cells: ML cultures were seeded with either low or high cell densities. Consistently, uniform and homogeneous differentiation was observed when started with few cells. The degree of heterogeneity was higher in ML cultures with high cell densities (Figure 5.13 and 5.14).
Together, these results suggest the existence of an *in vitro* environment with soluble factors that act auto-/paracrinely potentially including cell-cell contacts. These conditions can par-

tially maintain pluripotency marker expression even in the absence of LIF. Indeed, Davey *et al.* showed that besides the exogenous LIF growth factor which is withdrawn to initiate differentiation another ligand for the LIF receptor gp130 exists in ES cell cultures, which is secreted by ES cells [179, 180]. Thus, especially differentiating ES cells in the inner parts of EBs have 3 dimensionally contact to other ES cells. Cells are therefore highly exposed to secreted extracellular matrix. In addition to soluble factors and their receptors, also the mutual contacts between cell-adhesion molecules of neighboring cells could sustain the expression of pluripotency markers. Recently, the expression of E-cadherin and the E-cadherin-mediated cell-cell contact was reported to be beneficial if not essential for reprogramming of MEFs to iPS cells [181, 182, 183]. In addition, it was described that adhesion molecules like CD9 and Pecam1 are down-regulated in differentiating ES cells suggesting their importance for the undifferentiated state [184]. One might speculate, that the lack of cell-cell communication of differentiating ES cells hindered to mutual adhesion by either semisolid medium or low cellular density on TC plastic surface, accelerates the loss of pluripotency. Further analyses in the course of B. Jakob's Master thesis in our lab underlined this idea as the colony formation capacity declined faster in low density ML than in HD EB differentiation cultures [185].
Additionally, not only epigenetic regulation but also genetic changes might lead to heterogeneity in ES cells or their differentiation daughter cells. Ensenat-Waser *et al.* notice residual Oct4-eGFP^{positive} cells in differentiated ES cell cultures. The cells were resistant to *in vitro* differentiation due to a recurrent gain of chromosomes 8 and 9 [186]. However, as the authors used an unrelated cell line and as I could show an almost complete Oct4-eGFP loss upon differentiation, I assume that the heterogeneity observed here was due to cell-cell proximity effects than to alterations of the karyotype.
Finally, focusing on undifferentiated ES cells, it became clear that not every single ES cell exhibited *in vitro* pluripotency-associated functions: for example only 40 out of 100 V6.5 ES cells formed ES cell colonies and only 60 of 1,000 V6.5 ES cells formed EBs (Figure 5.10). This reflects a functional heterogeneity in undifferentiated ES cell cultures which probably is the result of heterogeneous cell states.
Altogether, cellular heterogeneity is characteristic for ES cell cultures and it is based on epigenetically mediated fluctuation of gene expression. Upon differentiation the degree of heterogeneity increases especially if cells remain in contact. For directed differentiation approaches (*e.g.* towards neural cells) this finding might help to establish protocols that give rise to homogeneously differentiated cells, with low numbers of teratoma-forming ES-like cells. Alternatively, the application of a differentiation protocol which leads to considerable heterogeneity could be used to obtain rare cell types that need the support by other cell types. In the end, it is beneficial for all research on ES cell differentiation to consider differentiation conditions.

6.3 Role of PRC2 in ES cell chromatin and function

To maintain pluripotency ES cells must conduct a defined molecular program that upon cell division enables the heritage of self renewal and differentiation potential. Therefore genes which are responsible for differentiation must be efficiently repressed without permanent silencing to allow for future expression. The PRC2 is essential for H3K27 trimethylation which serves as a reversible, repressive modification [131]. In ES cells lacking EED other core subunits of PRC2 are depleted on the protein level while their RNA remains transcribed

[131, 187]. Consequently, H3K27 methylation is almost absent in EED KO ES cells and the expression of PRC2 target genes was reported to be elevated [188].
In the scope of this thesis I confirmed that EED RNA and protein were depleted in EED KO ES cells (Figure 5.17 and 5.19) and that the HMT EZH2 was expressed on RNA level while EZH2 protein could not be detected (Figure 5.17 and 5.19). In parallel, H3K27 trimethylation levels were strongly reduced (Figure 5.18, 5.19 and 5.20). Despite the local absence of the repressive H3K27me3 mark at the transcriptional start sites of bivalently regulated genes like Sox21 or Bry, no derepression of these genes was observed, which is contradictory to the existing literature (Figure 5.17 and 5.18) [120, 119]. It can be speculated that in other studies different cell lines were used and that not all known bivalent genes show elevated transcription upon PRC2 depletion. Perhaps other repressive epigenetic mechanisms compensate the loss of PRC2. Alternatively, different culture conditions (media, feeders) or passage numbers influence the cells' transcriptome. EED KO ES cells like their wild type counterparts grew as morphologically undifferentiated colonies with typical ES cell morphology and AP activity (Figure 5.22). In contrast to some reports I did not observe a flattened colony morphology commensurate to differentiated cells [119]. The expression levels of pluripotency genes were similar to wild type cells or even elevated and the colony formation capacity was unaffected by EED KO (Figure 5.17 and 5.22). Wild type and EED KO ES cells proliferated at comparable levels and exhibited similar cell cycle distributions (Figure 5.21). These observations indicate that EED KO ES cells can be expanded and cultured in an undifferentiated pluripotent state. This is further supported by the fact that EED KO ES cells can be maintained under groundstate pluripotency culture conditions in the presence of MEK and GSK3 inhibitors [37] (preliminary data). It was earlier shown by Chamberlain *et al.* that ES cells without EED can contribute to chimeric mice up until embryonic day 12.5 [150]. Even though the authors claim that due to this finding EED is dispensable for pluripotency, this was not proven. The generation of life-birth following complementation of tetraploid blastocysts, the most stringent test for pluripotency, was not performed [42]. A recent report by Pereira *et al.* describes the requirement of EED for successful reprogramming of B cells following cell fusion [148]. Along these lines, it was shown that the transcription of EED is directly controlled by STAT3 and Oct4 in ES cells [147]. These findings indicate EED's important role for maintenance of the molecular pluripotency program in ES cells.
Though EED KO ES cells if cultured under ES cell conditions in the presence of LIF show typical characteristics of pluripotent cells, they have deficits in differentiation. This is reflected by the inability to give rise to alive offspring upon blastocyst injection, the inability of forming contracting cardiomyocytes *in vitro* and the persisting colony forming cells after 7 days of *in vitro* differentiation [150] (Figure 5.22). While the effect of EED deletion on the state of pluripotency seems mild, differentiation is compromised. Thus, EED KO ES cells exhibit problems to exit the pluripotent groundstate. Therefore, I hypothesize that PRC2 is not only involved in the repression of developmental genes in ES cells but EED is also essential for the silencing of genes during differentiation. It is known that *e.g.* the Oct4 promoter becomes H3K27 trimethylated during differentiation [146]. Oct4 gene expression must be silenced via alternative mechanisms in EED KO ES cells.
Besides the consequences of EED deletion on gene expression and cellular function, also the global chromatin in EED KO ES cells was analyzed. So far little is known about the role of PRC2 on the global nuclear organization of chromatin. Global levels of acetylated histones were increased (Figure 5.20). As it is known that HDACs, which remove acetyl groups from core histones, are assembled with the PRC2 in ES cells, this result is not unexpected

because of the complex's instability upon EED deletion [141]. Interestingly, besides the PRC2-mediated repressive H3K27me3 mark, another repressive mark, H3K9me3, was also reduced in EED KO ES cells, even though to a lesser extent (Figure 5.19). Earlier it was observed that PRC2 and the methylation activity of H3K9 are linked and that EED can directly bind to H3K9me3 [138, 139, 140, 132]. However, enzymes that directly methylate H3K9 are not part of the PRC2 core complex. It remains open whether in EED KO ES cells the activity of one or more of the 5 known H3K9 HMT is reduced or whether activities of KDMs are affected [189, 190]. As EED binds H3K9me3 with high affinity [132], it is possible that in KO ES cells the lack of this particular binding leads to reduced global levels of H3K9me3. In ES cells the PRC2 might assemble with H3K9 HMTs and also an enhancement of the enzymatic activation of H3K9 HMTs upon EED-H3K9me3 binding is conceivable. Further it must be assessed which genomic regions are affected by the apparent global H3K9me3 decrease. This can be done *e.g.* by applying genome-wide ChIP technologies.
In parallel to decreased H3K9me3 levels, the nuclear distribution of H3K9me3-enriched chromatin was changed in EED KO ES cells (Figure 5.21). Less foci of bigger size and with well-defined borders were found in EED KO as compared to wild type ES cells. This nuclear architecture reminds of differentiated cell types with respect to the high-defined distinction between eu- and heterochromatin regions. However, Meshorer *et al.* reported that the number of heterochromatin spots increased while their size decreased during the differentiation of ES cells to NSCs [104]. It is worth investigating whether other differentiated cell types besides NSCs also exhibit more and smaller heterochromatin foci or whether this appearance is specific for NSCs. It was speculated that by changing nuclear organization from poorly defined and diffusely distributed heterochromatin to distinct clusters, the gene expression repertoire and developmental potential of cells becomes restricted [104]. In case of EED KO ES cells this is only partially true, because most features of pluripotent cells (including gene expression of pluripotency markers) are preserved whereas the differentiation potential is disturbed. Thus, EED KO ES cells are inflexible concerning their developmental possibilities which might be reflected by well-defined and distinct chromatin domains. FRAP analyses revealed that EED KO like wild type ES cells contained similarly large proportions of mobile linker histone chromatin fractions (Figure 5.21). In contrast to differentiated cell types which were reported to have increased immobile chromatin fractions [104], EED KO ES cells recovered fluorescence fully. However, the halftime of recovery was reduced, indicating that chromatin mobility in general is retained, but slowed down.
In summary, EED KO ES cells exhibit typical properties of pluripotent cells, but appear to be restricted to the undifferentiated state. EED KO ES cells have difficulties to exit pluripotency upon differentiation induction - they could be described as 'trapped in the pluripotent state'.

6.4 The end of pluripotency

In the course of this thesis, I performed analyses to better define the loss and end of pluripotency. Applying an *in vitro* differentiation approach for ES cells using the HD method to form EBs I was able to show that functional properties delineating pluripotency, like self renewal and differentiation capacity, were immediately and strongly reduced in early differentiated ES cell cultures (Figure 5.10). This is surprising if one considers that in these early stages pluripotency genes remained highly expressed and SSEA1 levels changed only marginally or not at all (Figure 5.8 and 5.9). Most of the analyzed pluripotency-associated transcription

factors (Oct4, Rex1, Sox2, Nanog) or surface markers (SSEA1) were increased after 1 day of LIF withdrawal. A potential contamination with residual feeder cells in undifferentiated ES cell samples leading to lower pluripotency marker levels in day 0 as compared to 1-day differentiated samples, seems unlikely because functionally pluripotent cells with *e.g.* colony formation capacity were most frequent in undifferentiated ES cell samples. The assays performed here to test for pluripotency were not as stringent as teratoma formation, generation of chimeras with germline contribution or the complementation of tetraploid blastocysts, but they were able to mirror pluripotency levels (Figure 5.10). From these observations it can be concluded that ES cells after short-term differentiation of only 1 to 2 days show a functional loss of pluripotency before this is designated by declining levels of pluripotency markers. Similar results were described previously [191]. It is, however, conceivable that RNA of pluripotency-associated genes was synthesized and hence, is detectable, but RNA is not translated into protein. An alternative scenario is that pluripotency-associated proteins are present and hence traceable, but no longer produced. Therefore, I hypothesize that in very early stages of ES cell differentiation functional pluripotency loss is based on immediate molecular switches, *e.g.* post-translational modifications, that alter protein functions and subsequently cellular identities.

The progression of differentiation and thus the loss of pluripotency is also dependent on the method by which ES cells are differentiated. By detecting Oct4-eGFP levels I found that differentiation in MC or as ML at low cellular densities yielded the fastest and most uniform differentiation progression (Figure 5.11 and 5.13). Palmqvist *et al.* reported that the capacity of R1 ES cells to give rise to chimeric mice upon injection into blastocysts declines from 100% to about 20% within 24 h and to almost 0% after 48 h of differentiation [191]. In the same study ES cells were differentiated attached to culture dishes in the absence of LIF. Other differentiation methods, *e.g.* aggregation of ES cells to EBs, might give other outcomes, because the degree of cellular heterogeneity is higher in aggregation EBs than in ML cultures. For the generation of chimeric animals randomly 5-15 cells are injected into blastocysts. Hence, cellular heterogeneity will have an impact on the level and degree of chimera formation. Individual undifferentiated cells within heterogeneous differentiation cultures would be sufficient to take part in blastocyst seeding and consequently generate chimeric mice, even though other cells, maybe the majority, of co-injected cells have features of differentiated cells. Therefore it is important to know the composition of cell populations of which single cells are injected into blastocysts. Based on my data, I assume that differentiating ES cells without mutual contact (*i.e.* clonal EBs or low cell density ML) stop contributing to chimeric animals at earlier differentiation time points, whereas the chimeric outcome of heterogenous differentiated cells is a stochastic event.

The question of whether the 'end of pluripotency' is a point of no return or whether a time window of ambiguity exists which allows a regain of pluripotency, is difficult to approach directly. Due to the fact that currently no good markers exist that recognize cells in the process of early commitment, the identification of cells within a potential time window of ambiguity seems challenging. Generally, developmental processes are unidirectional and one would not expect de-differentiation without malignant transformation [192] or without external manipulation, like the induction of pluripotency by ectopic expression of factors like Oct4, Sox2 and Klf4 in somatic cells [53]. Here Oct4-enhancer driven eGFP in OG2 ES cells was used to assess whether expression of the pluripotency factor Oct4 can be re-elevated if once reduced, *i.e.* whether ES cell culture conditions alone can rescue Oct4-eGFP expression in 3 days differentiated ES cells. The results presented here suggest that if Oct4-eGFP levels fall

below a threshold, Oct4-eGFP can not be reactivated by culturing cells under ES cell growth conditions on MEFs (Figure 5.16). Only contaminating Oct4-eGFP^{high} cells overgrew the cultures (Figure 5.15 and 5.16). To deeper unravel the end of pluripotency, earlier differentiated cell types must be subjected to analyses. However, adequate markers for such kind of analysis have yet to be identified.
Though also pluripotent, EpiSCs represent a cell type distinct from ES cells and exhibit characteristics of more differentiated cells. EpiSCs are generally incapable of contributing to chimerism upon blastocyst injection [39]. ES cells can reversibly differentiate to epiblast-like cells that represent an intermediate cellular entity between ES cells and EpiSCs. ES and epiblast-like cells are described to be in a dynamic equilibrium [36]. ES cells, epiblast like cells as well as EpiSCs express Oct4 [36]. However, in contrast to EpiSCs, epiblast-like cells regulate their gene expression not via DNA methylation but rather via reversible histone modifications [36]. Therefore, the end of pluripotency is most probably defined by robust epigenetic marks which guide a cell's fate beyond a point of no return. Robust epigenetic silencing mechanism are more difficult to revert and include DNA methylation and higher order compaction by heterochromatin-associated proteins like HP1. This hypothesis is further supported by the observation that differentiated ES cells lacking Dnmt1, Dnmt3a and Dnmt3b (triple KO) can reactivate Oct4-eGFP expression after rescue in ES cell culture condition (unpublished data, communication with D. Meilinger of H. Leonhardt lab). However, appropriate culture conditions that supply either LIF or a cocktail of small molecule inhibitors for LSD1, ALK5, MEK, FGFR, and GSK3 were shown to revert EpiSCs to ES cells, including the erasure of DNA methylation marks [38, 39].
Finally, I conclude that for studies on the end of pluripotency it is essential (i) to consider the differentiation method, (ii) to analyze cells on the single cell level rather than in bulk cultures and (iii) to rely on functional assays instead of marker expression. However, in recent time there is striking progress in the field of cellular reprogramming with the identification of reprogramming genes that can replace one another (like nuclear receptor Nr5a2 or E-cadherin replace Oct4 [193, 183]) and small molecules that enhance reprogramming. Thus, the step to reprogram cells by just applying optimal culture conditions and creating a stimulating microenvironment appears not out of reach. As culture conditions for the groundstate of pluripotency exist that support self renewal of pluripotent cells, it is conceivable that somatic cells if treated with appropriate small molecules can stochastically turn on pluripotency gene expression. Consequently, these cells would selectively survive and expand. This reflects the potential that every cell, differentiated or uncommitted, holds in its genetic information. By deeper understanding of cellular programs and epigenetic regulation, I assume that in future the 'end of pluripotency' can be safely reverted without genetic approaches which will open gateways towards safe regenerative therapies.

7 Material and Methods

7.1 Material

7.1.1 Mice

Strain	Characteristica	Source
C57BL6 Ly5.1	wild type, inbred	Charles River
C57BL6 Ly5.2	wild type, inbred	Charles River
NMRI	wild type, outbred	Harlan
B6;CBA-Tg(Pou5f-eGFP)2Mnn/J	eGFP under transgenic Oct4 promoter control	kindly provided by Prof. Schöler
DR4	C57BL6 with four antibiotic resistance genes	kindly provided by Prof. Lübbert
C57BL6J-Thy^{c-2J}	C57BL6 albino	Charles River

7.1.2 Mouse ES cell lines

Name	Genetic background	Specific feature	Source
V6.5	129/Sv X C57BL6	wild type	open biosystems
D3	129/Sv X 129/Sv	wild type	
OG2	CBA X C57BL6	eGFP under transgenic Oct4 promoter control	kindly provided by Prof. Schöler
J1	129/Sv X 129/Sv	wild type	kindly provided by Dr. Wutz, Cambridge UK
EED KO J1	129/Sv X 129/Sv	knockout of eed	kindly provided by Dr. Wutz, Cambridge UK
EED KO E14	129/Sv X 129/Sv	knockout of eed	kindly provided by Dr. Wutz, Cambridge UK

7.1.3 Cell culture media and supplements

Standard ES cell medium

Ingredient	Concentration	Volume	Distributor
DMEM high glucose		400 ml	PAA
FCS, ES cell tested	15%	75 ml	PAA
Sodium pyruvate	1 mM	5 ml	PAA
Penicillin, Streptomycin	100 U/ml, 0.1 mg/ml	5 ml	PAA
L-Glutamine	2 mM	5 ml	PAA
Non-essential aminoacids	1x	5 ml	PAA
Beta-Mercaptoethanol	0.1 mM	3.5 μl in 5 ml Hepes	Sigma, PAA
LIF-conditioned medium		500 μl	own production

2 inhibitor ES cell medium

Ingredient	Concentration	Volume	Distributor
DMEM F12 Ham	50%	50 ml	Invitrogen
Neurobasal	50%	50 ml	Invitrogen
N2	0.5%	0.5 ml	Invitrogen
B27	1%	1 ml	Invitrogen
Glutamax	2 mM	1 ml	Invitrogen
Insulin	1 mg/ 100 ml	1 mg	Sigma
BSA	2.5 mg/100 ml		Sigma
Beta-Mercaptoethanol	0.1 mM	0.7 μl in 1 ml Hepes	Sigma, PAA
LIF-conditioned medium		100 μl	own production
PD0325901	1 μM	10 μl von 10 mM stock	Axon medchem
CHIR 99021	3 μM	30 μl von 10 mM stock	Axon medchem

Differentiation medium

Ingredient	Concentration	Volume	Distributor
DMEM high glucose		425 ml	PAA
FCS	10%	50 ml	Biochrome
Sodium pyruvate	1 mM	5 ml	PAA
Penicillin, Streptomycin	100 U/ml, 0.1 mg/ml	5 ml	PAA
L-Glutamine	2 mM	5 ml	PAA
Non essential aminoacids	1x	5 ml	PAA
Beta-Mercaptoethanol	0.1 mM	3.5 μl in 5 ml Hepes	Sigma, PAA

EB formation methylcellulose medium

Ingredient	Concentration	Volume	Distributor
M3120 ES-cult	1x	40 ml	Stem Cell Technologies
FCS	15%	15 ml	Biochrome
L-Glutamine	2 mM	1 ml	PAA
mSCF	40 ng/ml	40 μl	Peprotech
MTG	150 μM	124 μl	Sigma
IMDM		34 ml	Invitrogen

MEF medium

Ingredient	Concentration	Volume	Distributor
DMEM low glucose		500 ml	PAA
FCS	10%	50 ml	Biochrome
Sodium pyruvate	1 mM	5 ml	PAA
Penicillin, Streptomycin	100 U/ml, 0.1 mg/ml	5 ml	PAA
L-Glutamine	2 mM	5 ml	PAA

BM culture medium

Ingredient	Concentration	Volume	Distributor
IMDM		500 ml	Invitrogen
FCS	20%	100 ml	Sigma
BSA	0.1%	6.7 ml of 7.5% solution	Invitrogen
Sodium pyruvate	1 mM	5 ml	PAA
Penicillin, Streptomycin	100 U/ml, 0.1 mg/ml	5 ml	PAA
L-Glutamine	2 mM	5 ml	PAA
IL-3	10 ng/ml		Peprotech
IL-6	20 ng/ml		Peprotech
mSCF	50 ng/ml		Peprotech

Hematopoietic methylcellulose medium

Ingredient	Concentration	Volume	Distributor
MethoCult	1x	40 ml	Stem Cell Technologies
FCS	30%	30 ml	Biochrome
Penicillin, Streptomycin	100 U/ml, 0.1 mg/ml	1 ml	PAA
L-Glutamine	2 mM	1 ml	PAA
BSA	1%		Invitrogen
BM culture medium	1/6	500 μl per 2.5 ml	see above
Beta-Mercaptoethanol	0.1 mM	0.7 μl in 1 ml PBS	Sigma, PAA
PWM	2%		Stem Cell Technologies
IL-3	10 ng/ml		Peprotech
IL-6	20 ng/ml		Peprotech
mSCF	50 ng/ml		Peprotech

7.1.4 Antibodies

Primary antibodies

Target	Species	Distributor
H3	rabbit, polyclonal	Abcam
H3K4me3	rabbit, polyclonal	Abcam
H3K4me3	rabbit, polyclonal	Diagenode
H3K9ac	rabbit, polyclonal	Abcam
H3K9me3	rabbit, polyclonal	Upstate
H3K27me3	rabbit, polyclonal	Abcam
H3K27me3	rabbit, polyclonal	Diagenode
H4	rabbit, polyclonal	Upstate
H4K8ac	rabbit, polyclonal	Upstate
H4K12ac	rabbit, polyclonal	Upstate
H4K16ac	rabbit, polyclonal	Upstate
pan acH4	rabbit, polyclonal	Upstate
SSEA1	mouse, monoclonal	hybridoma bank
c-Kit	mouse, monoclonal	own production
Sca-1-PE	mouse, monoclonal	BD
CD4 (-biotin)	rat, monoclonal	own production
CD8 (-biotin)	rat, monoclonal	own production
Mac1 (-biotin)	rat, monoclonal	own production
Gr1 (-biotin)	rat, monoclonal	own production
Ter119 (-biotin)	rat, monoclonal	own production
B220 (-biotin)	rat, monoclonal	own production
Ly5.1	mouse, monoclonal	BD
EZH2	rabbit, polyclonal	Diagenode
EED	rabbit, polyclonal	Santa Cruz
GAPDH	mouse, monoclonal	Santa Cruz

Secondary antibodies / reagents

Target	Label	Distributor
mouse	Cy2	Dianova
mouse	Cy3	Dianova
rabbit	PE	Dianova
rabbit	Cy2	Dianova
biotin (streptavidin)	PE-Cy5	BD
biotin (streptavidin)	APC	Dianova
mouse	HRP	Amersham
rabbit	HRP	Amersham
rat	goat, micro beads	Miltenyi
goat	biotin	BD

7.1.5 Primers

All quantitative real time PCRs (either for gene expression or for ChIP analyses) were performed using an annealing temperature of 60°C. Primers were ordered from Eurofins MWG Operon.

Gene expression primers

Gene	Sequence	Product size (bp)
beta-actin	GATATCGCTGCGCTGGTCGTC ACGCAGCTCATTGTAGAAGGTGTGG	132
eed	GCACAGAGATGAAGTTCTGAGTGCTG ATAAGACTCCTTAATTGCATTCATCATCCT	133
oct4	CCGTGAAGTTGGAGAAGGTG GAAGCGACAGATGGTGGTCT	194
nanog	TCTTCCTGGTCCCCACAGTTT GCAAGAATAGTTCTCGGGATGAA	100
sox2	GCGGAGTGGAAACTTTTGTCC CGGGAAGCGTGTACTTATCCTT	157
rex1	GGC CAG TCC AGA ATA CCA GA GAA CTC GCT TCC AGA ACC TG	232
bry	CAGCCCACCTACTGGCTCTA GAGCCTCGAAAGAACTGAGC	123
nestin	CAG AGA GGC GCT GGA ACA GAG ATT AGA CAT AGG TGG GAT GGG AGT GCT	469

ChIP primers

Gene	Sequence	Product size (bp)
oct4	TCCGCCAGCACAGGAATG CAGAGCCTCAGATGGAGATACC	95
nanog	TTCAGATAGGCTGATTTGGTTGG GATCATAGAAAGAAGAGTTAAATGTCTAATGC	115
klf4	TCGGTCCCTCTCCGCGTTCC TCCCGTAGGGTGGGGGTGAG	199
irx2	TAACACGGCCTGAAATCTTCTC GCATCCCACTTCTACAGTCCTC	198
hoxa3	AATTACCTCCCTGCATCTCAAA TTATCAGAGCAGACCCACAATG	165
pax5	ATGGGAGTTTGTTTTCCTGTGT AGTGATGTTTGGCCTAATCCTG	174
dlx1	ATGTCTCCTTCTCCCATGTCC ACTGCACGGAACTGATGTAGG	178
tcf4	CGGATGTGAATGGATTACAATG ATTGTTCTTCGGTCTTGTTGGT	184

7.1.6 Buffers and solutions

PBS
137 mM NaCl, 2.7 mM KCl, 10 mM Na_2HPO_4, 1.76 mM KH_2PO_4, pH 7.4

FACS-buffer
PBS, 0.3 % BSA, 0.1% NaN_3, pH 7.4

Flow FisH buffer
21.4 mM Tris HCl pH 7.1, 21.4 mM NaCl, 80.25% v/v deionized formamide, 1.07% BSA

Protein sample buffer
100 mM Tris HCl pH 6.8, 200 mM DTT, 4% SDS, 0.2% bromophenol blue, 20% glycerol

Trypsin
0.05% trypsin in PBS, commercially purchased from PAA

Gelatin
0.1% in PBS

Gey's Solution
20% Stock A:
NH_4Cl 35.0 g, KCl 1.85 g, Na_2HPO_4-12·H_2O 1.5 g, KH_2PO_4 0.12 g, Glucose 5.0 g, Phenol red 50 mg, bring to 1 L
5% Stock B:
$MgCl_2$-6·H_20 0.42 g, $MgSO_4$-7·H_20 0.14 g, $CaCl_2$ 0.34 g, bring to 100 ml
5% Stock C:
$NaHCO_3$ 2.25 g, bring to 100 ml
70% water

Western blot stripping solution
100 mM Beta-Mercaptoethanol, 2% SDS, 62.5 mM Tris HCl pH 6.7

7.1.7 Commercial kits and reagents

Kit / Reagent	Distributor
M-MLV Reverse transcriptase kit	Invitrogen
rDNase I	Ambion
Alkaline Phosphatase kit	Sigma
ABsolute SybrGreen Mix	Thermofisher
ChIP Kit	Upstate
PeqGold RNAPure	Peq Lab
RNeasy Mini kit	Qiagen
Fixation and Permeabilization buffers	eBioscience
AnnexinV-FITC Apoptosis detection kit	BD
HDAC activity kit	Upstate
Customized PCR gene expression array (Table 5.2)	SABiosciences
TSA	Sigma
VPA	Sigma
ATRA	Sigma
DAPI	Sigma
Hoechst 33343	Sigma
Hoechst 33258	Sigma
Prolong Gold, mounting medium	Invitrogen
Mouse embryonic stem cell Nucleofection kit	Amaxa
RNase and DNase free water	Sigma
Protease inhibitor cocktail	Applichem
Nitrocellulose membrane PROTRAN	Whatman
Tissue-Tek	OCT

7.1.8 Cell culture plastic, technical devices and software

Cell culture plastic	Distributor
2 ml cryotubes	PAA
3.5 cm TC plates	Greiner
3.5 cm suspension plates	Sarstedt
6 cm TC plates	PAA
10 cm TC plates	Greiner
10 cm petri dish	Greiner
15 cm petri dish	Sarstedt
75 cm^2 TC flasks, red cap	Sarstedt
24 well plates TC	Nunc
24 well plates, suspension	Greiner
48 well plates TC	Greiner
15 ml tubes	Greiner
50 ml tubes	Greiner
flexiPERM chamber	Sarstedt
70 μm cell strainer	Greiner

Technical device	Distributor
Nucleofector I	Amaxa / Lonza
Bioruptor	Diagenode
FACS Canto I	BD
Real time Cycler Rotor Gene 3000	Corbett
Fluorescence microscope DM IRBE	Leica
Cell culture microscope EVOS	AMG
Spectra Thermo, ELISA reader	Tecan

Software	Distributor
ImageJ	NIH
FlowJo	Tree Star, Inc.
FACS Diva	BD
Rotor Gene 6	Corbett
Micron EVOS	AMG

7.2 Methods

7.2.1 Mouse cell isolation and transplantation

MEF isolation

MEFs were isolated from E12.5 - E14.5 mouse embryos of wild type mice. Pregnant mothers were sacrificed and embryos were freed from residual extraembryonic tissue. The heads and inner organs were removed by using forceps and scalpel. The remaining embryonic tissue was incubated in trypsin solution over night at 4°C to allow diffusion of the enzyme inside the tissue. The enzymatic activity was induced by 30 min incubation at 37°C and stopped by the addition of a large volume of MEF medium. The tissue was further disrupted by thorough pipetting. Large tissue particles were allowed to settle down and the supernatant containing single MEF suspension was spun down at 200x g and cells were resuspended and plated in MEF medium at a density of 1/3 embryo per 10 cm TC plate. One or two days later MEFs were trypsinized and one plate was frozen in three cryotubes, labelled "passage 0".

BM isolation

Male C57BL6 Ly5.1 mice at an age of 8 to 12 weeks were sacrificed, femur and tibia bones were isolated and the BM was flushed out with 0.3% BSA in PBS by using needle and syringe. Single cell suspension was obtained by thorough pipetting and the pass though a 70 μm cell strainer. Erythrocytes were depleted by incubation in hypotonic Gey's solution for 6 min on ice and the BM cells were subsequently collected in a phase of FCS by centrifugation.

BM transplantation

Freshly isolated or cultured and treated BM cells were injected (20,000 cells per animal) intravenously into lethally irradiated (11 Gy) female C57BL6 Ly5.2 mice together with $1 \cdot 10^5$ Ly5.2 competitor BM cells. Before transplantation the cultured cells were washed twice with PBS. After an engraftment period of 16 weeks blood of the transplanted animals was collected from the tail veins, white blood cells were purified by Ficoll gradient centrifugation and finally used for flow cytometric analyses.
BM transplantation were performed together with V. Hornich and A.M. Müller.

7.2.2 Cell culture

All cells were cultured at 37°C and 5% CO2 in a humidified atmosphere. Cells were frozen in 10% DMSO in FCS.

BM

Freshly isolated BM cells were cultured for two days in 24 well suspension plates at a density of $1 \cdot 10^6$ cells per 1 ml BM culture medium accordingly supplemented with TSA or VPA.

MEF

MEFs were either used directly upon isolation or thawed and were used for no more than 6 passages. MEFs were maintained in TC flasks (T75 or T175) with MEF medium and split

once or twice a week by washing them once with PBS, incubating them with minimum volume of trypsin at 37°C for maximal 5 min, washing them out with MEF medium and distributing them at equal amounts into three new flasks. For mitotic inactivation confluently grown MEFs were treated with mitomycin C (10 μg/ml) for two to three hours, washed at least two times with PBS, trypsinized and counted. Inactivated MEFs were plated at a density of $1 \cdot 10^6$ cells per 6 cm TC plate. After some hours or the next day MEFs had attached and were read as feeder cells for subsequent ES cell culture.

ES cells

Usually, ES cells were thawed and cultured in standard ES cell medium on inactivated MEF feeders in 6 cm TC plates. Medium was changed every day and cells were passaged at a ratio of 1/10 every second day. For this, cells were washed twice with 5 ml of PBS and trypsinized by incubation with 0.5 ml trypsin for 5 min at 37°C. Trypsin reaction was stopped by the addition of 5 ml of ES cell medium and cells were dissociated by pipetting. After centrifugation at 90x g the pellet was resuspended in ES cell medium and 1/10 was given to a new culture dish onto MEFs in ES cell medium. ES cells cultured in 2 inhibitor medium were grown on gelatin coated 3.5 cm or 6 cm TC plates and passaging was done by the usage of accutase.
To obtain feeder-free ES cells the heterogenous cell suspension of one 6 cm plate (comprising ES cells and MEFs) was given to a gelatine coated 10 cm TC plate for 45 min. This allows MEFs to strongly attach to the bottom of the dish while ES cells only loosely adhere and dead cells as well as cell clusters remain in suspension. ES cells are isolated by removing the suspension phase and washing off the loosely adhered ES cell fraction from the fixed MEFs.

ES cell differentiation

For the induction of differentiation, feeder-free ES cells were cultured in the absence of LIF and MEFs with reduced FCS concentration. This was either achieved by the formation of EBs or by the growth as a dish-adhered ML. EBs were generated by clustering 1,000 ES cells in 30 μl differentiation medium as HDs at the lids of 15 cm petri dished in the presence of PBS for humidification. After two days the formed EBs from one 15 cm lid (usually 120 EBs) were transferred into 10 cm petri dishes in 10 ml of fresh differentiation medium and cultured for up to 7 days. For further analyses EBs were dissociated by harvesting free floating EBs, allowing them to settle down by gravity, washing them twice in PBS and incubating them for 5 to 10 min at 37°C in trypsin. By the addition of medium, thorough pipetting and the help of a 70 μm cell strainer single cell suspensions could be made.
ML differentiation was performed by plating feeder-free ES cells in differentiation medium on 10 cm TC plates at appropriate density. Cells were harvested by trypsination as explained above.
Differentiation towards clonal-derived EBs in MC medium was done as explained below for the EB formation assay. For harvesting MC-derived EBs the semisolid medium was diluted by warm PBS, EBs were washed out of the dish and subsequently dissociated to single cells with trypsin.

'Beating body' assay

For the differentiation of ES cells towards spontaneously contracting cardiomyogenic cells, first EBs were generated in HDs for two days as explained above. The EBs were transferred

to petri dishes for three more days and finally individual EBs were moved into gelatin coated wells of 48 well TC plates. From then on the differentiation medium was changed every day and EBs were subjected to an everyday microscopic observation to identify contractions.

EB formation assay

To analyze the potential of cells to form EBs, 1,000 feeder-free ES cells or differentiated cells were plated in 1 ml EB formation MC medium into 3.5 cm petri dishes. In this semisolid medium the formation of EBs is the result of clonal proliferation and not of aggregation. One week after plating the number of EBs was enumerated by light microscopy.

Colony formation assay for ES cells

To analyze the potential of cells to form colonies, defined numbers of feeder-free ES cells or differentiated cells were transferred onto a MEF feeder layer in standard ES cell medium. After four days the colonies were fixed and the activity of their AP was visualized by applying the Alkaline Phosphatase Kit according to manufacturer (see Material). Only $AP^{positive}$ colonies were enumerated by light microscopy.

Colony formation assay for HPCs

Freshly isolated or 2-day cultured BM cells were plated at densities between 1,000 and 5,000 cells per 1 ml hematopoietic MC medium as triplicates in 3.5 cm suspension culture plates. After 10 days all colonies consisting of at least 50 single cells were enumerated. For the secondary colony formation, colonies were washed out of the dish with warm PBS , cells were counted and plated again under the same conditions as before. After 10 days frequencies of secondary colonies were determined.

7.2.3 Molecular biology

RNA isolation

Total RNA of cells was purified by using peqGOLD RNA Pure, an optimized guanidine isothiocyanate/phenol reagent for RNA extraction, or by the Qiagen spin column RNeasy Mini Kit. RNA isolation was performed as recommended by the manufacturer. The concentration and purity was measured photospectrometrically.

cDNA synthesis

Purified RNA was reverse transcribed by the M-MLV reverse transcriptase. Briefly, 1 μg of total RNA were used and first remaining genomic DNA was digested for 30 min at 37°C by DNase. The reaction was stopped by the addition of 7% v/v 25 mM EDTA and by 10 min heat inactivation at 65°C. Oligo dT primers (5' TTT TTT TTT TTT TTT T 3') were allowed to anneal to poly A RNA for 5 min at 65°C followed by rapid chill down on ice. Together with 5 mM dNTPs and reverse transcriptase as well as with buffers (provided by the manufacturer, see Material) cDNA was synthesized for 1 h at 37°C. Usually cDNA was further diluted with RNase and DNase free water before subsequent PCR.

ChIP

ChIP was done by applying a ChIP kit (see Materials), individual steps were performed as recommended by the manufacturer and a protease inhibitor cocktail was added to all solutions.
For ChIP, chromatin of $1{\cdot}10^6$ cells was cross-linked to DNA for 10 min at 37°C by 1% formaldehyde in medium. Next, cells were washed twice in ice cold PBS and subsequently resuspended in 200 μl SDS lysis buffer. DNA was sheared in the Bioruptor at 4°C in 60 cycles with one cycle comprising 30 s of sonication and 30 s of no sonication. One percent was used as input material and the remaining chromatin was split equally to H3K27me3 and isotype control precipitation. Following over night incubation with 5 μl of antibody (H3K27me3 or isotype control) DNA was isolated by phenol chloroform and ethanol precipitation. DNA of IPs and input was dissolved in 30 and 100 μl water, respectively, and used for real time PCR.
ChIP analyses were performed together with M. Becker.

Quantitative realtime PCR

Realtime PCRs were performed with cDNA and ChIP-DNA.
For gene expression analyses generally 1 μl cDNA was mixed with 10 μl 2x SybrGreen Mix, 8.5 μl water and each 0.25 μl of 100 pM primers. Analyses were referred to beta-actin by the delta-delta Ct calculation. However, Ct values for beta-actin were tried to be aligned for comparative samples. All reactions were carried out as duplicates in the Corbett Rotor Gene RG 3000 real time cycler with the following PCR program: 95°C 15 min, 40x (95°C 10 s, 60°C 20 s, 72°C 30 s, 80°C 20 s), 50°C 1 min, 67°C to 95°C with 0.5°C temperature increase per 5 s. Ct values were determined by Rotor Gene 6 software.
The SABioscience gene expression PCR array was used with cDNA which was synthesized from Qiagen purified RNA. After dilution (1:5) each 1 μl cDNA together with water and SybrGreen Mix was placed per well, as recommended by the manufacturer. Roche Light Cycler software determined Cp values automatically and results were normalized to HPRT.
ChIP-DNA and input DNA were used as template for quantification of H3K27me3 enrichment at certain genomic regions. Each 1 μl of template DNA was mixed with 10 μl 2x SybrGreen Mix, 8.5 μl water and each 0.25 μl of 100 pM primers. All reactions were carried out as duplicates in the Corbett Rotor Gene RG 3000 real time cycler with the following PCR program: 95°C 15 min, 40x (95°C 10 s, 60°C 20 s, 72°C 30 s, 80°C 20 s), 50°C 1 min, 67°C to 95°C with 0.5°C temperature increase per 5 s. Ct values were determined by Rotor Gene 6 software. Analyses were referred to non-precipitated input DNA by the delta-delta Ct calculation.

Western blot

Protein samples were prepared from $1 \cdot 10^6$ cells which were washed at least twice in PBS to clean from FCS protein contamination. The cells were lysed in 100 μl protein lysis buffer and sheared by passing through a 21 gauge needle several times. Samples were heated up to 95°C for 5 min and proteins were separated by SDS-PAGE in 10% SDS gels. Proteins were next blotted onto nitrocellulose membranes followed by 30 min blocking of unspecific binding sites in 5% milk in PBS 0.1% Tween20 at RT. Primary antibodies were incubated over night at 4°C in 1% milk PBS 0.1% Tween20 with the membrane. After three washes secondary HRP-coupled antibodies were incubated for 2 h at RT in PBS 0.1% Tween20, before proteins

were detected by ECL addition and chemiluminescence measurement, either by X-ray film or by Biorad Imaging system. Membranes were stripped from antibodies by 30 min incubation with stripping solution at 56°C.

HDAC activity assay

Nuclei of unfractionated or MACS-separated BM cells were prepared by first incubating the cells in a buffer containing 10 mM Hepes pH 7.9, 10 mM KCl, 0.1 mM EDTA, 0.1 mM EGTA and 2.5 mM DTT, followed by lysis in 0.5% NP40. Nuclear proteins were then extracted with a buffer containing 20 mM Hepes pH 7.9, 400 mM NaCl, 1 mM EDTA and 2.5 mM DTT. Equal amounts of nuclear protein extracts from unfractionated, Lin^+ or $Lin^{-/int}$ cell populations were subjected to HDAC enzymatic activity measurement using a fluorimetric assay kit according to the manufacturer's instructions. For analysis, triplicates of nuclear extracts from the different cell populations were incubated with fluorochrome-conjugated substrate. The release of fluorochrome as a measure of HDAC activity was quantified in a fluorimeter with an excitation wavelength of 360 nM and detection of emission at 440 nM wavelength. As a control, nuclear extracts of unfractionated BM cells were treated with 4 μM TSA for 60 min prior to HDAC activity measurement, as recommended by the manufacturer. HDAC activity assays were done with the help of V. Hornich and A.M. Müller.

7.2.4 Flow cytometry

All flow cytometric analyses were done on a BD FACS Canto I using FACS Diva and FlowJo software.

Surface staining

For the detection of cellular surface antigens on living cells, approx. $2 \cdot 10^5$ cells were needed and washed once in 1 ml of FACS buffer before staining.
For SSEA1 detection: ES or EB cells were incubated with 0.25 μl of mouse SSEA1 in 100 μl FACS buffer for 20 min at 4°C, washed once in 1 ml of FACS buffer, incubated for 20min with anti-mouse Cy3 diluted 1:200 in FACS buffer and washed before analysis. BM cells were stained for their LKS immunophenotype by first blocking Fc-receptors with a specific monoclonal antibody for 15 min. Lin markers were bound by biotin-labelled rat antibodies against CD4, CD8, Mac1, Gr1, B220 and Ter119 which were incubated together with the cells for 20 min at a concentration of 0.25 μl per antibody in 50 μl FACS buffer at 4°C. Cells were washed twice in order to remove as much unbound biotin-labelled antibody as possible and subsequently incubated with 0.1 μl streptavidin-PE-Cy5, 1 μl anti-Sca1-PE and 1 μl anti-cKit-FITC in 100 μl FACS buffer for 30 min at 4°C. After a final wash BM cells were analyzed.

Chromatin flow cytometric protocols

Two different protocols were used to intranuclearly stain histone modifications for flow cytometry:
In protocol A, modified from a Flow FisH protocol [194], cells were resuspended in 300 μl freshly prepared flow FisH buffer and incubated for 10 min at 80°C. Cells were allowed to cool down to RT. After centrifugation (960x g) and removal of the supernatant, transparent

cell pellets were resuspended in 200 μl PBS and cells were transferred into a FACS tube containing 1 ml PBS. Next, cells were pelleted again and washed successively in PBS and FACS buffer. As the fixation procedure does not allow prior cell surface immunofluorescent staining, cell surface staining was performed together with intranuclear staining. For SSEA1/histone modification-specific immunofluorescent stainings, first, 0.1 μl mouse anti-SSEA1 primary antibody was added to cells in 100 μl FACS buffer. Cells were incubated for 20 min at RT. After washing with 1 ml FACS buffer, a secondary anti-mouse-Cy3 antibody (1/200) was added and incubated at RT for 20 min. Following repeated washes, histone modification-specific antibodies or a rabbit polyclonal isotype control were added at the indicated concentrations (Table 5.1) in 100 μl FACS buffer and incubated for 1 h at RT. The cells were then washed twice in 1 ml FACS buffer and incubated with appropriate secondary antibodies for 45 min at RT. For single stainings of histone modifications, anti-rabbit-PE (1/500) or anti-mouse-Cy3 (1/200) antibodies were used. For 2-color analysis, anti-rabbit-Cy2 antibody (1/200) together with anti-mouse-Cy3 antibody (1/200) were used. After immunofluorescent staining, the cells were washed in 1 ml FACS buffer and resuspended in 120 μl FACS buffer for analysis.
In protocol B, cells were resuspended in 100 μl fixation/permeabilization buffer (formaldehyde basis; eBioscience) and incubated for 10 min at RT. Next, cells were pelleted (960x g) and washed once in 200 μl permeabilization buffer (saponin basis; eBioscience) before incubating with primary histone modification-specific antibodies in 100 μl permeabiliza- tion buffer for 1 h at RT at the indicated antibody concentrations (Table 5.1). Cells were spun down and washed twice in 200 μl permeabilization buffer. Next, appropriate secondary antibodies were added to 100 μl permeabilization buffer, and the cells were incubated for 45min at RT. Finally, the cells were washed once in permeabilization buffer, transferred to FACS tubes, washed with FACS buffer and resuspended in 120 μl FACS buffer for analysis. As formaldehyde-based fixation does not cause antibody or fluorochrome degradation, surface immunofluorescent staining was done prior to fixation. Fixation in self-prepared 4% formaldehyde solution and permeabilization in 0.1% saponin also gave a successful staining outcome, but yielded lower signal intensities.

AnnexinV apoptosis detection

Frequencies of living and apoptotic cells were analyzed by an Apoptosis detection kit. Approx. $2 \cdot 10^5$ freshly harvested cells were washed once in 1x binding buffer and were incubated for 15 min at RT with 5 μl AnnexinV-FITC in 100 μl 1x binding buffer. Immediately cells were analyzed.

Cell cycle analysis

To stain and analyze DNA content, $2{\cdot}10^5$ feeder-free ES cells were fixed in 70% ice cold ethanol for at least 30 min at -20°C. Following 2 washes in PBS, cells were incubated for 30 min in 200 μl PBS with 100 μg/ml RNase and 50 μg/ml propidium iodide at 37°C. Immediately cells were analyzed.

7.2.5 Cell sorting and separating

FACS

In order to sort differentiated cells that had reduced Oct4-eGFP levels from a heterogeneous 3-day old EB population, a gate of GFP medium intensity excluding Oct4-eGFP^{high} ES cells was defined. With the kind support of Ch. Linden in the FACSort facility of the Department of Virology and Immunology, University of Würzburg, cells were purely sorted and culture could be maintained under sterile conditions. BD FACS Vantage cell sorter and Diva software were used.
Sorted cells were re-analyzed at FACS Canto I with respect to Oct4-eGFP immediately after sorting. All remaining cells were plated at different cell concentrations in 24 well plates onto MEFs in standard ES cell medium. HDAC inhibitors TSA or VPA were only added for the first 24 h of culture post sort and subsequently withdrawn. After 2, 4 or 6 days cells from individual wells were washed with PBS, allowed to detach from the dish by trypsin treatment and finally subjected to Oct4-eGFP flow cytometric analysis.

MACS

Magnetic cell separation was used to separate Lin$^+$ from Lin$^-$ BM cells. For this purpose freshly isolated BM cells were first incubated with the Lin cocktail antibodies (CD4, CD8, Mac1, Gr1, B220, Ter119, all rat) followed by incubation with goat anti-rat micro beads. According to the manufacturer labelled BM cells were passed through a magnetic field with Lin$^+$ cells remaining inside the column and with Lin$^-$ cells passing through. The purity of MACS was controlled by subsequent flow cytometric analysis after a staining with anti-goat biotin and streptavidin-PE-Cy5 and revealed that the Lin$^-$ fraction comprised 10-20% Lin$^-$ and 80% Lin^{int} cells. Therefore I denotated them as Lin$^{-/int}$ cells. The Lin$^+$ compartment comprised 70% Lin$^+$ and 30% Lin^{int} cells (see also Figure 5.6 B).

7.2.6 Microscopy

Immunofluorescence staining of ES cells

For immunofluorescent imaging of undifferentiated ES cells, first MEFs were plated onto gelatin-coated round coverslips in 24 well plates and subsequently ES cells were transferred onto the feeder cells. Usually 1 or 2 days later cells were washed twice in PBS and fixed by 4% formaldehyde for 10 min at RT. After another wash in PBS cells were permeabilized with 0.1% TritonX in PBS for 10 min at RT. DAPI or Hoechst 33258 was added for 5 min at a concentration of 50 μg/ml in PBS. Cells were washed for 5 min in PBS, for 1 min in H_2O and finally the coverslip was inverted and placed on a drop of ProLong Gold mounting medium on a glass slide.
Staining of H3K9me3 in the nuclei of wild type and EED KO ES cells was done with fixed ES cell colonies on coverslips as explained above. After permeabilization the samples were blocked with gelatin in PBS 0.1% TritonX for 30 min at RT and together with the antibody incubated over night. Following washing in PBS 0.1% TritonX anti-rabbit-Cy2 was added for 2 h and finally ES cell colonies were embedded as described above. Heterochromatin foci were captured by deconvolution imaging of entire ES cell colonies and subsequently frequency and size were analyzed by ImageJ software.

EB sections

EBs from HD differentiation were collected and frozen in Tissue-Tek embedding medium. Cryosections of 10 μm thickness were prepared and the sections were fixed by 4% formaldehyde. DAPI staining was subsequently done as described above, including permeabilization with TritonX.

FRAP

In order to analyze the chromatin dynamics of wild type and EED KO ES cells, a linker histone H1-eGFP construct was transfected into ES cells and bleached by laser scanning confocal microscopy. The time for fluorescence recovery was measured.
First, $4 \cdot 10^6$ feeder depleted ES cells were transfected with 10 μg plasmid by electroporation (Amaxa, mouse ES cell nucleofection kit). Transfected cells were plated on coverslips in flexiPERM chambers onto a layer of MEF feeder cells. Flow cytometric analyses 1 day after transfection revealed a transfection efficiency of not more than 10% and weak fluorescence, suggesting a detrimental effect of too much H1 protein in ES cells. One day after transfection cells were subjected to FRAP, which was performed at the imaging facility of the Rudolf Virchow Center, Würzburg, by M. Becker and G. Harms. Nuclei were visualized by addition of Hoechst 33342 (10 μg/ml) to the cells immediately before bleaching.

8 Bibliography

[1] D. Arendt. The evolution of cell types in animals: emerging principles from molecular studies. *Nat. Rev. Genet.*, 9:868–882, Nov 2008.

[2] D. R. Bell and G. Van Zant. Stem cells, aging, and cancer: inevitabilities and outcomes. *Oncogene*, 23:7290–7296, Sep 2004.

[3] T. Reya, S. J. Morrison, M. F. Clarke, and I. L. Weissman. Stem cells, cancer, and cancer stem cells. *Nature*, 414:105–111, Nov 2001.

[4] Y. Kato and Y. Tsunoda. Totipotency and pluripotency of embryonic nuclei in the mouse. *Mol. Reprod. Dev.*, 36:276–278, Oct 1993.

[5] G. R. Martin. Isolation of a pluripotent cell line from early mouse embryos cultured in medium conditioned by teratocarcinoma stem cells. *Proc. Natl. Acad. Sci. U.S.A.*, 78:7634–7638, Dec 1981.

[6] M. J. Evans and M. H. Kaufman. Establishment in culture of pluripotential cells from mouse embryos. *Nature*, 292:154–156, Jul 1981.

[7] R. T. Tecirlioglu and A. O. Trounson. Embryonic stem cells in companion animals (horses, dogs and cats): present status and future prospects. *Reprod. Fertil. Dev.*, 19:740–747, 2007.

[8] J. A. Thomson, J. Itskovitz-Eldor, S. S. Shapiro, M. A. Waknitz, J. J. Swiergiel, V. S. Marshall, and J. M. Jones. Embryonic stem cell lines derived from human blastocysts. *Science*, 282:1145–1147, Nov 1998.

[9] L. Conti and E. Cattaneo. Neural stem cell systems: physiological players or in vitro entities? *Nat. Rev. Neurosci.*, 11:176–187, Mar 2010.

[10] T. Schroeder. Hematopoietic stem cell heterogeneity: subtypes, not unpredictable behavior. *Cell Stem Cell*, 6:203–207, Mar 2010.

[11] R. J. Deans and A. B. Moseley. Mesenchymal stem cells: biology and potential clinical uses. *Exp. Hematol.*, 28:875–884, Aug 2000.

[12] V. Jaks, M. Kasper, and R. Toftgard. The hair follicle-a stem cell zoo. *Exp. Cell Res.*, 316:1422–1428, May 2010.

[13] N. Barker, M. van de Wetering, and H. Clevers. The intestinal stem cell. *Genes Dev.*, 22:1856–1864, Jul 2008.

[14] J. Voog and D. L. Jones. Stem cells and the niche: a dynamic duo. *Cell Stem Cell*, 6:103–115, Feb 2010.

[15] T. A. Mitsiadis, O. Barrandon, A. Rochat, Y. Barrandon, and C. De Bari. Stem cell niches in mammals. *Exp. Cell Res.*, 313:3377–3385, Oct 2007.

[16] Y. C. Hsu, D. C. Lee, and I. M. Chiu. Neural stem cells, neural progenitors, and neurotrophic factors. *Cell Transplant*, 16:133–150, 2007.

[17] I. H. Oh and K. R. Kwon. Concise review: multiple niches for hematopoietic stem cell regulations. *Stem Cells*, 28:1243–1249, Jul 2010.

[18] C. D. Jude, J. J. Gaudet, N. A. Speck, and P. Ernst. Leukemia and hematopoietic stem cells: balancing proliferation and quiescence. *Cell Cycle*, 7:586–591, Mar 2008.

[19] Y. Sang, M. F. Wu, and D. Wagner. The stem cell–chromatin connection. *Semin. Cell Dev. Biol.*, 20:1143–1148, Dec 2009.

[20] A. Krtolica, D. Ilic, O. Genbacev, and R. K. Miller. Human embryonic stem cells as a model for embryotoxicity screening. *Regen Med*, 4:449–459, May 2009.

[21] G. Weitzer. Embryonic stem cell-derived embryoid bodies: an in vitro model of eutherian pregastrulation development and early gastrulation. *Handb Exp Pharmacol*, pages 21–51, 2006.

[22] H. Boeuf, C. Hauss, F. D. Graeve, N. Baran, and C. Kedinger. Leukemia inhibitory factor-dependent transcriptional activation in embryonic stem cells. *J. Cell Biol.*, 138:1207–1217, Sep 1997.

[23] A. Suzuki, A. Raya, Y. Kawakami, M. Morita, T. Matsui, K. Nakashima, F. H. Gage, C. Rodriguez-Esteban, and J. C. Izpisua Belmonte. Nanog binds to Smad1 and blocks bone morphogenetic protein-induced differentiation of embryonic stem cells. *Proc. Natl. Acad. Sci. U.S.A.*, 103:10294–10299, Jul 2006.

[24] P. Cartwright, C. McLean, A. Sheppard, D. Rivett, K. Jones, and S. Dalton. LIF/STAT3 controls ES cell self-renewal and pluripotency by a Myc-dependent mechanism. *Development*, 132:885–896, Mar 2005.

[25] J. Hall, G. Guo, J. Wray, I. Eyres, J. Nichols, L. Grotewold, S. Morfopoulou, P. Humphreys, W. Mansfield, R. Walker, S. Tomlinson, and A. Smith. Oct4 and LIF/Stat3 additively induce Krüppel factors to sustain embryonic stem cell self-renewal. *Cell Stem Cell*, 5:597–609, Dec 2009.

[26] I. Chambers and S. R. Tomlinson. The transcriptional foundation of pluripotency. *Development*, 136:2311–2322, Jul 2009.

[27] S. H. Orkin, J. Wang, J. Kim, J. Chu, S. Rao, T. W. Theunissen, X. Shen, and D. N. Levasseur. The transcriptional network controlling pluripotency in ES cells. *Cold Spring Harb. Symp. Quant. Biol.*, 73:195–202, 2008.

[28] C. J. Lengner, G. G. Welstead, and R. Jaenisch. The pluripotency regulator Oct4: a role in somatic stem cells? *Cell Cycle*, 7:725–728, Mar 2008.

[29] D. Strumpf, C. A. Mao, Y. Yamanaka, A. Ralston, K. Chawengsaksophak, F. Beck, and J. Rossant. Cdx2 is required for correct cell fate specification and differentiation of trophectoderm in the mouse blastocyst. *Development*, 132:2093–2102, May 2005.

[30] H. Niwa, J. Miyazaki, and A. G. Smith. Quantitative expression of Oct-3/4 defines differentiation, dedifferentiation or self-renewal of ES cells. *Nat. Genet.*, 24:372–376, Apr 2000.

[31] I. G. Brons, L. E. Smithers, M. W. Trotter, P. Rugg-Gunn, B. Sun, S. M. Chuva de Sousa Lopes, S. K. Howlett, A. Clarkson, L. Ahrlund-Richter, R. A. Pedersen, and L. Vallier. Derivation of pluripotent epiblast stem cells from mammalian embryos. *Nature*, 448:191–195, Jul 2007.

[32] L. Cui, K. Johkura, F. Yue, N. Ogiwara, Y. Okouchi, K. Asanuma, and K. Sasaki. Spatial distribution and initial changes of SSEA-1 and other cell adhesion-related molecules on mouse embryonic stem cells before and during differentiation. *J. Histochem. Cytochem.*, 52:1447–1457, Nov 2004.

[33] M. G. Carter, C. A. Stagg, G. Falco, T. Yoshikawa, U. C. Bassey, K. Aiba, L. V. Sharova, N. Shaik, and M. S. Ko. An in situ hybridization-based screen for heterogeneously expressed genes in mouse ES cells. *Gene Expr. Patterns*, 8:181–198, Feb 2008.

[34] T. Graf and M. Stadtfeld. Heterogeneity of embryonic and adult stem cells. *Cell Stem Cell*, 3:480–483, Nov 2008.

[35] I. Chambers, J. Silva, D. Colby, J. Nichols, B. Nijmeijer, M. Robertson, J. Vrana, K. Jones, L. Grotewold, and A. Smith. Nanog safeguards pluripotency and mediates germline development. *Nature*, 450:1230–1234, Dec 2007.

[36] K. Hayashi, S. M. Lopes, F. Tang, and M. A. Surani. Dynamic equilibrium and heterogeneity of mouse pluripotent stem cells with distinct functional and epigenetic states. *Cell Stem Cell*, 3:391–401, Oct 2008.

[37] J. Wray, T. Kalkan, and A. G. Smith. The ground state of pluripotency. *Biochem. Soc. Trans.*, 38:1027–1032, Aug 2010.

[38] S. Bao, F. Tang, X. Li, K. Hayashi, A. Gillich, K. Lao, and M. A. Surani. Epigenetic reversion of post-implantation epiblast to pluripotent embryonic stem cells. *Nature*, 461:1292–1295, Oct 2009.

[39] H. Zhou, W. Li, S. Zhu, J. Y. Joo, J. T. Do, W. Xiong, J. B. Kim, K. Zhang, H. R. Scholer, and S. Ding. Conversion of mouse epiblast stem cells to an earlier pluripotency state by small molecules. *J. Biol. Chem.*, 285:29676–29680, Sep 2010.

[40] N. G. Kooreman and J. C. Wu. Tumorigenicity of pluripotent stem cells: biological insights from molecular imaging. *J R Soc Interface*, Sep 2010.

[41] A. Pluck and C. Klasen. Generation of chimeras by microinjection. *Methods Mol. Biol.*, 561:199–217, 2009.

[42] Z. Wang and R. Jaenisch. At most three ES cells contribute to the somatic lineages of chimeric mice and of mice produced by ES-tetraploid complementation. *Dev. Biol.*, 275:192–201, Nov 2004.

[43] Geron Corporation. Geron initiates clinical trial of human embryonic stem cell based therapy, First patient treated at Shephard Center in Atlanta. *www.geron.com*, Oct 2010.

[44] C. E. Murry and G. Keller. Differentiation of embryonic stem cells to clinically relevant populations: lessons from embryonic development. *Cell*, 132:661–680, Feb 2008.

[45] S. W. Choi. Analyse des neuralen Differenzierungspotentials androgenetischer muriner embryonaler Stammzellen in vitro und in vivo. *PhD Thesis*, Jun 2010.

[46] T. C. Dinger, S. Eckardt, S. W. Choi, G. Camarero, S. Kurosaka, V. Hornich, K. J. McLaughlin, and A. M. Müller. Androgenetic embryonic stem cells form neural progenitor cells in vivo and in vitro. *Stem Cells*, 26:1474–1483, Jun 2008.

[47] S. W. Choi, S. Eckaedt, R. Ahmad, W. Wolber, J.K. McLaughlin, A-L. Siren, and A.M. Müller. Two paternal genomes are compatible with dopaminergic in vitro and in vivo differentiation. *Int. J. Dev. Biol.*, accepted for publication, 2010.

[48] A. M. Bratt-Leal, R. L. Carpenedo, and T. C. McDevitt. Engineering the embryoid body microenvironment to direct embryonic stem cell differentiation. *Biotechnol. Prog.*, 25:43–51, 2009.

[49] I. Desbaillets, U. Ziegler, P. Groscurth, and M. Gassmann. Embryoid bodies: an in vitro model of mouse embryogenesis. *Exp. Physiol.*, 85:645–651, Nov 2000.

[50] M. V. Wiles and G. Keller. Multiple hematopoietic lineages develop from embryonic stem (ES) cells in culture. *Development*, 111:259–267, Feb 1991.

[51] J. Heo, J. S. Lee, I. S. Chu, Y. Takahama, and S. S. Thorgeirsson. Spontaneous differentiation of mouse embryonic stem cells in vitro: characterization by global gene expression profiles. *Biochem. Biophys. Res. Commun.*, 332:1061–1069, Jul 2005.

[52] S. Yamanaka and H. M. Blau. Nuclear reprogramming to a pluripotent state by three approaches. *Nature*, 465:704–712, Jun 2010.

[53] K. Takahashi and S. Yamanaka. Induction of pluripotent stem cells from mouse embryonic and adult fibroblast cultures by defined factors. *Cell*, 126:663–676, Aug 2006.

[54] K. Takahashi, K. Tanabe, M. Ohnuki, M. Narita, T. Ichisaka, K. Tomoda, and S. Yamanaka. Induction of pluripotent stem cells from adult human fibroblasts by defined factors. *Cell*, 131:861–872, Nov 2007.

[55] Q. Hu, A. M. Friedrich, L. V. Johnson, and D. O. Clegg. Memory in Induced Pluripotent Stem Cells: Reprogrammed Human Retinal Pigmented Epithelial Cells Show Tendency for Spontaneous Redifferentiation. *Stem Cells*, Sep 2010.

[56] K. Kim, A. Doi, B. Wen, K. Ng, R. Zhao, P. Cahan, J. Kim, M. J. Aryee, H. Ji, L. I. Ehrlich, A. Yabuuchi, A. Takeuchi, K. C. Cunniff, H. Hongguang, S. McKinney-Freeman, O. Naveiras, T. J. Yoon, R. A. Irizarry, N. Jung, J. Seita, J. Hanna, P. Murakami, R. Jaenisch, R. Weissleder, S. H. Orkin, I. L. Weissman, A. P. Feinberg, and G. Q. Daley. Epigenetic memory in induced pluripotent stem cells. *Nature*, 467:285–290, Sep 2010.

[57] C. E. Müller-Sieburg, R. H. Cho, M. Thoman, B. Adkins, and H. B. Sieburg. Deterministic regulation of hematopoietic stem cell self-renewal and differentiation. *Blood*, 100:1302–1309, Aug 2002.

[58] J. Fuller. Hematopoietic stem cells and aging. *Sci Aging Knowledge Environ*, 2002:pe11, Jun 2002.

[59] S. Huang, P. Law, K. Francis, B. O. Palsson, and A. D. Ho. Symmetry of initial cell divisions among primitive hematopoietic progenitors is independent of ontogenic age and regulatory molecules. *Blood*, 94:2595–2604, Oct 1999.

[60] N. Carlesso and A. A. Cardoso. Stem cell regulatory niches and their role in normal and malignant hematopoiesis. *Curr. Opin. Hematol.*, 17:281–286, Jul 2010.

[61] F. Rosenbauer and D. G. Tenen. Transcription factors in myeloid development: balancing differentiation with transformation. *Nat. Rev. Immunol.*, 7:105–117, Feb 2007.

[62] E. C. Forsberg, S. S. Prohaska, S. Katzman, G. C. Heffner, J. M. Stuart, and I. L. Weissman. Differential expression of novel potential regulators in hematopoietic stem cells. *PLoS Genet.*, 1:e28, Sep 2005.

[63] M. H. Cottler-Fox, T. Lapidot, I. Petit, O. Kollet, J. F. DiPersio, D. Link, and S. Devine. Stem cell mobilization. *Hematology Am Soc Hematol Educ Program*, pages 419–437, 2003.

[64] M. Tavassoli and J. J. Minguell. Homing of hemopoietic progenitor cells to the marrow. *Proc. Soc. Exp. Biol. Med.*, 196:367–373, Apr 1991.

[65] M. A. Kharfan-Dabaja, Y. R. Abou Mourad, H. F. Fernandez, M. C. Pasquini, and E. S. Santos. Hematopoietic cell transplantation in acute promyelocytic leukemia: a comprehensive review. *Biol. Blood Marrow Transplant.*, 13:997–1004, Sep 2007.

[66] S. Chou, P. Chu, W. Hwang, and H. Lodish. Expansion of human cord blood hematopoietic stem cells for transplantation. *Cell Stem Cell*, 7:427–428, Oct 2010.

[67] G. Sauvageau, U. Thorsteinsdottir, C. J. Eaves, H. J. Lawrence, C. Largman, P. M. Lansdorp, and R. K. Humphries. Overexpression of HOXB4 in hematopoietic cells causes the selective expansion of more primitive populations in vitro and in vivo. *Genes Dev.*, 9:1753–1765, Jul 1995.

[68] H. Araki, N. Mahmud, M. Milhem, R. Nunez, M. Xu, C. A. Beam, and R. Hoffman. Expansion of human umbilical cord blood SCID-repopulating cells using chromatin-modifying agents. *Exp. Hematol.*, 34:140–149, Feb 2006.

[69] M. Milhem, N. Mahmud, D. Lavelle, H. Araki, J. DeSimone, Y. Saunthararajah, and R. Hoffman. Modification of hematopoietic stem cell fate by 5aza 2'deoxycytidine and trichostatin A. *Blood*, 103:4102–4110, Jun 2004.

[70] M. P. Lutolf and H. M. Blau. Artificial stem cell niches. *Adv. Mater. Weinheim*, 21:3255–3268, Sep 2009.

[71] M. P. Lutolf, R. Doyonnas, K. Havenstrite, K. Koleckar, and H. M. Blau. Perturbation of single hematopoietic stem cell fates in artificial niches. *Integr Biol (Camb)*, 1:59–69, Jan 2009.

[72] A. E. Boitano, J. Wang, R. Romeo, L. C. Bouchez, A. E. Parker, S. E. Sutton, J. R. Walker, C. A. Flaveny, G. H. Perdew, M. S. Denison, P. G. Schultz, and M. P. Cooke. Aryl hydrocarbon receptor antagonists promote the expansion of human hematopoietic stem cells. *Science*, 329:1345–1348, Sep 2010.

[73] G. Egger, G. Liang, A. Aparicio, and P. A. Jones. Epigenetics in human disease and prospects for epigenetic therapy. *Nature*, 429:457–463, May 2004.

[74] M. Spivakov and A. G. Fisher. Epigenetic signatures of stem-cell identity. *Nat. Rev. Genet.*, 8:263–271, Apr 2007.

[75] C. Bonifer, M. Hoogenkamp, H. Krysinska, and H. Tagoh. How transcription factors program chromatin–lessons from studies of the regulation of myeloid-specific genes. *Semin. Immunol.*, 20:257–263, Aug 2008.

[76] X. Cheng and R. M. Blumenthal. Mammalian DNA methyltransferases: a structural perspective. *Structure*, 16:341–350, Mar 2008.

[77] S. C. Wu and Y. Zhang. Active DNA demethylation: many roads lead to Rome. *Nat. Rev. Mol. Cell Biol.*, 11:607–620, Sep 2010.

[78] E. I. Campos and D. Reinberg. Histones: annotating chromatin. *Annu. Rev. Genet.*, 43:559–599, 2009.

[79] B. M. Turner. Cellular memory and the histone code. *Cell*, 111:285–291, Nov 2002.

[80] A. J. Ruthenburg, H. Li, D. J. Patel, and C. D. Allis. Multivalent engagement of chromatin modifications by linked binding modules. *Nat. Rev. Mol. Cell Biol.*, 8:983–994, Dec 2007.

[81] H. Lehrmann, L. L. Pritchard, and A. Harel-Bellan. Histone acetyltransferases and deacetylases in the control of cell proliferation and differentiation. *Adv. Cancer Res.*, 86:41–65, 2002.

[82] J. C. Rice and C. D. Allis. Histone methylation versus histone acetylation: new insights into epigenetic regulation. *Curr. Opin. Cell Biol.*, 13:263–273, Jun 2001.

[83] K. Agger, J. Christensen, P. A. Cloos, and K. Helin. The emerging functions of histone demethylases. *Curr. Opin. Genet. Dev.*, 18:159–168, Apr 2008.

[84] J. C. van Wolfswinkel and R. F. Ketting. The role of small non-coding RNAs in genome stability and chromatin organization. *J. Cell. Sci.*, 123:1825–1839, Jun 2010.

[85] W. W. Franke, U. Scheer, H. Zentgraf, M. F. Trendelenburg, U. Müller, G. Krohne, and H. Spring. Organization of transcribed and nontranscribed chromatin. *Results Probl Cell Differ*, 11:15–36, 1980.

[86] L. Ho and G. R. Crabtree. Chromatin remodelling during development. *Nature*, 463:474–484, Jan 2010.

[87] A. L. Clayton, C. A. Hazzalin, and L. C. Mahadevan. Enhanced histone acetylation and transcription: a dynamic perspective. *Mol. Cell*, 23:289–296, Aug 2006.

[88] S. K. Kurdistani, S. Tavazoie, and M. Grunstein. Mapping global histone acetylation patterns to gene expression. *Cell*, 117:721–733, Jun 2004.

[89] J. E. Bolden, M. J. Peart, and R. W. Johnstone. Anticancer activities of histone deacetylase inhibitors. *Nat Rev Drug Discov*, 5:769–784, Sep 2006.

[90] Z. Wang, C. Zang, K. Cui, D. E. Schones, A. Barski, W. Peng, and K. Zhao. Genome-wide mapping of HATs and HDACs reveals distinct functions in active and inactive genes. *Cell*, 138:1019–1031, Sep 2009.

[91] N. Pecuchet, T. Cluzeau, C. Thibault, N. Mounier, and S. Vignot. [Histone deacetylase inhibitors: highlight on epigenetic regulation]. *Bull Cancer*, 97:917–935, Aug 2010.

[92] M. Yoshida, M. Kijima, M. Akita, and T. Beppu. Potent and specific inhibition of mammalian histone deacetylase both in vivo and in vitro by trichostatin A. *J. Biol. Chem.*, 265:17174–17179, Oct 1990.

[93] B. Monti, E. Polazzi, and A. Contestabile. Biochemical, molecular and epigenetic mechanisms of valproic acid neuroprotection. *Curr Mol Pharmacol*, 2:95–109, Jan 2009.

[94] A. Duenas-Gonzalez, M. Candelaria, C. Perez-Plascencia, E. Perez-Cardenas, E. de la Cruz-Hernandez, and L. A. Herrera. Valproic acid as epigenetic cancer drug: preclinical, clinical and transcriptional effects on solid tumors. *Cancer Treat. Rev.*, 34:206–222, May 2008.

[95] I. M. Adcock. Histone deacetylase inhibitors as novel anti-inflammatory agents. *Curr Opin Investig Drugs*, 7:966–973, Nov 2006.

[96] Y. Zhang, S. Kwon, T. Yamaguchi, F. Cubizolles, S. Rousseaux, M. Kneissel, C. Cao, N. Li, H. L. Cheng, K. Chua, D. Lombard, A. Mizeracki, G. Matthias, F. W. Alt, S. Khochbin, and P. Matthias. Mice lacking histone deacetylase 6 have hyperacetylated tubulin but are viable and develop normally. *Mol. Cell. Biol.*, 28:1688–1701, Mar 2008.

[97] B. N. Singh, G. Zhang, Y. L. Hwa, J. Li, S. C. Dowdy, and S. W. Jiang. Nonhistone protein acetylation as cancer therapy targets. *Expert Rev Anticancer Ther*, 10:935–954, Jun 2010.

[98] H. J. Woo, S. J. Lee, B. T. Choi, Y. M. Park, and Y. H. Choi. Induction of apoptosis and inhibition of telomerase activity by trichostatin A, a histone deacetylase inhibitor, in human leukemic U937 cells. *Exp. Mol. Pathol.*, 82:77–84, Feb 2007.

[99] V. Balasubramaniyan, E. Boddeke, R. Bakels, B. Kust, S. Kooistra, A. Veneman, and S. Copray. Effects of histone deacetylation inhibition on neuronal differentiation of embryonic mouse neural stem cells. *Neuroscience*, 143:939–951, Dec 2006.

[100] D. Huangfu, R. Maehr, W. Guo, A. Eijkelenboom, M. Snitow, A. E. Chen, and D. A. Melton. Induction of pluripotent stem cells by defined factors is greatly improved by small-molecule compounds. *Nat. Biotechnol.*, 26:795–797, Jul 2008.

[101] A. Mattout and E. Meshorer. Chromatin plasticity and genome organization in pluripotent embryonic stem cells. *Curr. Opin. Cell Biol.*, 22:334–341, Jun 2010.

[102] S. Efroni, R. Duttagupta, J. Cheng, H. Dehghani, D. J. Hoeppner, C. Dash, D. P. Bazett-Jones, S. Le Grice, R. D. McKay, K. H. Buetow, T. R. Gingeras, T. Misteli, and E. Meshorer. Global transcription in pluripotent embryonic stem cells. *Cell Stem Cell*, 2:437–447, May 2008.

[103] J. L. Golob, S. L. Paige, V. Muskheli, L. Pabon, and C. E. Murry. Chromatin remodeling during mouse and human embryonic stem cell differentiation. *Dev. Dyn.*, 237:1389–1398, May 2008.

[104] E. Meshorer, D. Yellajoshula, E. George, P. J. Scambler, D. T. Brown, and T. Misteli. Hyperdynamic plasticity of chromatin proteins in pluripotent embryonic stem cells. *Dev. Cell*, 10:105–116, Jan 2006.

[105] H. F. Jørgensen, V. Azuara, S. Amoils, M. Spivakov, A. Terry, T. Nesterova, B. S. Cobb, B. Ramsahoye, M. Merkenschlager, and A. G. Fisher. The impact of chromatin modifiers on the timing of locus replication in mouse embryonic stem cells. *Genome Biol.*, 8:R169, 2007.

[106] J. H. Lee, S. R. Hart, and D. G. Skalnik. Histone deacetylase activity is required for embryonic stem cell differentiation. *Genesis*, 38:32–38, Jan 2004.

[107] E. Bartova, G. Galiova, J. Krejci, A. Harnicarova, L. Strasak, and S. Kozubek. Epigenome and chromatin structure in human embryonic stem cells undergoing differentiation. *Dev. Dyn.*, 237:3690–3702, Dec 2008.

[108] J. Krejci, R. Uhlirova, G. Galiova, S. Kozubek, J. Smigova, and E. Bartova. Genome-wide reduction in H3K9 acetylation during human embryonic stem cell differentiation. *J. Cell. Physiol.*, 219:677–687, Jun 2009.

[109] Y. Bian, R. Alberio, C. Allegrucci, K. H. Campbell, and A. D. Johnson. Epigenetic marks in somatic chromatin are remodelled to resemble pluripotent nuclei by amphibian oocyte extracts. *Epigenetics*, 4:194–202, Apr 2009.

[110] B. Wen, H. Wu, Y. Shinkai, R. A. Irizarry, and A. P. Feinberg. Large histone H3 lysine 9 dimethylated chromatin blocks distinguish differentiated from embryonic stem cells. *Nat. Genet.*, 41:246–250, Feb 2009.

[111] T. Aoto, N. Saitoh, T. Ichimura, H. Niwa, and M. Nakao. Nuclear and chromatin reorganization in the MHC-Oct3/4 locus at developmental phases of embryonic stem cell differentiation. *Dev. Biol.*, 298:354–367, Oct 2006.

[112] B. Keenen and I. L. de la Serna. Chromatin remodeling in embryonic stem cells: regulating the balance between pluripotency and differentiation. *J. Cell. Physiol.*, 219:1–7, Apr 2009.

[113] S. Assou, D. Cerecedo, S. Tondeur, V. Pantesco, O. Hovatta, B. Klein, S. Hamamah, and J. De Vos. A gene expression signature shared by human mature oocytes and embryonic stem cells. *BMC Genomics*, 10:10, 2009.

[114] Z. Yan, Z. Wang, L. Sharova, A. A. Sharov, C. Ling, Y. Piao, K. Aiba, R. Matoba, W. Wang, and M. S. Ko. BAF250B-associated SWI/SNF chromatin-remodeling complex is required to maintain undifferentiated mouse embryonic stem cells. *Stem Cells*, 26:1155–1165, May 2008.

[115] J. Landry, A. A. Sharov, Y. Piao, L. V. Sharova, H. Xiao, E. Southon, J. Matta, L. Tessarollo, Y. E. Zhang, M. S. Ko, M. R. Kuehn, T. P. Yamaguchi, and C. Wu. Essential role of chromatin remodeling protein Bptf in early mouse embryos and embryonic stem cells. *PLoS Genet.*, 4:e1000241, Oct 2008.

[116] L. Ho, R. Jothi, J. L. Ronan, K. Cui, K. Zhao, and G. R. Crabtree. An embryonic stem cell chromatin remodeling complex, esBAF, is an essential component of the core pluripotency transcriptional network. *Proc. Natl. Acad. Sci. U.S.A.*, 106:5187–5191, Mar 2009.

[117] C. Schaniel, Y. S. Ang, K. Ratnakumar, C. Cormier, T. James, E. Bernstein, I. R. Lemischka, and P. J. Paddison. Smarcc1/Baf155 couples self-renewal gene repression with changes in chromatin structure in mouse embryonic stem cells. *Stem Cells*, 27:2979–2991, Dec 2009.

[118] L. Ho, J. L. Ronan, J. Wu, B. T. Staahl, L. Chen, A. Kuo, J. Lessard, A. I. Nesvizhskii, J. Ranish, and G. R. Crabtree. An embryonic stem cell chromatin remodeling complex, esBAF, is essential for embryonic stem cell self-renewal and pluripotency. *Proc. Natl. Acad. Sci. U.S.A.*, 106:5181–5186, Mar 2009.

[119] B. E. Bernstein, T. S. Mikkelsen, X. Xie, M. Kamal, D. J. Huebert, J. Cuff, B. Fry, A. Meissner, M. Wernig, K. Plath, R. Jaenisch, A. Wagschal, R. Feil, S. L. Schreiber, and E. S. Lander. A bivalent chromatin structure marks key developmental genes in embryonic stem cells. *Cell*, 125:315–326, Apr 2006.

[120] H. F. Jørgensen, S. Giadrossi, M. Casanova, M. Endoh, H. Koseki, N. Brockdorff, and A. G. Fisher. Stem cells primed for action: polycomb repressive complexes restrain the expression of lineage-specific regulators in embryonic stem cells. *Cell Cycle*, 5:1411–1414, Jul 2006.

[121] K. Cui, C. Zang, T. Y. Roh, D. E. Schones, R. W. Childs, W. Peng, and K. Zhao. Chromatin signatures in multipotent human hematopoietic stem cells indicate the fate of bivalent genes during differentiation. *Cell Stem Cell*, 4:80–93, Jan 2009.

[122] M. Adli, J. Zhu, and B. E. Bernstein. Genome-wide chromatin maps derived from limited numbers of hematopoietic progenitors. *Nat. Methods*, 7:615–618, Aug 2010.

[123] H. Weishaupt, M. Sigvardsson, and J. L. Attema. Epigenetic chromatin states uniquely define the developmental plasticity of murine hematopoietic stem cells. *Blood*, 115:247–256, Jan 2010.

[124] A. M. Pietersen and M. van Lohuizen. Stem cell regulation by polycomb repressors: postponing commitment. *Curr. Opin. Cell Biol.*, 20:201–207, Apr 2008.

[125] X. Shen, Y. Liu, Y. J. Hsu, Y. Fujiwara, J. Kim, X. Mao, G. C. Yuan, and S. H. Orkin. EZH1 mediates methylation on histone H3 lysine 27 and complements EZH2 in

maintaining stem cell identity and executing pluripotency. *Mol. Cell*, 32:491–502, Nov 2008.

[126] P. J. Rugg-Gunn, B. J. Cox, A. Ralston, and J. Rossant. Distinct histone modifications in stem cell lines and tissue lineages from the early mouse embryo. *Proc. Natl. Acad. Sci. U.S.A.*, 107:10783–10790, Jun 2010.

[127] O. Alder, F. Lavial, A. Helness, E. Brookes, S. Pinho, A. Chandrashekran, P. Arnaud, A. Pombo, L. O'Neill, and V. Azuara. Ring1B and Suv39h1 delineate distinct chromatin states at bivalent genes during early mouse lineage commitment. *Development*, 137:2483–2492, Aug 2010.

[128] L. E. Surface, S. R. Thornton, and L. A. Boyer. Polycomb group proteins set the stage for early lineage commitment. *Cell Stem Cell*, 7:288–298, Sep 2010.

[129] N. D. Montgomery, D. Yee, S. A. Montgomery, and T. Magnuson. Molecular and functional mapping of EED motifs required for PRC2-dependent histone methylation. *J. Mol. Biol.*, 374:1145–1157, Dec 2007.

[130] D. Pasini, A. P. Bracken, J. B. Hansen, M. Capillo, and K. Helin. The polycomb group protein Suz12 is required for embryonic stem cell differentiation. *Mol. Cell. Biol.*, 27:3769–3779, May 2007.

[131] N. D. Montgomery, D. Yee, A. Chen, S. Kalantry, S. J. Chamberlain, A. P. Otte, and T. Magnuson. The murine polycomb group protein Eed is required for global histone H3 lysine-27 methylation. *Curr. Biol.*, 15:942–947, May 2005.

[132] R. Margueron, N. Justin, K. Ohno, M. L. Sharpe, J. Son, W. J. Drury, P. Voigt, S. R. Martin, W. R. Taylor, V. De Marco, V. Pirrotta, D. Reinberg, and S. J. Gamblin. Role of the polycomb protein EED in the propagation of repressive histone marks. *Nature*, 461:762–767, Oct 2009.

[133] K. H. Hansen, A. P. Bracken, D. Pasini, N. Dietrich, S. S. Gehani, A. Monrad, J. Rappsilber, M. Lerdrup, and K. Helin. A model for transmission of the H3K27me3 epigenetic mark. *Nat. Cell Biol.*, 10:1291–1300, Nov 2008.

[134] T. Suganuma and J. L. Workman. WD40 repeats arrange histone tails for spreading of silencing. *J Mol Cell Biol*, 2:81–83, Apr 2010.

[135] A. Kanhere, K. Viiri, C. C. Araujo, J. Rasaiyaah, R. D. Bouwman, W. A. Whyte, C. F. Pereira, E. Brookes, K. Walker, G. W. Bell, A. Pombo, A. G. Fisher, R. A. Young, and R. G. Jenner. Short RNAs are transcribed from repressed polycomb target genes and interact with polycomb repressive complex-2. *Mol. Cell*, 38:675–688, Jun 2010.

[136] M. C. Tsai, O. Manor, Y. Wan, N. Mosammaparast, J. K. Wang, F. Lan, Y. Shi, E. Segal, and H. Y. Chang. Long noncoding RNA as modular scaffold of histone modification complexes. *Science*, 329:689–693, Aug 2010.

[137] E. Vire, C. Brenner, R. Deplus, L. Blanchon, M. Fraga, C. Didelot, L. Morey, A. Van Eynde, D. Bernard, J. M. Vanderwinden, M. Bollen, M. Esteller, L. Di Croce, Y. de Launoit, and F. Fuks. The Polycomb group protein EZH2 directly controls DNA methylation. *Nature*, 439:871–874, Feb 2006.

[138] C. C. de la Cruz, A. Kirmizis, M. D. Simon, K. Isono, H. Koseki, and B. Panning. The polycomb group protein SUZ12 regulates histone H3 lysine 9 methylation and HP1 alpha distribution. *Chromosome Res.*, 15:299–314, 2007.

[139] A. Kuzmichev, K. Nishioka, H. Erdjument-Bromage, P. Tempst, and D. Reinberg. Histone methyltransferase activity associated with a human multiprotein complex containing the Enhancer of Zeste protein. *Genes Dev.*, 16:2893–2905, Nov 2002.

[140] R. G. Sewalt, M. Lachner, M. Vargas, K. M. Hamer, J. L. den Blaauwen, T. Hendrix, M. Melcher, D. Schweizer, T. Jenuwein, and A. P. Otte. Selective interactions between vertebrate polycomb homologs and the SUV39H1 histone lysine methyltransferase suggest that histone H3-K9 methylation contributes to chromosomal targeting of Polycomb group proteins. *Mol. Cell. Biol.*, 22:5539–5553, Aug 2002.

[141] J. van der Vlag and A. P. Otte. Transcriptional repression mediated by the human polycomb-group protein EED involves histone deacetylation. *Nat. Genet.*, 23:474–478, Dec 1999.

[142] H. M. Herz and A. Shilatifard. The JARID2-PRC2 duality. *Genes Dev.*, 24:857–861, May 2010.

[143] J. C. Peng, A. Valouev, T. Swigut, J. Zhang, Y. Zhao, A. Sidow, and J. Wysocka. Jarid2/Jumonji coordinates control of PRC2 enzymatic activity and target gene occupancy in pluripotent cells. *Cell*, 139:1290–1302, Dec 2009.

[144] X. Shen, W. Kim, Y. Fujiwara, M. D. Simon, Y. Liu, M. R. Mysliwiec, G. C. Yuan, Y. Lee, and S. H. Orkin. Jumonji modulates polycomb activity and self-renewal versus differentiation of stem cells. *Cell*, 139:1303–1314, Dec 2009.

[145] D. Pasini, P. A. Cloos, J. Walfridsson, L. Olsson, J. P. Bukowski, J. V. Johansen, M. Bak, N. Tommerup, J. Rappsilber, and K. Helin. JARID2 regulates binding of the Polycomb repressive complex 2 to target genes in ES cells. *Nature*, 464:306–310, Mar 2010.

[146] G. Li, R. Margueron, M. Ku, P. Chambon, B. E. Bernstein, and D. Reinberg. Jarid2 and PRC2, partners in regulating gene expression. *Genes Dev.*, 24:368–380, Feb 2010.

[147] H. Ura, M. Usuda, K. Kinoshita, C. Sun, K. Mori, T. Akagi, T. Matsuda, H. Koide, and T. Yokota. STAT3 and Oct-3/4 control histone modification through induction of Eed in embryonic stem cells. *J. Biol. Chem.*, 283:9713–9723, Apr 2008.

[148] C. F. Pereira, F. M. Piccolo, T. Tsubouchi, S. Sauer, N. K. Ryan, L. Bruno, D. Landeira, J. Santos, A. Banito, J. Gil, H. Koseki, M. Merkenschlager, and A. G. Fisher. ESCs require PRC2 to direct the successful reprogramming of differentiated cells toward pluripotency. *Cell Stem Cell*, 6:547–556, Jun 2010.

[149] J. Wang, J. Mager, E. Schnedier, and T. Magnuson. The mouse PcG gene eed is required for Hox gene repression and extraembryonic development. *Mamm. Genome*, 13:493–503, Sep 2002.

[150] S. J. Chamberlain, D. Yee, and T. Magnuson. Polycomb repressive complex 2 is dispensable for maintenance of embryonic stem cell pluripotency. *Stem Cells*, 26:1496–1505, Jun 2008.

[151] M. Leeb, D. Pasini, M. Novatchkova, M. Jaritz, K. Helin, and A. Wutz. Polycomb complexes act redundantly to repress genomic repeats and genes. *Genes Dev.*, 24:265–276, Feb 2010.

[152] I. H. Su, M. W. Dobenecker, E. Dickinson, M. Oser, A. Basavaraj, R. Marqueron, A. Viale, D. Reinberg, C. Wulfing, and A. Tarakhovsky. Polycomb group protein ezh2 controls actin polymerization and cell signaling. *Cell*, 121:425–436, May 2005.

[153] S. Philipp, M. Puchert, S. Adam-Klages, V. Tchikov, S. Winoto-Morbach, S. Mathieu, A. Deerberg, L. Kolker, N. Marchesini, D. Kabelitz, Y. A. Hannun, S. Schutze, and D. Adam. The Polycomb group protein EED couples TNF receptor 1 to neutral sphingomyelinase. *Proc. Natl. Acad. Sci. U.S.A.*, 107:1112–1117, Jan 2010.

[154] J. A. Simon and C. A. Lange. Roles of the EZH2 histone methyltransferase in cancer epigenetics. *Mutat. Res.*, 647:21–29, Dec 2008.

[155] H. Niwa, T. Burdon, I. Chambers, and A. Smith. Self-renewal of pluripotent embryonic stem cells is mediated via activation of STAT3. *Genes Dev.*, 12:2048–2060, Jul 1998.

[156] M. Boiani and H. R. Scholer. Regulatory networks in embryo-derived pluripotent stem cells. *Nat. Rev. Mol. Cell Biol.*, 6:872–884, Nov 2005.

[157] T. C. Doetschman, H. Eistetter, M. Katz, W. Schmidt, and R. Kemler. The in vitro development of blastocyst-derived embryonic stem cell lines: formation of visceral yolk sac, blood islands and myocardium. *J Embryol Exp Morphol*, 87:27–45, Jun 1985.

[158] P. E. Szabo, K. Hubner, H. Scholer, and J. R. Mann. Allele-specific expression of imprinted genes in mouse migratory primordial germ cells. *Mech. Dev.*, 115:157–160, Jul 2002.

[159] N. Fox, I. Damjanov, A. Martinez-Hernandez, B. B. Knowles, and D. Solter. Immunohistochemical localization of the early embryonic antigen (SSEA-1) in postimplantation mouse embryos and fetal and adult tissues. *Dev. Biol.*, 83:391–398, Apr 1981.

[160] N. Kojima, B. A. Fenderson, M. R. Stroud, R. I. Goldberg, R. Habermann, T. Toyokuni, and S. Hakomori. Further studies on cell adhesion based on Le(x)-Le(x) interaction, with new approaches: embryoglycan aggregation of F9 teratocarcinoma cells, and adhesion of various tumour cells based on Le(x) expression. *Glycoconj. J.*, 11:238–248, Jun 1994.

[161] H. Kurosawa, T. Imamura, M. Koike, K. Sasaki, and Y. Amano. A simple method for forming embryoid body from mouse embryonic stem cells. *J. Biosci. Bioeng.*, 96:409–411, 2003.

[162] S. M. Dang, M. Kyba, R. Perlingeiro, G. Q. Daley, and P. W. Zandstra. Efficiency of embryoid body formation and hematopoietic development from embryonic stem cells in different culture systems. *Biotechnol. Bioeng.*, 78:442–453, May 2002.

[163] S. Atkinson and L. Armstrong. Epigenetics in embryonic stem cells: regulation of pluripotency and differentiation. *Cell Tissue Res.*, 331:23–29, Jan 2008.

[164] M. Bibikova, L. C. Laurent, B. Ren, J. F. Loring, and J. B. Fan. Unraveling epigenetic regulation in embryonic stem cells. *Cell Stem Cell*, 2:123–134, Feb 2008.

[165] T. P. Rasmussen. Embryonic stem cell differentiation: a chromatin perspective. *Reprod. Biol. Endocrinol.*, 1:100, Nov 2003.

[166] Q. Gan, T. Yoshida, O. G. McDonald, and G. K. Owens. Concise review: epigenetic mechanisms contribute to pluripotency and cell lineage determination of embryonic stem cells. *Stem Cells*, 25:2–9, Jan 2007.

[167] H. Niwa. How is pluripotency determined and maintained? *Development*, 134:635–646, Feb 2007.

[168] V. Azuara, P. Perry, S. Sauer, M. Spivakov, H. F. Jørgensen, R. M. John, M. Gouti, M. Casanova, G. Warnes, M. Merkenschlager, and A. G. Fisher. Chromatin signatures of pluripotent cell lines. *Nat. Cell Biol.*, 8:532–538, May 2006.

[169] T. Suganuma and J. L. Workman. Crosstalk among Histone Modifications. *Cell*, 135:604–607, Nov 2008.

[170] S. Winter and W. Fischle. Epigenetic markers and their cross-talk. *Essays Biochem.*, 48:45–61, Sep 2010.

[171] W. Fischle, Y. Wang, and C. D. Allis. Histone and chromatin cross-talk. *Curr. Opin. Cell Biol.*, 15:172–183, Apr 2003.

[172] R. Eskeland, M. Leeb, G. R. Grimes, C. Kress, S. Boyle, D. Sproul, N. Gilbert, Y. Fan, A. I. Skoultchi, A. Wutz, and W. A. Bickmore. Ring1B compacts chromatin structure and represses gene expression independent of histone ubiquitination. *Mol. Cell*, 38:452–464, May 2010.

[173] A. Eberharter and P. B. Becker. Histone acetylation: a switch between repressive and permissive chromatin. Second in review series on chromatin dynamics. *EMBO Rep.*, 3:224–229, Mar 2002.

[174] P. Collas. The current state of chromatin immunoprecipitation. *Mol. Biotechnol.*, 45:87–100, May 2010.

[175] K. W. McCool, X. Xu, D. B. Singer, F. E. Murdoch, and M. K. Fritsch. The role of histone acetylation in regulating early gene expression patterns during early embryonic stem cell differentiation. *J. Biol. Chem.*, 282:6696–6706, Mar 2007.

[176] P. Sampath, D. K. Pritchard, L. Pabon, H. Reinecke, S. M. Schwartz, D. R. Morris, and C. E. Murry. A hierarchical network controls protein translation during murine embryonic stem cell self-renewal and differentiation. *Cell Stem Cell*, 2:448–460, May 2008.

[177] E. Karantzali, H. Schulz, O. Hummel, N. Hubner, A. Hatzopoulos, and A. Kretsovali. Histone deacetylase inhibition accelerates the early events of stem cell differentiation: transcriptomic and epigenetic analysis. *Genome Biol.*, 9:R65, 2008.

[178] C. B. Ware, L. Wang, B. H. Mecham, L. Shen, A. M. Nelson, M. Bar, D. A. Lamba, D. S. Dauphin, B. Buckingham, B. Askari, R. Lim, M. Tewari, S. M. Gartler, J. P. Issa, P. Pavlidis, Z. Duan, and C. A. Blau. Histone deacetylase inhibition elicits an evolutionarily conserved self-renewal program in embryonic stem cells. *Cell Stem Cell*, 4:359–369, Apr 2009.

[179] R. E. Davey and P. W. Zandstra. Spatial organization of embryonic stem cell responsiveness to autocrine gp130 ligands reveals an autoregulatory stem cell niche. *Stem Cells*, 24:2538–2548, Nov 2006.

[180] R. E. Davey, K. Onishi, A. Mahdavi, and P. W. Zandstra. LIF-mediated control of embryonic stem cell self-renewal emerges due to an autoregulatory loop. *FASEB J.*, 21:2020–2032, Jul 2007.

[181] T. Chen, D. Yuan, B. Wei, J. Jiang, J. Kang, K. Ling, Y. Gu, J. Li, L. Xiao, and G. Pei. E-cadherin-mediated cell-cell contact is critical for induced pluripotent stem cell generation. *Stem Cells*, 28:1315–1325, Aug 2010.

[182] P. Samavarchi-Tehrani, A. Golipour, L. David, H. K. Sung, T. A. Beyer, A. Datti, K. Woltjen, A. Nagy, and J. L. Wrana. Functional genomics reveals a BMP-driven mesenchymal-to-epithelial transition in the initiation of somatic cell reprogramming. *Cell Stem Cell*, 7:64–77, Jul 2010.

[183] R. Li, J. Liang, S. Ni, T. Zhou, X. Qing, H. Li, W. He, J. Chen, F. Li, Q. Zhuang, B. Qin, J. Xu, W. Li, J. Yang, Y. Gan, D. Qin, S. Feng, H. Song, D. Yang, B. Zhang, L. Zeng, L. Lai, M. A. Esteban, and D. Pei. A mesenchymal-to-epithelial transition initiates and is required for the nuclear reprogramming of mouse fibroblasts. *Cell Stem Cell*, 7:51–63, Jul 2010.

[184] M. Oka, K. Tagoku, T. L. Russell, Y. Nakano, T. Hamazaki, E. M. Meyer, T. Yokota, and N. Terada. CD9 is associated with leukemia inhibitory factor-mediated maintenance of embryonic stem cells. *Mol. Biol. Cell*, 13:1274–1281, Apr 2002.

[185] B. Jakob. Analysing the loss of pluripotency in mouse embryonic stem cells. *Master Thesis*, July 2010.

[186] R. Ensenat-Waser, A. Santana, N. Vicente-Salar, J. C. Cigudosa, E. Roche, B. Soria, and J. A. Reig. Isolation and characterization of residual undifferentiated mouse embryonic stem cells from embryoid body cultures by fluorescence tracking. *In Vitro Cell. Dev. Biol. Anim.*, 42:115–123, 2006.

[187] D. Pasini, A. P. Bracken, M. R. Jensen, E. Lazzerini Denchi, and K. Helin. Suz12 is essential for mouse development and for EZH2 histone methyltransferase activity. *EMBO J.*, 23:4061–4071, Oct 2004.

[188] L. A. Boyer, K. Plath, J. Zeitlinger, T. Brambrink, L. A. Medeiros, T. I. Lee, S. S. Levine, M. Wernig, A. Tajonar, M. K. Ray, G. W. Bell, A. P. Otte, M. Vidal, D. K. Gifford, R. A. Young, and R. Jaenisch. Polycomb complexes repress developmental regulators in murine embryonic stem cells. *Nature*, 441:349–353, May 2006.

[189] F. Lohmann, J. Loureiro, H. Su, Q. Fang, H. Lei, T. Lewis, Y. Yang, M. Labow, E. Li, T. Chen, and S. Kadam. KMT1E mediated H3K9 methylation is required for the maintenance of embryonic stem cells by repressing trophectoderm differentiation. *Stem Cells*, 28:201–212, Feb 2010.

[190] K. Agger, P. A. Cloos, J. Christensen, D. Pasini, S. Rose, J. Rappsilber, I. Issaeva, E. Canaani, A. E. Salcini, and K. Helin. UTX and JMJD3 are histone H3K27 demethylases involved in HOX gene regulation and development. *Nature*, 449:731–734, Oct 2007.

[191] L. Palmqvist, C. H. Glover, L. Hsu, M. Lu, B. Bossen, J. M. Piret, R. K. Humphries, and C. D. Helgason. Correlation of murine embryonic stem cell gene expression profiles with functional measures of pluripotency. *Stem Cells*, 23:663–680, May 2005.

[192] N. E. Fusenig, D. Breitkreutz, P. Boukamp, P. Tomakidi, and H. J. Stark. Differentiation and tumor progression. *Recent Results Cancer Res.*, 139:1–19, 1995.

[193] J. C. Heng, B. Feng, J. Han, J. Jiang, P. Kraus, J. H. Ng, Y. L. Orlov, M. Huss, L. Yang, T. Lufkin, B. Lim, and H. H. Ng. The nuclear receptor Nr5a2 can replace Oct4 in the reprogramming of murine somatic cells to pluripotent cells. *Cell Stem Cell*, 6:167–174, Feb 2010.

[194] G. M. Baerlocher, I. Vulto, G. de Jong, and P. M. Lansdorp. Flow cytometry and FISH to measure the average length of telomeres (flow FISH). *Nat Protoc*, 1:2365–2376, 2006.

9 Acknowledgments

First and foremost I want to thank Prof. Albrecht Müller for all the trust, advancement, help, support and experience that he always offered and offers me! Thank you so much!

I also thank my co-supervisors Prof. Constanze Bonifer and Prof. Ulrich Scheer and I appreciate the Graduate School of Life Sciences and the Research Training Group 1048 for advisory and financial support, respectively.

I would like to acknowledge my dear companion and great help Vroni whom I learnt a lot from and whom I could work together with in a trustful manner (in the lab as well as in the christmas bakery)!

I am grateful to Dr. Matthias Becker for all the stimulating, inspiring and 'horizon-opening' discussions we had and the cool work we did together!

I particularly thank all the current and former members of the Müller group for their friendship, support and the familiar atmosphere in the lab! Especially I am happy to have spent these important years of my life with my nice friends Andrea, Jenny, Linda, Nikos, Ruhel, Soon and Xiaoli (anyway: the sad lab rulez)!

I would like to express my heart-felt gratitude to my family and my friends! Thank you for your constant encouragement and for giving me the self-confidence necessary for the completion of my PhD and for survival in the science business! In particular, I thank my mother, my grandmother, my brother as well as Martina & Frank, Traudel, my lovely Maria and my dear Sandra. Finally I give my deep thank to Christoph for everything I am.

10 Affidavit

I hereby declare that my thesis entitled

Defining the end of pluripotency in mouse embryonic stem cells

is the result of my own work. I did not receive any help or support from commercial consultants. All sources and / or materials applied are listed and specified in the thesis.

Furthermore, I verify that this thesis has not yet been submitted as part of another examination process neither in identical nor in similar form.

Würzburg, ...

Date, Signature

12 List of publications

2010 "Inhibition of histone deacetylases by trichostatin A leads to a HoxB4-independent increase of hematopoietic progenitor/stem cell frequencies as a result of selective survival"

Obier N, Uhlemann CF, Müller AM

Cytotherapy, 12(7):899-908.

2010 "Chromatin flow cytometry identifies changes in epigenetic cell states"

Obier N, Müller AM

Cells Tissues Organs, 191(3):167-74.

2009 Book Chapter "Möglichkeiten und Chancen der Stammzellforschung: Stammzellen für Alle?" in "Forschung contra Lebensschutz? Der Streit um die Stammzellforschung" Hilpert K (Ed.)

Müller AM, Obier N, Choi S *et al.*

Herder Verlag, ISBN: 978-3-451-02233-3